UNIVERSITY OF OKLAHOMA

GRADUATE COLLEGE

USING RADAR TO REVEAL LARGE-SCALE IN-FLIGHT BEHAVIORS OF MIGRATORY BIRDS

A DISSERTATION

SUBMITTED TO THE GRADUATE FACULTY

in partial fulfillment of the requirements for the

Degree of

DOCTOR OF PHILOSOPHY

By

KYLE GERALD HORTON
Norman, Oklahoma
2017

USING RADAR TO REVEAL LARGE-SCALE IN-FLIGHT BEHAVIORS OF MIGRATORY BIRDS

A DISSERTATION APPROVED FOR THE
DEPARTMENT OF BIOLOGY

BY

Dr. Jeffrey Kelly, Chair

Dr. Eli Bridge

Dr. Jeffrey Buler

Dr. Phillip Chilson

Dr. Michael Patten

Acknowledgements

I write this section with a bit of emotion, a bit of reflection, and an abundant amount of sincerity. If this, at times, comes across as mawkish, that's because it is. This is a genuine thank you to the people who have helped me along this fun journey. A journey that I could not have accomplished by myself. To say "I" throughout this dissertation would be a mischaracterization, instead, I write "we".

First, I thank my advisor, Jeff Kelly. This is first, because it is foremost. Jeff has opened the right doors at all the right moments. His opinion I value utmost. His steady language I cherish. Uncle J, a nickname, unbeknownst to him – I suspect – carries my full weight of endearment. Jeff is a friend, colleague, confidant, and mentor of the first rate. He carries a wealth of knowledge he would never admit to having. Jeff has shaped this work, my character, and my academic philosophy. I thank him for letting me shoot high, and being there when I miss. I thank him for the many conversations, good, bad, uncomfortable – they likely meant more to me than he could ever image. Thank you.

I thank the following four people, Carolyn Burt, Benjamin Van Doren, Andrew Farnsworth, and Phillip Stepanian for different, but equally important reasons.

I start with Carolyn. Carolyn has instilled an education in me I didn't know I needed. A side of things I have been, for far too long, blind to see. An education in feminism. An instruction that tests my biases, assumptions, privileges – daily – both in society and in academia. An education you won't find listed on my CV, but one that rivals the letters that will follow my name. One that I continue to grow in. An education that will carry through the various incarnations of my professional and personal life. She is also my companion, my rock, a voice of reason, a person that tells me, "you're wrong, Kyle". A person who cares about my success, my future, our journeys together, and a person to share countless memories with. Whether tromping through a cloud forest or bopping around campus for Pokómon, I thank her for telling

me to put research aside from time-to-time – however resistant I may be. For these reasons and more, I thank you and I love you.

I thank Benjamin for his scientific prowess. Unmatched in my opinion. His numeric touch prevalent throughout this dissertation. His proficiency has been frustrating and contagious at the same time. I thank Benjamin for the countless, timely, academic exchanges. His attention to detail, statistical craft, and use of language have made our collaborations a delight. I thank him for the tireless dedication to this work. I thank him for the continued input. I am a better scientist for it, and the science we have done is better because of it. Thank you.

I thank Andrew for his excitement and passion for studying migratory birds. His doctoral work inspired and excited an undergraduate years ago, *à* propos we were able to work together on my own doctoral work. I thank him for facilitating the many connections I've acquired through our collaborations. I thank him for always providing a natural history perspective. I thank him for the continued encouragement and kind reflection.

I thank Phil for being my first and best friend in Norman. Beyond friendship, Phil's shared knowledge in radar is the only reason I approach mastery in radar ornithology. Our work at OU laid the groundwork for the fondest memories of my doctoral work. Thank you for the guidance. Thank you for listening and understanding my frustrations. Thank you for giving this biologist the time of day.

I would like to thank my committee members, Eli Bridge, Jeffrey Buler, Phillip Chilson, and Michael Patten. I thank each of them for their support, guidance, and timely feedback. I thank Eli for always championing my work. I thank Jeff for his continued encouragement and lively radar discussions. I thank Phil for the opportunities he's opened up to me. I thank Michael for his interest in my work, his sense of humor, and timely feedback on anything and everything I sent him.

I'd like to thank Dan Sheldon for the many engaging radar conversations, and his willingness to share his knowledge in radar processing. I'd like to thank Kyle Broadfoot for his camaraderie. Our adventures in Rome and Washington will last a lifetime. I'd like to thank Frank La Sorte and Daniel Fink for their interest in my questions and willingness to contribute eBird data. I'd like to thank Wesley Hochachka for his statistical input in the infancy of this work. I'd like to thank all the members of the OU Aeroecology group. I'd like to thank Sara Morris for her continued mentorship. I thank Sara for exposing me to the world of ornithology. I thank Sara for exciting me about bird migration.

Lastly, I'd like to thank my family, my biggest fans. Thank you for listening and understanding how much this degree means to me. Thank you for supporting my journey, coast-to-coast.

Table of Contents

List Of Tables

List Of Figures

Abstract

Chapter 1: Of all migratory taxa, birds have garnered the greatest attention. In the Western Hemisphere billions of avian migrants pass between Nearctic and Neotropical ecozones. Landscape and climate change make understanding behavioral plasticity of paramount importance to study how migrants cope with change. Yet quantifying the passage of these movements has posed tremendous challenges and has often required creative methodology. Particularly challenging are the scales of movements (100s to 1000s of kilometers) and altitudes of migrants' flights (100s to 1000s of meters above ground level). Although technological advances have vastly improved our abilities to investigate these phenomena, tools for studying these behaviors in real-time and in-flight – critical for advancing biological and conservation knowledge – have remained rather static. Many studies use stopover methods that gather information before and after migratory flights (e.g. ground observations, banding). But these methods do not directly improve our knowledge of birds' behaviors *during* flights, when we need detailed information about changes in direction, speed, altitude, and orientation to study migration biology. I use weather surveillance radar to investigate the in-flight behaviors employed by migratory birds as they transition to and from their wintering and breeding grounds. I explore regional (Chapter 2), seasonal (Chapter 3), altitudinal (Chapter 4), and latitudinal (Chapter 5) dependencies on how migrants utilize and cope with winds aloft.

Chapter 2: The shortest possible migratory route for birds is not always the best route to travel. Substantial research effort has established that birds in captivity are capable of orienting toward the direction of an intended goal, but efforts to examine how free-living birds use navigational information under conditions that potentially make direct flight toward that goal inefficient have been limited in spatiotemporal scales and in the number of individuals observed because of logistical and technological limitations. Using novel and recently developed techniques for

analysis of Doppler polarimetric weather surveillance radar data, we examined two impediments for nocturnally migrating songbirds in eastern North America following shortest-distance routes: crosswinds and oceans. We found that migrants in flight often drifted sideways on crosswinds, but most strongly compensated for drift when near the Atlantic coast. Coastal migrants' tendency to compensate for wind drift also increased through the night, while no strong temporal differences were observed at inland sites. Such behaviors suggest that birds migrate in an adaptive way to conserve energy by assessing while airborne the degree to which they must compensate for wind drift.

Chapter 3: Migrating birds make strategic decisions at multiple temporal and spatial scales. They must select flight altitudes, speeds, and orientations in order to maintain preferred directions of movement and to minimize energy expenditure and risk. Spring flights follow a rapid phenology, but how this rapid transit translates to in-flight decisions is not clear. We described flight strategies of nocturnally migrating landbirds using six weather surveillance radars during spring (2013–2015) and fall (2013–2014) migratory periods in the eastern United States to investigate seasonal decision- making patterns and how climate change may influence these trends. During spring, we found groundspeed and airspeed of migrants to be significantly higher than those of fall migrants; compensation for wind drift was also significantly greater during spring. Our results indicate that birds make more rapid and precise flights in spring that are only partially explained by meteorological phenomena. Future applications at greater spatial scales will allow direct comparisons of in-flight behaviors with predictions from migration theory.

Chapter 4: The lower atmosphere (i.e. aerosphere) is critical habitat for migrant birds. This habitat is vast and little is known about the spatio-temporal patterns of distribution and abundance of migrants in it. Increased human encroachment into the aerosphere makes understanding where and when migratory birds use this

airspace a key to reducing human–wildlife conflicts. We use weather surveillance radar to describe large-scale height distributions of nocturnally migrating birds and interpret these distributions as aggregate habitat selection behaviors of individual birds. As such, we detail wind cues that influence selection of flight heights. Using six radars in the eastern USA during the spring (2013–2015) and autumn (2013 and 2014), we found migrants tended to adjust their heights according to favorable wind profit. We found that migrants' flight altitudes correlated most closely with the altitude of maximum wind profit; however, absolute differences in flight heights and height of maximum wind profit were large. Migrants tended to fly slightly higher at inland sites compared with coastal sites during spring, but not during autumn. Migration activity was greater at coastal sites during autumn, but not during spring. This characterization of bird migration represents a critical advance in our understanding of migrant distributions in flight and a new window into habitat selection behaviors.

Chapter 5: Many migratory bird species travel thousands of kilometers each year and navigate with high spatial and temporal precision using a variety of tactics and strategies. One potentially important tactic is compensation for wind drift, whose characteristics may vary among species based on timing, body size, and prevailing atmospheric conditions. Until recently, methodological limitations have constrained studies of wind drift and its relationship to spatiotemporal variation in migration strategies at continental extents. Here, we use weather surveillance radar data and citizen science observations (eBird) compiled during spring migration within central North America to address the extent to which migratory birds drift or compensate as they travel north across a broad latitudinal gradient defined by changing atmospheric conditions. Migrants traveling northward in the spring shifted their flight strategies as they encountered stronger westerly crosswinds at higher latitudes. Greater compensation for wind drift and the use of faster flight speeds was most pronounced when

large-bodied species dominated species composition. Further supporting these linkages, we were able to accurately predict variation in the direction of in-flight nocturnal migration from ground-based estimates of species composition. This study reveals the complementary relationships between radar and citizen science, furthering our ability to document and understand broad-scale migration patterns and dynamics.

Chapter 1

Introduction

> *Our traditional view of natural systems, therefore, might well be less a meaningful reality than a perceptual convenience*
>
> – C.S. Holling (1973), Resilience and Stability of Ecological Systems

The structure and function of modern ecosystems shape and are shaped by the movements of organisms. All animals, at some point in their life cycle, move; but the mechanisms for these movements can vary in incredible ways. Whether through air, on land, or by water, animal movement behaviors differ in nearly every measurable aspect; e.g., locomotion type, speed, duration, scale, etc. (Hansson and Åkesson 2014). The proximate motivation for each of these movements may vary (e.g., homing, ranging, dispersal, foraging, etc.), they ultimately have fitness consequences. Yet, as simple as each may seem, they require remarkable feats of orientation and navigation, regardless of the distance spanned (Dingle 1996). Foraging trips by desert ants (*Cataglyphis* sp.), spanning no more than several hundred meters, rely on complex path integration (Müller and Wehner 1988), sensory perception of polarized light (Lehrer 1997), and subtle changes in gravitational forces (Wohlgemuth et al. 2001). The Wandering Albatross (*Diomedea exulans*) may travel upwards of 3500 kilometers in search of food (Weimerskirch et al. 2014), both navigating and sensing prey by olfaction (Bonadonna et al. 2005, Nevitt et al. 2008). These are but a few of the

remarkable movements animals undertake, but none may be more impressive than migratory movements.

Unlike other animal movements, migrations are predictable movements between two well-defined habitats where individuals suppress proximate responses to resources that would otherwise be favorable (Dingle 1996, Hansson and Åkesson 2014). Migrations tend to be longer (in duration and distance) than daily movements (e.g., foraging, station keeping, etc.), are more directed, rely on initiation cues (e.g., photoperiod, population density), and require specific patterns of energy allocation within the individual (Dingle 1996, Dingle and Drake 2007). Migration can be seen as a pre-emptive movement from deteriorating local conditions (push) or toward improving conditions (pull), which ultimately have fitness consequences. They can occur on micro- or macroscopic scales, and exhibit an immense amount of taxonomic variability (Alerstam et al. 2003). Of all migratory taxa, birds have received the greatest attention (Newton 2008).

Avian migrations are some of the fastest (Great Snipe, *Gallinago media*; Klaassen et al. 2011) and most enduring (Bar-tailed Gotwit, *Limosa lapponica*; Gill et al. 2009) movements recorded on earth. Arctic Terns (*Sterna paradisaea*) and Sooty Shearwaters (*Puffinus griseus*), champions of long-distance migration, span as much as 60,000 kilometers in a single year (Shaffer et al. 2006, Egevang et al. 2010). Equally as impressive, Bar-headed Geese (*Anser indicus*) make remarkable high elevation flights over the Himalayan Mountains (4-6 kilometers), a feat that requires numerous physiological adaptations (Hawkes et al. 2011). These are but a few cases exemplifying the diversity and scale of avian migratory movements. Migration has served as a model system for animal navigation, optimal migration theory (Alerstam and Hedenström 1998, Alerstam 2011), and indictor of biological responses to phenological shifts driven by global climate change (Butler 2003, Jonzón et al. 2006). These movements leave

ecologists, evolutionary biologists, animal behaviorists, and ornithologists asking new and exciting questions that have fundamental implications in biology.

Recent discoveries in avian migration have been aided by the growth of citizen science communities (Silvertown 2009, Hochachka et al. 2012) and a tremendous radiation in technological advances (Bridge et al. 2011). These advances aid in identifying departure and arrival dates (Deppe et al. 2015), individual migration tracks (Bridge et al. 2011, 2013), and population-level migration trajectories (La Sorte et al. 2013, 2016). Yet while these advances have vastly improved our ability to investigate migratory phenomena, tools for studying real-time nocturnal flights, and in-flight behaviors in particular, have remained rather static (Figure 1.1). Monitoring

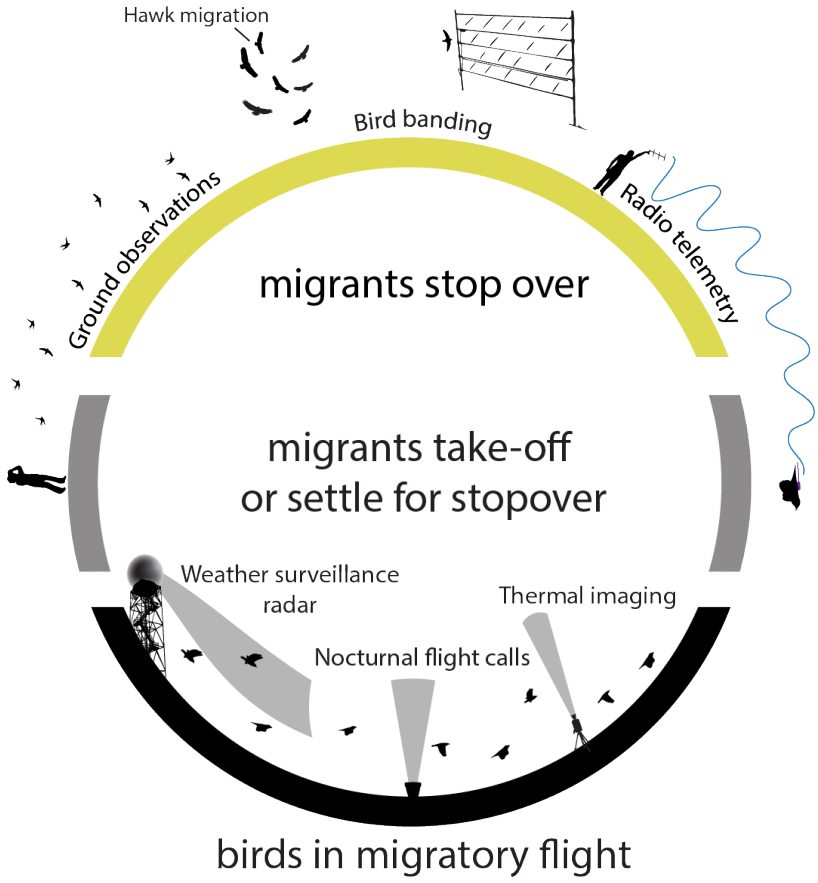

Figure 1.1: Tools commonly employed for the detection, quantification, and description of avian migration.

avian migrants in flight is difficult for innumerable reasons; simply the scale (100s to 1000s of kilometers) at which avian migration occurs imposes logistic limitations, not to mention that migrants typically fly at hundreds, if not thousands of meters above ground level. These factors restrict diurnal monitoring and pose even more serious challenges when migrants fly under the cover of darkness.

Tools for monitoring real-time migratory movements can be assigned to three basic modes of operation: visual, auditory, and radio detection (Kunz et al. 2007). Each of these tools lies on a continuum of sampling frequency, spatial coverage, species or taxonomic certainty, and cost; none of which maximize (or minimize, e.g., cost) all factors (i.e., the perfect tool). Research questions ultimately dictate the tool employed. For example, species-level certainty is limited to just a few techniques: flight calls (Farnsworth 2005) and radio telemetry (Bridge et al. 2011). Flight calls are unique, species-specific vocalizations given during migratory flight (Evans and O'Brien 2002). While our understanding of the meaning of these calls is still in its infancy (Farnsworth 2005), the frequency with which they are detected tend to correlate with aerial density (Larkin et al. 2002, Farnsworth et al. 2004, Horton et al. 2015a). Yet like other visual techniques (thermal-imaging, moon-watching), the use of flight calls as a monitoring tool suffers from a narrow detection range (hundreds of meters) and a laborious data extraction phase (Ross and Allen 2014, Horton et al. 2015b). Alternatively, radio telemetry presents a species-level technique for investigating migratory behaviors. Telemetry can yield long-distance tracks of individuals captured and fitted with small radio tags. In addition to providing the spatial (latitude, longitude) coordinates of individual migrants, parameters such as heart rate, wingbeat frequency, and flight altitude can be acquired (Bowlin et al. 2005, 2015). But because this process of data collection can be immensely time-consuming, it often requires years to amass sample sizes on the order of hundreds, but more frequently, tens of individuals.

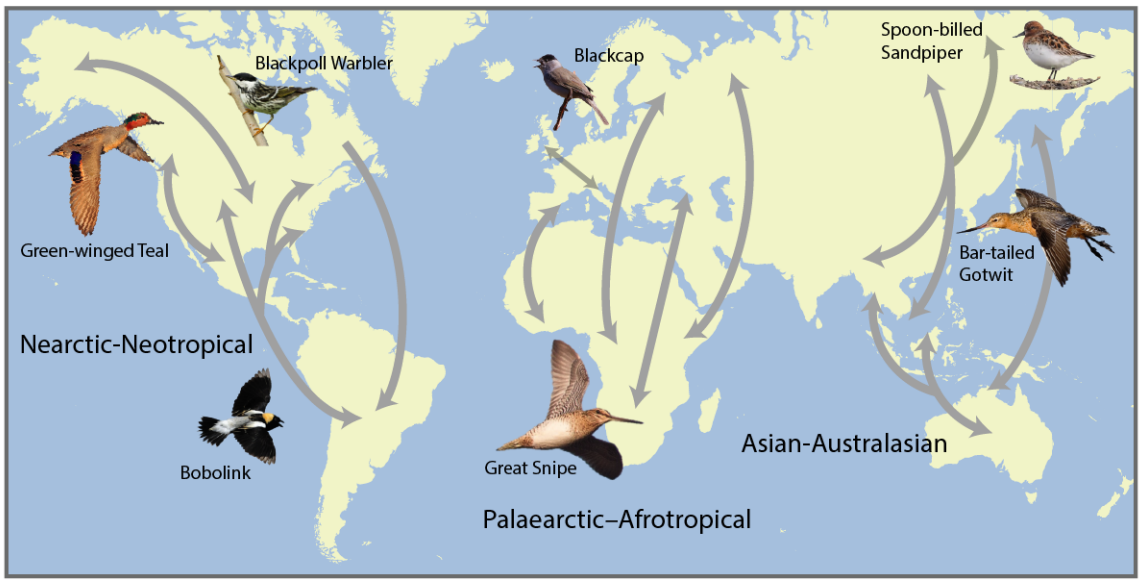

Figure 1.2: Three hemispheric avian migration systems: Nearctic-Neotropic, Palearctic-Afrotropic, and Asian-Australasian. Arrows represent generalized movement patterns.

In contrast to other techniques, radars, specifically weather surveillance radars, offer an invaluable tool for assessing system-level questions at a low cost (freely accessible in the United States), high temporal and spatial resolution, and can detect millions of individuals, albeit of unknown species (Gauthreaux and Belser 1998). Organismal biologists trained to focus on the individual as the fundamental unit of natural selection often struggle with the interpretation of radar data that is decoupled from species identities (Kelly and Horton 2016). However, there is ample evidence that this approach to understanding migration systems is likely to provide key insights into the macroscale dynamics of these hemispheric systems (Gauthreaux et al. 2003, Kelly and Horton 2016, Kelly et al. 2016). Since the 1960s, ecologists have recognized that complex ecosystems are not simply mechanistic combinations of their constituent parts, and do not vary as a direct function of these constituents (individuals; Holling 1973). Often individual-based simulations of behavior result either in analytically intractable models (Strigul et al. 2008) or those models do not capture

complex interactions that drive system behaviors (Odum 1971). Large-scale systems such as the three hemispheric-scale avian migration systems on earth (Figure 1.2) are driven by broadscale seasonal patterns in primary productivity. These processes drive the movements of billions of individuals of thousands of species. Understanding this global system of animal movement and its response to land use and climate change is an imperative for system ecologists and ornithologists alike. However, the prospect of cataloging the individual migration behaviors of members of each species of migrant and then combining them to reveal some emergent understanding of migrations systems seem a long way off and not likely to succeed even if the individual data could be amassed.

It is currently possible to measure the mass flow of all nocturnal migrants and assess their behavioral responses to long- and short-term environmental change in near real time. There are two primary hurdles to this systems approach. One is coping with the data volume and the other is coping with the bias among organismal biologists that these data are meaningless unless they can be tied directly to particular individuals of known species. Here I develop the workflows needed to overcome the data hurdle. I argue that individual-based data from hundreds to thousands of species is neither a practical approach to the questions of interest nor are they particularly well-suited to answering the systems-level questions at the heart of understanding large-scale processes of navigation and optimal migration theory, and how migration systems will respond to global change. I use weather surveillance radar to investigate the in-flight behaviors employed by migratory birds as they transition to and from their wintering and breeding grounds. I explore regional (Chapter 2), seasonal (Chapter 3), altitudinal (Chapter 4), and latitudinal (Chapter 5) dependencies on how migrant's utilize and cope with winds aloft.

Chapter 2

Migrating nocturnal songbirds drift when they can and compensate when they must

2.1 Introduction

How do birds migrate in unfavorable winds? Although migration is a nearly universal behavior of species among animal taxa (Alerstam et al. 2003) and has fascinated scientists for millennia (Evans 1966, Gauthreaux and Able 1970, Alerstam and Petterson 1976, Aristotle and Balme 1991, Alerstam and Hedenström 1998, Thorup et al. 2003, Chapman et al. 2010, 2011), this fundamental question about the behavior of billions of migrating birds remains unresolved. Decades of research have yielded contradictory results on how migrants cope with adverse wind conditions, whether they use common strategies in such situations, and how important these behaviors are to an organism's fitness (Evans 1966, Alerstam and Hedenström 1998, Thorup et al. 2003, Gauthreaux and Able 1970, Sergio et al. 2014, Liechti 2006). Recent studies have demonstrated that migrants can be selective in choosing when to fly as a means of avoiding adverse conditions and maximizing travel speeds (McLaren et al. 2014, Chapman et al. 2015a, 2015b). When in flight, the ability to reach breeding and wintering grounds successfully is predicated on the capacity of migrants to make time-sensitive decisions of how to orient to exploit wind patterns in order to maximize energetic efficiency and minimize lateral drift (Liechti 2006, McLaren et al. 2014).

Birds can avoid drifting off course by preferentially migrating in favorable tailwind conditions (Able 1977, Larkin and Thompson 1980, Erni et al. 2002, Schaub et al. 2004, Alerstam 2011), however costs (both time and energy) may be incurred if tailwinds are infrequent (Wikelski et al. 2003, Thorup et al. 2006, Alerstam 2011). Alternatively, birds can initiate flight under wind regimes with crosswind components at the cost of being drifted away from optimal north-south migration routes. In-flight migrants can use one of two strategies in crosswinds: they can maintain a constant heading towards their destination and allow crosswinds to influence their resultant flight tracks (Figure 2.1a); or they can counter a crosswind by orienting (i.e., heading) in an offset position, a strategy known as compensation (Figure 2.1b). Although compensation minimizes overall flight distance, diminished groundspeeds that result from flying in crosswinds may actually render this a suboptimal strategy (Alerstam 1979). Conversely, fully drifting birds can utilize their full heading vector to maximize groundspeed, at the cost of geographic displacement, which can reduce overall migration speed, increase energetic expenditure, and result in decreased fitness (Alerstam and Hedenström 1998, McLaren et al. 2012, Chapman et al. 2015a, Kranstauber et al. 2015).

Despite potential advantages for detours and variation in migration timing (Hahn et al. 2014, Arlt et al. 2015), encounters with inhospitable terrains (e.g., deserts, large lakes, seas, oceans) may account for a significant source of mortality (Schmaljohann et al. 2007, Diehl et al. 2014, Lok et al. 2015). Furthermore, longer duration flights that result from drift may take migrants further from key stopover habitats and delay arrival on breeding grounds, and both of these errors may be costly at the individual level (Hahn et al. 2014). Over small spatial extents (e.g., observed using tracking radars), birds exhibit within-night shifts in the mean track of nocturnal migration preceding a water crossing (Fortin et al. 1999, Zehnder et al. 2001), suggesting an active shift in migrant motivation. In Western Europe birds

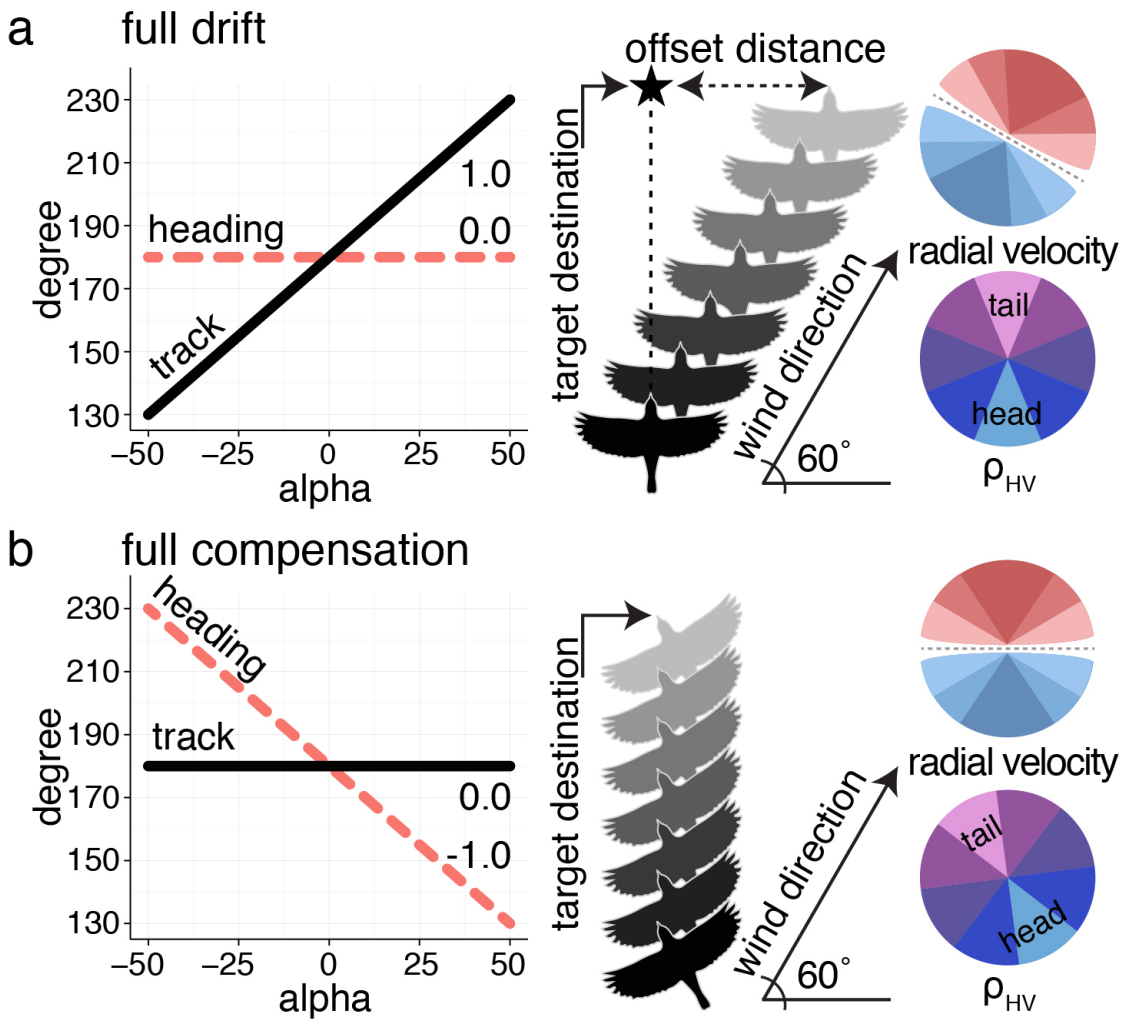

Figure 2.1: Generalized statistical (left), flight (middle), and radar (right) interpretations of (a) full drift and (b) full compensation. Full drift is characterized by a slope of 1 when monitoring track in relation to alpha and 0 when monitoring heading. Drift signifies a change in track with changing wind parameters but no change in migrant heading. For this reason, flight track is directed towards the prevailing wind direction. For simplicity, bird airspeeds are ignored. Track measures represented by radial velocity, blue (negative) indicating approaching targets and red (positive) representing targets receding from the radar. Radar correlation coefficient (ρ_{HV}) differentiates migrant head and tail features to measure heading.

partially compensate for wind drift in unfavorable winds (Alerstam 2011, McLaren et al. 2012). Although similar analyses have not been done at a regional scale, existing results from local scale studies suggest that at the regional scale migrants will increasingly exhibit compensatory behavior when approaching large ecological barriers (Peterson et al. 2014). However, the means to test hypotheses regarding these flight strategies, particularly at coherent regional and full-nightly scales, have not existed until recently.

The upgrade of the United States national weather radar network to dual-polarization is yielding new data to directly observe migrant heading (body axis direction) and track (the resultant direction of bird movements given wind motion) to assess long-standing theoretical predictions of these behaviors (Green and Alerstam 2002, Stepanian and Horton 2015). Here, using recently developed techniques for analysis of Doppler polarimetric weather radar data, we test the prediction that nocturnal migrant songbirds compensate for wind drift and that this compensation will be more extreme near an ocean barrier than over a contiguous continental land mass.

2.2 Methods

2.2.1 Weather surveillance radar data

We examined migrant flight strategies at six weather surveillance radars (WSR-88D): three coastal and three inland sites (Figure 2.2). The radars transmit at a wavelength of 10 cm (S-band), peak power of 750 kW, and sample (i.e., scan) 360° every 5 to 10 minutes depending on the volume coverage pattern (VCP). The VCP specifies the operational elevation angles of the antenna (e.g., 0.5°, 1.5°... 19.5°) and the temporal update time. Radars sampled the airspace at range intervals of 250 m at 0.5° azimuthal intervals (720 radials) from 2-230 km in range. We acquired 2013 and 2014 level-II data products from August 1st to November 15th from the

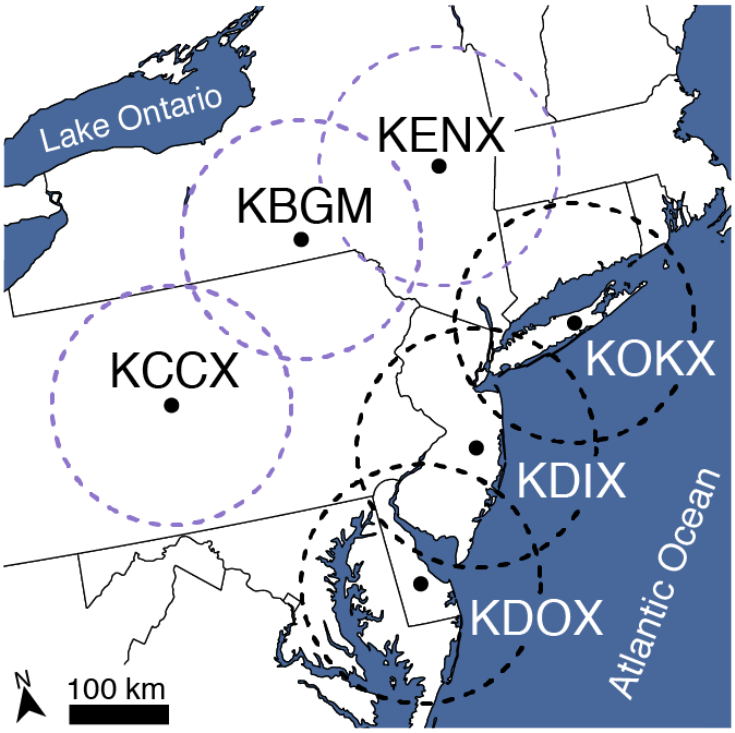

Figure 2.2: Radar locations and biological ranges (125 km) denoted by circles. Purple rings indicate inland classification and black coastal. Autumn data from 2013 and 2014 were assessed from August 6th to October 30th.

National Centers for Environmental Information (NCEI) archive (`http://www.ncdc.noaa.gov/has/has.dsselect`). We visually screened data from all nights to discard scans with weather contamination and anomalous propagation and restricted analyses to samples for the period between evening and morning civil twilight (sun angle 6° below horizon) (Farnsworth et al. 2015). We aggregated all measures (track, heading, migration intensity, and bird abundance) to tenths of the night (hereafter "deciles"). In addition to data quality measures described below, we included only nights containing measures from at least four radars. After screening and data quality protocols

we retained 55 of 214 potential sampling nights from August 6th to October 30th.

2.2.2 Track

We generated velocity azimuth displays (VAD) from ∼0.5° elevation angle radial velocity measures to estimate ground speed and heading direction of flying animals. We followed Sheldon et al. (2013) to dealias velocities when necessary and Browning and Wexler (1968) to estimate ground speed and track direction for each range annulus. Radial velocities required dealiasing when the inbound or outbound speeds of targets exceeded the Nyquist velocity of the radar (Sheldon et al. 2013). We included estimates up to 2 km above ground level (a.g.l.; ∼125 km range), retaining only those estimates with root mean squared error less than 5. We aggregated height profiles of flight track by column averaging. We estimated target airspeed by:

$$\text{airspeed}_y = \text{VADgroundspeed} \times cos(\text{VADdirection}) - \text{windspeed} \times cos(\text{wind direciton}) \tag{2.1}$$

$$\text{airspeed}_x = \text{VADgroundspeed} \times sin(\text{VADdirection}) - \text{windspeed} \times sin(\text{wind direciton}) \tag{2.2}$$

$$\text{target airspeed} = \sqrt{\text{airspeed}_x{}^2 + \text{airspeed}_y{}^2} \tag{2.3}$$

Nightly airspeeds across radar stations averaged 7.8 ms^{-1}, and pooled nightly mean airspeeds were greater than 4.5 ms^{-1}.

2.2.3 Heading

We determined migrant heading using the co-polar cross-correlation coefficient (ρ_{HV}) radar product from the ∼0.5° tilt angle scans following Stepanian and Horton (2015) (Figure 2.1). We fit models to three sequential range gates (250 m intervals from the radar – 750 m in total) across all azimuths to ensure sufficient data for

extraction. We eliminated individual volumes, the smallest sampling unit for WSR-88Ds, with non-biological characteristics (i.e., -33 dBZ) and estimated heading only for ranges with more than 300 azimuthal samples. We visually inspected all heading extractions below 2 km a.g.l. to ensure that automation captured well-defined symmetry axes. We included extractions that explained greater than 15% of the variance (Stepanian and Horton 2015) (i.e., R^2 greater than 0.15) and standard deviation in heading angle less than 20°. As a result, these criteria typically removed scans with light migratory movements, movements in which birds may have oriented in many different directions (i.e., low directional alignment), and those in close proximity to weather systems.

2.2.4 Relative migration intensity and abundance

To assess relative nightly migration intensity we calculated average reflectivity factor (dBZ) from the ∼0.5° tilt angle from 5-150 km from each radar. To reduce underestimates of migration intensity, we omitted all clear-air echo returns (-33 dBZ) in our averaging process. We weighted all statistical analyses by migration intensity.

To estimate migration abundance, we derived the number of birds for each ∼0.5° tilt angle sweep from 20 to 125 km following Chilson et al. (2012). To mitigate clutter contamination we used more distant starting range gates and omitted volumes with greater than 35 dBZ. Reflectivity factor (dBZ) was converted to dBη following:

$$\eta[\text{dB}] = \text{Z}[\text{dBZ}] + \beta, \tag{2.4}$$

where

$$\beta = 10log_{10}\left(\frac{10^3\pi^5|Km|^2}{\lambda^4}\right). \tag{2.5}$$

We used an average WSR-88D wavelength (λ) of 10.7 cm and $|\text{Km}|^2$ for liquid water of 0.93, the dielectric constant. This yielded $\beta = 13.37$. We chose a cross section (σ) of 17.5 cm^2, representative of landbirds (Larkin 1991), to convert η to

birds/km^3. To extract the number of birds per sweep we calculated the volume of each range gate as follows:

$$V_{rad} = \frac{0.35\sqrt{2\pi}}{2ln2}\left(\frac{\pi {r_o}^2 \theta_1 \phi_1 \Delta r}{4}\right), \tag{2.6}$$

where r_o^2 is the mid-range of the range gate, Δr equals the range gate spacing (250 m), and θ_1 and ϕ_1 the half power beam width (0.96°). We aggregated measures of bird abundance to nightly averages.

2.2.5 Quantifying wind speed and direction

We gathered nightly pressure level gridded North American Regional Reanalysis (NARR, `http://wwwt.emc.ncep.noaa.gov/mmb/rreanl/index.html`) pressure and monolevel data to estimate winds aloft within the radar coverage areas (Mesinger et al. 2006). Wind speed and direction are mapped at a 32 km spatial resolution, and update every three hours. We used pressure level measures to calculate speed and direction of winds aloft from u (zonal velocity; east-west) and v (meridional velocity; north-south) measures from 2 isobaric levels: 900 and 950 hPa. We used monolevel surface geopotential height data to determine site-specific ground-level pressure levels. We linked all radar measures with the closest temporal wind measurements. Because coastal and inland sites differed in height above sea level (mean height above sea level ±SD; inland: 593.0 ±125.8 m; coastal: 28.3 ±15.3 m), we used 950 hPa winds (mean height ±95%CI, 573.14 ±2.34 m a.g.l.) for coastal sites and 900 hPa for inland sites (mean height ±95%CI, 630.77 ±3.57 m a.g.l.). For analyses of wind scenarios east and west of the PDM, only winds with speeds greater than 5 ms^{-1} were included because they yielded consistent (low standard deviation) wind directions within the

sampling region.

2.2.6 Statistics

We conducted statistical analyses in R, version 3.0.2 (R Core Team 2017), with GAMM implemented using the mgcv package (Wood 2015) and linear mixed models implemented using the lme4 package (Bates et al. 2014).

2.2.7 Generalized additive mixed model (GAMM)

To examine the temporal variation of migrant heading and track, we used a generalized additive mixed model. Because migrant behavior tends to covary with winds aloft, we used a non-parametric spline fit for wind direction, and decile as a fixed effect. We used a single random effect of the interaction of year, radar station, and ordinal date.

2.2.8 Linear mixed models (LMM)

Alpha, the difference between a bird's track and its heading, provides information about the extent to which birds compensate for wind drift (Green and Alerstam 2002). This relationship defines migrants' preferred direction of movement (PDM) (Chapman et al. 2011, Kemp et al. 2012 p. 2012), and measures migrant flight strategy via the slope of alpha (0 = complete compensation, 1 = complete drift; Fig. 1a-b). Intermediate values represent a mixture of these behaviors (i.e., partial compensation for drift). Our two fixed effects addressed the temporal and site-specific features of drift propensity: 1) region (coastal or inland) and 2) the interaction of alpha, region, and decile. We used multiple levels of random effects to account for non-independence among samples. We included three random slope and intercept terms: 1) interaction of year, radar station, and ordinal date, 2) interaction between

year and radar station, and 3) ordinal date. In addition to accounting for pseudoreplication from temporally correlated samples, this random effect structure statistically incorporated variation in drift propensity and PDM over time and space, leaving the fixed effects to describe the average patterns in which we were interested. We used 2000 bootstrapped replicates to estimate 95% confidence intervals.

We implemented a similar mixed model approach to test for mean differences in heading and track across coastal and inland regions, modeling heading or track as a function of region. We included random intercepts following the same structure as above with the addition of decile as a random effect. To calculate means of migrant heading and track, we used mixed models, accounting for non-independence of samples by designating random effects of decile and sampling period for each station.

2.3 Results and Discussion

We examined strategies of nocturnally migrating birds using Doppler polarimetric radars at three coastal and three inland sites in the eastern United States during autumn of 2013 and 2014 (Figure 2.2). Each radar site provides independent scans of migrants' headings and tracks for areas nearing 49,000 km^2. Radars collected data every five to ten minutes, yielding approximately 1.6 million samples from 55 nights (Table 2.1).

The typical direction of headings and tracks of birds was toward the southwest (Figure 2.3). Tracks were more southerly than birds' headings, indicating that on average birds were being drifted by crosswinds. The difference between heading and track was 33.66° at inland sites and 42.32° near the coast; the smaller difference at inland sites indicates a greater propensity of birds to drift sideways (Figure 2.3). We found that birds flying near the Atlantic coast increasingly oriented and tracked westward, away from the coast, with each subsequent decile of the night (direction of heading 2.24° per decile more westward, and direction of travel 2.37° per decile;

Figure 2.3). In contrast, birds flying over inland sites showed near-zero changes in both the heading and direction they flew with each subsequent decile of the night (direction of heading -0.03° per decile, and direction of travel 0.06° per decile; Figure 2.3)

Migrants at inland sites displayed moderate to high propensity to drift (0.63-0.77, Figure 2.4), whereas migrants at coastal sites showed both an overall lower propensity to drift (0.29-0.65, Figure 2.4) and a change in the magnitude of drift through the night. At coastal sites, the propensity to drift decreased through the night, and behaviors diverged markedly after the middle of the night (i.e., decile 5, Figure 2.4). Migrant PDM showed little variability across the night at inland sites (mean ±95% CI, 206.41 ±8.27 to 212.02 ±5.56°) in comparison to a 2.32° per decile increase in PDM at coastal sites (mean ±95% CI, 209.22 ±6.32° to 232.68 ±8.11°).

Typical nocturnal winds blew to the southeast, and southwest-bound birds consistently oriented across these winds to the west and partially compensated for coastward wind drift. In conditions of prevailing crosswinds, a partial compensation strategy may maximize migration speeds of migrants: by allowing a certain amount of drift, birds can increase ground speeds to expend less energy per unit distance (Alerstam and Hedenström 1998, McLaren et al. 2012). When winds were east of the PDM, migrant heading and track differed significantly (paired test of means, coastal and inland: $p < 0.0001$; Figure 2.5a-b), whereas differences were not evident when winds were west of the PDM (paired test of means, coastal: $p = 0.14$, inland: $p = 0.69$; Figure 2.5c-d).

The prediction that migrants compensate for drift more drastically when encountering a migration barrier is consistent with these results. Birds over inland sites without ecological barriers compensated on average for only 29.0% of the effect of wind, whereas birds near coastal sites compensated for drift to an increasingly greater extent over the course of the night, reaching the highest level of wind drift

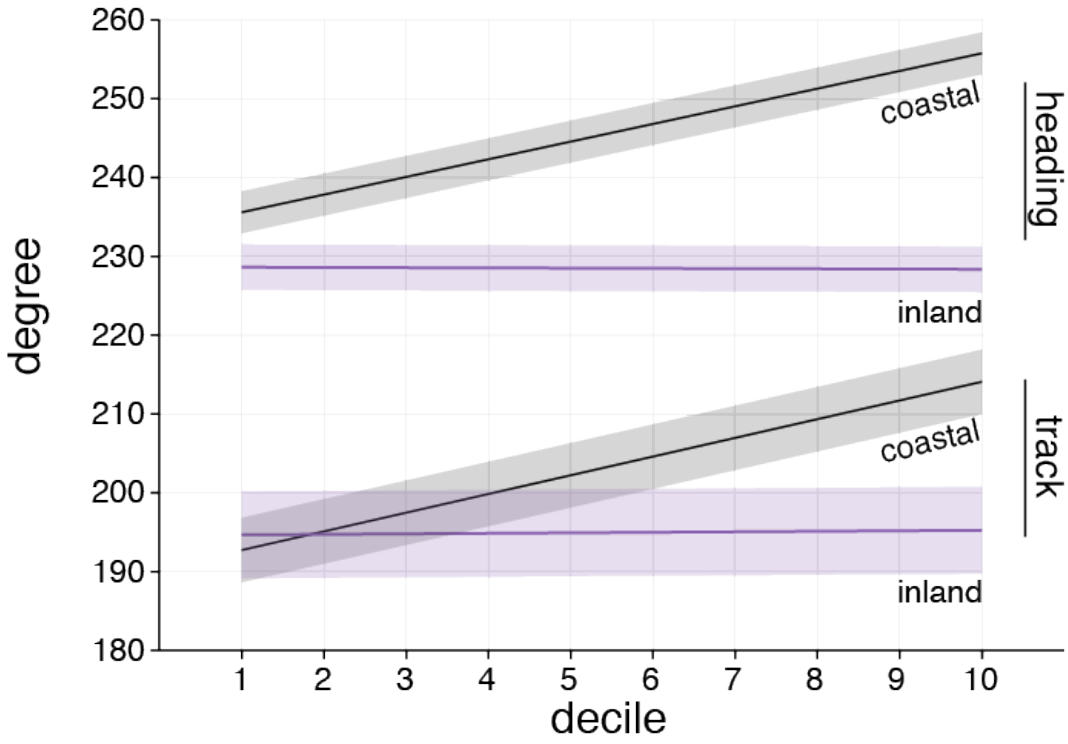

Figure 2.3: Modeled mean heading and track directions as inferred by GAMM to account for fixed and random spatiotemporal effects. Birds followed mean tracks between 203.56-204.91° at coastal sites and 190.07-203.64° at inland sites (Table 2.2). Birds' headings were further west than they traveled, between 241.60-252.06° for coastal sites and 226.26-229.71° for inland sites (Table 2.2). We found differences in means of coastal and inland track directions (LMM: $p < 0.05$) as well as heading directions (LMM: $p < 0.001$). Linear change in migrant heading and track for coastal and inland regions revealed significant temporal shifts in coastal track (GAMM: $p < 0.001$) and heading (GAMM: $p < 0.001$). Inland sites showed non-significant, near-zero changes in track (GAMM: $p = 0.763$) and heading (GAMM: $p = 0.804$). Wind heading was a significant non-parametric factor for all cases (GAMM: $p < 0.01$).

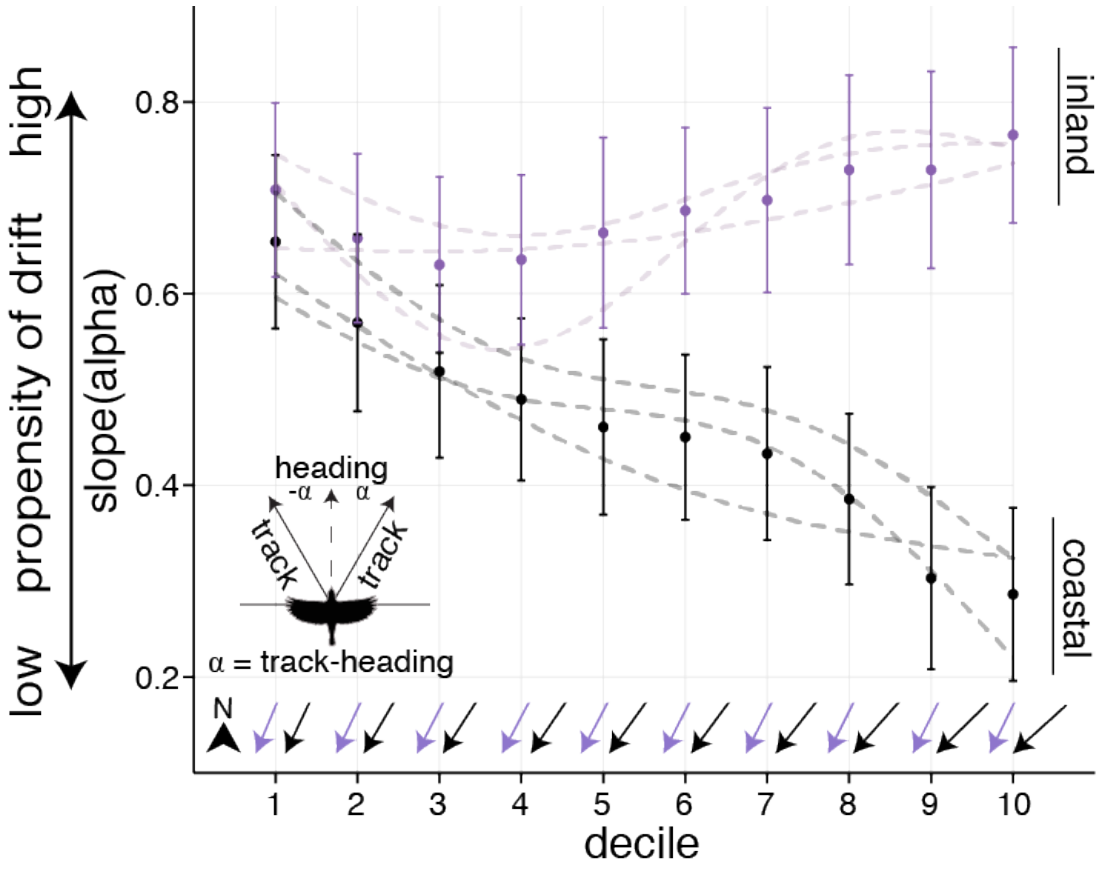

Figure 2.4: Mixed-effect model output depicting migrant behavior through the night for coastal and inland regions. Higher values of the slope of alpha indicate a stronger propensity for a drift behavior (0 = full compensation; 1 = full drift). Transparent lines represent site-specific behaviors and error bars 95% confidence intervals. Arrows represent preferred direction of movement. Individual radar coefficients interpolated using a generalized additive model.

compensation (76.5%) at KDOX during decile 10. Aversion to a water crossing close to sunrise and into the daylight hours may be a product of dwindling fat stores through the night and atmospheric changes after sunrise that make migration less efficient for most birds (Alerstam 1979, Richardson 1991). Previous research with orientation cages, individual releases, and radio tracking has established that birds with substantive fat stores are likely to orient in directions that would bring them

over a barrier, whereas those lacking sufficient fat usually do not (Sandberg 1994, Bäckman et al. 1997, Sandberg et al. 2002, Deutschlander and Muheim 2009, Deppe et al. 2015). Over smaller spatial extents, within-night shifts in the mean track of nocturnal migration precede a water crossing (Fortin et al. 1999, Zehnder et al. 2001) and active inland reorientation occurs near coasts (Able 1975, Richardson 1982, Bruderer and Liechti 1998). However, no studies have captured the large-scale phenomena we documented using weather radars. Analyses at this scale are based on detection of upwards of 5 million migrating birds (mean ±95% CI 1,034,440 ±42,668; Table 2.3-2.4), thus representing the behavioral response of a significant fraction of the migrant bird assemblage.

Whether birds migrate when winds are unfavorable and to what degree they compensate for resulting drift have been long-standing questions in migration biology (Evans 1966, Gauthreaux and Able 1970, Alerstam and Hedenström 1998, Thorup et al. 2003, Chapman et al. 2011, 2015a). We show for the first time at a regional scale, in a regularly and heavily traveled airspace of the Nearctic-Neotropic migration system, that birds routinely migrate under crosswind wind conditions and compensate in a context specific manner. This result is consistent with migrants knowing their location relative to migration barriers while in flight and actively assessing the degree to which they need to compensate for wind. While we cannot exclude completely other more complex explanations, such complexity requires systematic and differential turnover of migrants employing different behavioral strategies between regions and within nights – an unlikely scenario for which there is no observational evidence. Consequently, it seems more plausible that birds are changing their in-flight behaviors based on a spatiotemporal context. These changes in behavior may be facilitated by visual cues (e.g., rivers and coasts) (Bingman et al. 1982, Cochran and Kjos 1985), compass direction (Able and Able 1997, Deutschlander and Muheim 2010), and likely the interaction of multiple sensory systems. Regardless of the biological cues used

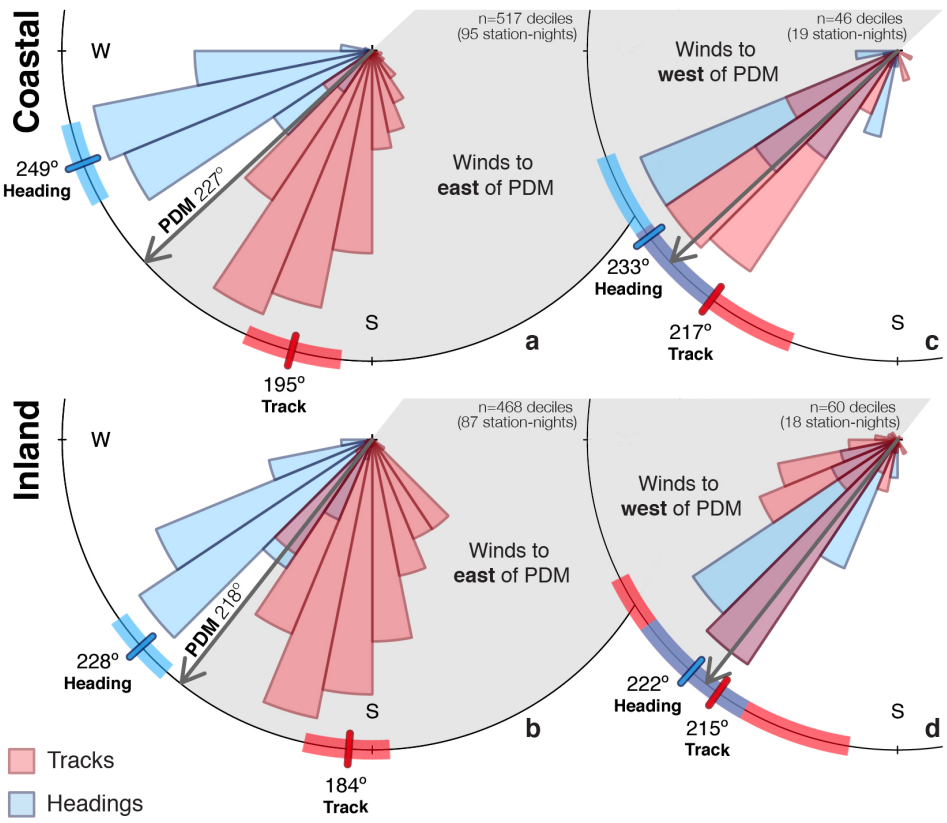

Figure 2.5: Migrating birds' tracks and headings for winds east (a-b) and west (c-d) of the preferred direction of movement (PDM). The area of each sector is proportional to the frequency of directions in that sector, weighted by migration intensity (dBZ). Mean directions plotted as tick marks on the circle border, 95% confidence intervals shown as transparent rectangles behind tick marks. Mean heading and track directions were calculated from decile samples.

for active assessments, our results strongly suggest that migrants choose to drift, not compensate, under a wide range of winds when they face no impending inhospitable barrier.

New independent measures of migrant heading provided by polarimetric data significantly improve our ability to quantify migrant behavior at regional to continental spatial extents. Increasing automation of radar analysis will further enable

exploration and quantification of the full complement of United States weather radar data to achieve real-time monitoring of the phenology, distribution, abundance, and behaviors of billions of birds during their biannual migrations. Although greatly underused, the U.S. weather surveillance radar network provides the largest sensor array worldwide for the monitoring of nocturnally migrating animals (i.e., birds as well as bats and insects). These analyses fill knowledge gaps in our understanding of migratory behaviors at large scales while fulfilling a primary requirement to shed light on past, present, and future behavioral strategies of aerial taxa.

Table 2.1: Sample sizes of radar measures of heading and track. Samples sizes collected for heading and track measures. Measures are collected every 250 m in range from the radar. All preserved measures met screening criteria described in methods.

Inland	2013	2014	Total
Radar	n	n	n
KBGM; Binghamton, NY	167,121	184,030	351,151
KENX; Albany, NY	82,444	115,203	197,647
KCCX; State College, PA	144,738	97,269	242,007
Coastal	2013	2014	Total
Radar	n	n	n
KDIX; Mt. Holly, NJ	152,909	149,308	302,217
KDOX; Dover, DE	143,844	137,493	281,337
KOKX; New York, NY	103,270	120,421	223,691
Total	794,326	803,724	1,598,050

Table 2.2: Mean fall heading and track directions. Heading and track directions for inland and coastal radar sites weighted by migration intensity (dBZ). Bootstrapped 95% confidence intervals in parentheses.

Inland	Mean Heading (degree) (95% CI)	Mean Track (degree) (95% CI)
KBGM; Binghamton, NY	229.71° (224.85, 234.60)	190.07° (182.29, 198.45)
KENX; Albany, NY	226.26° (219.63, 232.46)	192.25° (183.49, 200.84)
KCCX; State College, PA	227.60° (221.63, 233.73)	203.64° (195.38, 212.92)
Coastal	Mean Heading (degree) (95% CI)	Mean Track (degree) (95% CI)
KDIX; Mt. Holly, NJ	244.53° (238.96, 250.41)	204.91° (196.47, 213.98)
KDOX; Dover, DE	241.60° (234.64, 248.63)	203.59° (195.85, 210.84)
KOKX; New York, NY	252.06° (244.55, 260.02)	203.56° (195.01, 212.27)

Table 2.3: Inland migrant abundance within sampling regions. Mean and range of migrant birds within the sampling region of each radar site (20-125 km). Means and ranges based on nightly averages. Number of birds calculated using a cross-section of 17.5 cm^2, representative of landbirds (Larkin 1991). 95% confidence intervals in parentheses.

Inland	2013			2014		
Radar	Mean birds (±95% CI)	Range of birds	Sampling nights	Mean birds (±95% CI)	Range of birds	Sampling nights
KBGM; Binghamton, NY	601,784 (±146,773)	54,553 to 5,245,856	22	447,842 (±64,057)	55,312 to 2,291,963	28
KENX; Albany, NY	872,263 (±159,171)	169,560 to 5,467,045	18	614,674 (±86,336)	36,042 to 2,630,611	23
KCCX; State College, PA	716,796 (±134,147)	69,071 to 5,491,108	10	348,084 (±56,628)	42,810 to 1,736,133	22

Table 2.4: Coastal migrant abundance within sampling regions. Mean and range of migrant birds within the sampling region of each radar site (20-125 km). Means and ranges based on nightly averages. Number of birds calculated using a cross-section of 17.5 cm^2, representative of landbirds (Larkin 1991). 95% confidence intervals in parentheses.

Coastal	2013			2014		
Radar	Mean birds (±95% CI)	Range of birds	Sampling nights	Mean birds (±95% CI)	Range of birds	Sampling nights
KDIX; Mt. Holly, NJ	1,606,117 (±169,060)	225,224 to 5,209,128	23	1,011,452 (±188,222)	50,270 to 5,477,626	30
KDOX; Dover, DE	528,723 (±82,920)	87,230 to 2,924,113	20	500,336 (±121,354)	61,712 to 3,669,654	29
KOKX; New York, NY	920,513 (±117,751)	240,696 to 3,898,720	22	937,613 (±188,392)	24,266 to 5,238,237	28

Chapter 3

Seasonal differences in landbird migration strategies

3.1 Introduction

The capacity of avian migrants to make time- and place-sensitive decisions in response to seasonal conditions underlies their abilities to successfully reach breeding and wintering grounds (Alerstam 1979, Alerstam and Hedenström 1998). Western hemisphere migratory journeys may span several thousand kilometers, from wintering grounds in Central and South America and southern portions of the United States to northern breeding grounds in the United States and Canada (Newton 2008). Spring migratory movements are generally completed more quickly than fall movements (Newton 2008, Nilsson et al. 2013, La Sorte et al. 2013, 2016). The need for haste in spring is well documented (Newton 2008, Nilsson et al. 2013, La Sorte et al. 2013): birds arriving late to breeding grounds often suffer reduced fitness (Kokko 1999). However, mechanisms facilitating this increased pace of movement – and how global climate change will influence migration speeds – are less well understood.

Timing differences can stem from variation in stopover behavior and flight strategy. Seasonal differences in stopover behavior have been reported (Morris et al. 1994), but in-flight behaviors remain poorly known, particularly at relevant temporal and spatial extents. Existing natural variation in migration speeds (Bäckman and

Alerstam 2003, Nilsson et al. 2013) provides an opportunity to test predictions about the role of in-flight behaviors in determining overall migration speed, defined as the time required to transit between wintering and breeding grounds. Our understanding of the mechanisms that operate en route at the migration assemblage level, such as how migrants actively manage their flight altitude, speed, and orientation, are imperative for forecasting future implications for migratory birds, particularly with mounting evidence that climate change alters migration phenology (Butler 2003, Jonzén et al. 2006).

Prevailing wind conditions and birds' flight strategies, in combination, exert the greatest influence on migration speeds (Kemp et al. 2010, Nilsson et al. 2014), but few studies have examined these factors in North America at an assemblage level (La Sorte et al. 2014). We hypothesize that migrants select flight strategies in spring that facilitate faster migration with increased airspeeds and greater compensation for wind drift (B*ä*ckman and Alerstam 2003, Nilsson et al. 2013). To study these behaviors at large spatial scales, we use recent advances in radar remote sensing (Stepanian and Horton 2015) to measure the aggregated behaviors of millions of individual birds during spring and fall along the east coast of the United States. We examine these patterns at both coastal and inland sites because recent work has shown that in-flight behaviors differ substantially across these regional landscapes (Horton et al. 2016c).

3.2 Methods

3.2.1 Weather surveillance radar data

We used level-II weather surveillance radar (hereafter WSR-88D) products from six coastal radars from 2013-15 (Figure 3.1, Figure 3.2). WSR-88Ds sample the airspace every 5 to 10 minutes, sequentially scanning at 0.5 or 1.0° azimuthal intervals and collecting data every 250 m in range from the radar. These radars transmit at 10 cm wavelength, peak power of 750 kW, and possess a typical biological range of

∼80-125 km (Crum and Alberty 1993, Gauthreaux and Belser 1998). The National Weather Service (NWS) within the National Oceanic and Atmospheric Administration (NOAA) operates five of these radars (KBGM, KCCX, KDIX, KENX, KOKX) and the Department of Defense (DOD) operates one (KDOX). For low elevation scans (<1.5°), DOD radars sample the airspace at 1.0° azimuthal intervals, rather than the 0.5° intervals that are typical of NOAA operated radars. We downloaded data from these radars from NOAA's National Centers for Environmental Information (NCEI; `http://www.ncdc.noaa.gov/has/has.dsselect`) from March 1st to June 15th for spring seasons and August 1st to November 15th for fall seasons. We retained data between evening and morning civil twilight (sun angle 6° below the horizon), discarding the remaining diurnal data as well as any sweeps containing weather (i.e., contamination from precipitation that obscured bird movements). We summarized radar measures to tenths of the night (i.e., deciles) to control for changes in the duration of nights within and between seasons.

To determine the intensity of migratory movements with respect to height above ground level, we used the lowest five elevation scans from 5-20 km to generate vertical profiles of reflectivity at 10 m intervals following Buler and Diehl (2009). For reflectivity averaging we omitted measures with a value of -33 dBZ and values over 35dBZ to limit clutter contamination. Measures of -33 dBZ represent the minimum detection threshold for WSR-88Ds and are interpreted as having no biological scatters (also, termed clear-air). Using the lowest elevation sweeps (∼0.5°), we used velocity azimuth display (VAD) techniques on radial velocity fields to determine migrant track, the direction of bird movements over the ground (Figure 3.1b; Browning and Wexler 1968, Green and Alerstam 2002). When necessary, we dealiased measures of radial velocity (Sheldon et al. 2013). We eliminated VADs with poor fits (RMSE>5), and to limit insect contamination we excluded VADs with RMSE less than one (Dokter et al. 2011). This filtering eliminated 284,429 10-m height bins (11.9%) during spring

and 172,100 (5.6%) during fall. The resultant mean RMSE for sites varied from 3.21 and 3.67.

Because radar-derived velocities are an average of behaviors of individuals within a pulse volume, conflicting or diverse migratory strategies within a volume could theoretically be masked, and average airspeed estimates could be biased low. At times when flight speeds and trajectories within a sampling volume are diverse, we expect the spread, or width, of the Doppler spectrum to be large. Spectrum width is a measure of velocity dispersion (Figure 3.1c) that is archived at level-II (Crum and Alberty 1993, Crum et al. 1993), but it is used infrequently in biological applications (Diehl and Larkin 2005). To examine the diversity of radial velocities within pulse volumes for evidence that any observed velocity differences could be due to averaging of multiple behaviors, we examined average spectrum width from 20-125km for each sweep. We omitted clear-air measures (i.e., cases with no migration) from these averages.

To determine migrant heading, the direction of the body axis, we used polarimetric azimuth displays (Figure 3.1d) (Stepanian and Horton 2015). In-flight migrants have an anatomical axis of symmetry coincident with their body orientation, and they show strong azimuthal patterns in polarimetric fields (Zrnić and Ryzhkov 1998, Stepanian and Horton 2015). From these data, we defined the axis of symmetry, based on correlation coefficient (ρ_{HV}, Figure 3.1d) (Stepanian and Horton 2015). This axis is the azimuth of orientation of migrants, which is independent of radial velocity and wind measurements.

All measures of migrant track, heading, and groundspeed were projected at 10m height intervals up to 2km above ground level. For purposes of averaging we weighted all measures following the distribution of the vertical profile of reflectivity

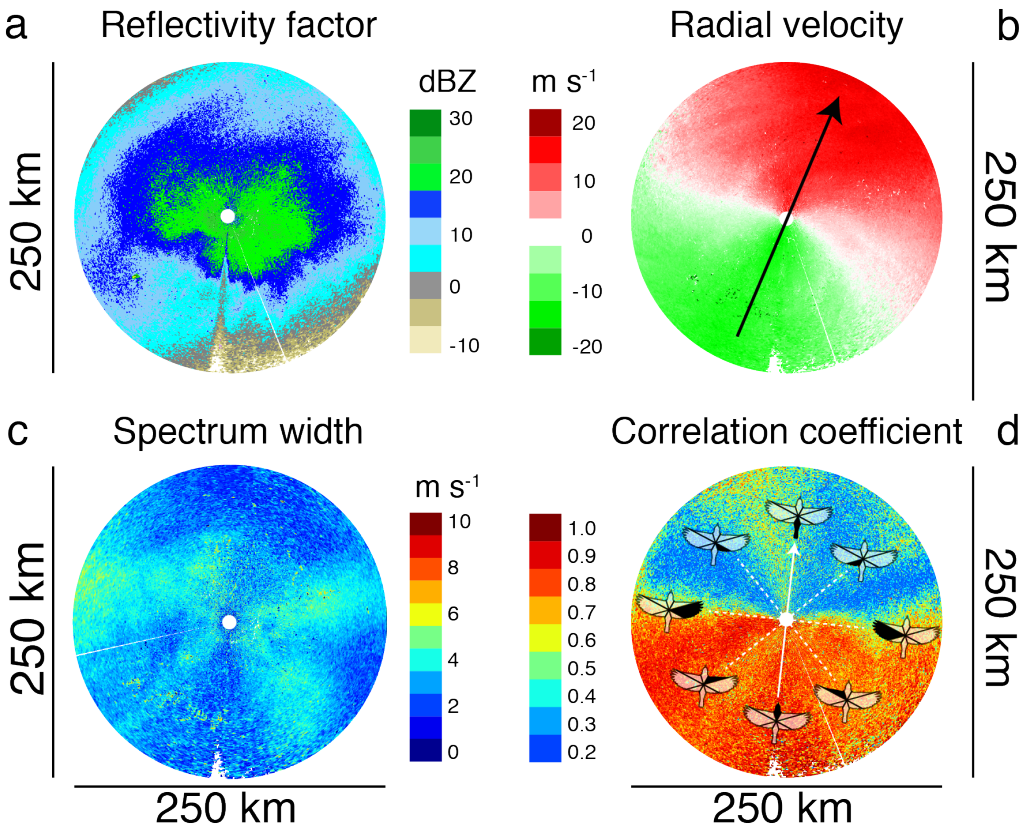

Figure 3.1: Radar measures of (a) reflectivity, (b) radial velocity, (c) spectrum width, and (d) co-polar correlation coefficient from KBGM (Binghamton, NY, USA) for May 4th, 2015 05:33 UTC (∼4 hours after local sunset). Radar measures displayed as plan position indicators (PPI) from the lowest elevation sweeps (∼0.5°). (a) Reflectivity factor represents general migrant abundance on a logarithmic scale (dBZ). (b) Radial velocity measures migrant groundspeeds approaching (green) and receding (red) from the radar (ms^{-1}), and is used to determine mean track direction (black arrow). (c) Spectrum width measures pulse volume variation in radial velocity (ms^{-1}). (d) Co-polar correlation coefficient is used to measure migrant heading.

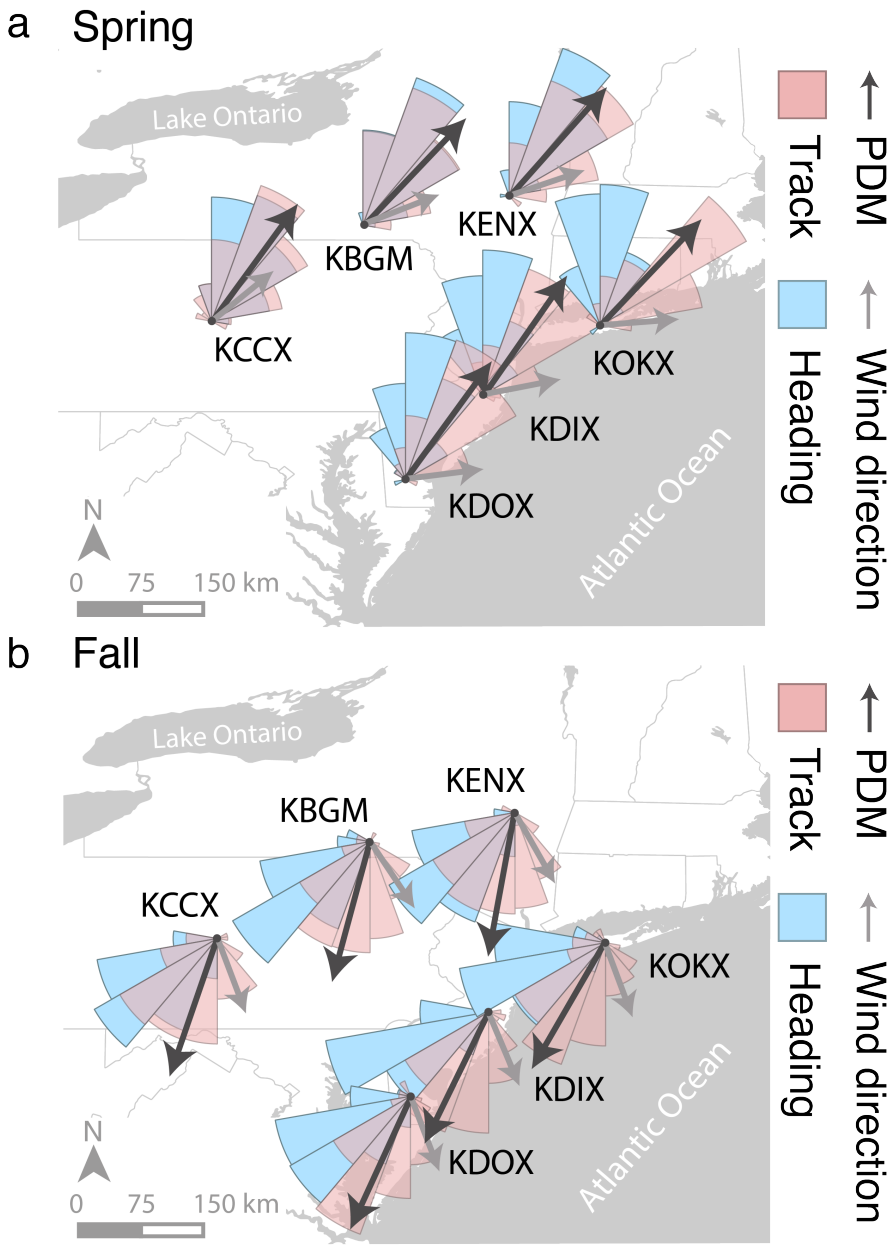

Figure 3.2: Rose diagrams depict distributions of migrant track (red) and heading (blue) for (a) spring and (b) fall migratory seasons. Black arrows denote preferred direction of movement (PDM) and grey arrows mean nightly wind direction. Track and heading distributions were weighted by scaled reflectivity factor, and wind direction by the product of reflectivity factor and wind speed. See Table 3.1-3.2 for site-specific summaries of track, heading, wind direction, and PDM.

(dBZ).

3.2.2 Winds aloft

In addition to determining the mean track direction of migrants aloft, VADs also reveal migrant groundspeed (i.e., speed relative to the ground). Groundspeed includes contributions from migrants via powered flight (airspeed) and wind speed and direction. Given estimates of groundspeed, wind direction, and wind speed, we calculated migrant airspeeds through vector subtraction. We used North American Regional Reanalysis (NARR) data to determine wind direction and speed aloft, with a spatial resolution of ∼32km and temporal resolution of every three hours (Mesinger et al. 2006). For each 10m measure of groundspeed, we linked the closest spatial and temporal measures of wind speed and direction. As an additional step to limit insect contamination, we eliminated height intervals (10m samples) with airspeeds less than 5 ms^{-1} (Larkin 1991, Gauthreaux and Belser 1998). This filtering eliminated 118,892 10-m height bins (5.0%) during spring and 335,997 (10.9%) during fall. When summarizing wind vectors we weighted directions by migration intensity (reflectivity) and wind speed (ms^{-1}). To follow the conventions of track and heading directions, we summarized winds to represent the direction toward which winds were moving (Green and Alerstam 2002). In summary, we apply two independent techniques for ameliorating insect contamination in our radar data, filtering by RMSE (Dokter et al. 2011) and airspeeds (Diehl et al. 2003, Buler and Dawson 2014, Van Doren et al. 2014, Horton et al. 2015a, Farnsworth et al. 2016), and investigate the seasonal variability in radial velocities using spectrum width. In contrast, most recent radar ornithology studies have applied only one of these methods. Therefore, our dataset is likely to contain less insect contamination than most, if not all, existing studies that

have used weather surveillance radar.

3.2.3 Statistics

To determine flight behaviors (i.e., wind drift or compensation), we used a mixed model approach, regressing track on the difference between track and heading (α) (Green and Alerstam 2002). This approach yields two important metrics describing migrant flight strategy: 1) slope of α, a measure of drift propensity (0 – complete wind drift compensation, 1– complete wind drift); and 2) y-intercept, a measure of preferred direction of movement (PDM) (Chapman et al. 2011, Kemp et al. 2012). To limit pseudoreplication from repeated measure decile samples, we used a series of random effects, including radar site, year, and ordinal date as random intercepts and α as a random slope (Horton et al. 2016c, Van Doren et al. 2016). For temporal examinations decile was included as a fixed effect.

We used a linear mixed model (LMM) to test for seasonal and site differences in groundspeeds, airspeeds, and spectrum width, and to calculate radar-specific means of migrant track, heading, groundspeed, and airspeed. We weighted all analyses by scaled radar reflectivity factor (dBZ). We conducted statistical analyses in R, version 3.0.2 (R Core Team 2014), and linear mixed models were implemented using the lme4 and lmerTest packages (Kuznetsova et al. 2014, Bates et al. 2014). We determined the marginal variance explained by fixed effects using the piecewiseSEM package in R (Lefcheck 2015).

3.3 Results

Using weather surveillance radars measures (Figure 3.1a-d) we sampled a total of 67 spring nights (1,756 deciles) and 78 fall nights (2,129 deciles) (Table 3.1).

3.3.1 Flight speeds

Migrant groundspeeds were significantly faster during spring (LMM; $p < 0.001$), averaging 4.1 $\pm$0.5 ms^{-1} (mean $\pm$95% CI) faster across coastal and inland regions (Figure 3.3a). Within each season, migrants at inland sites tended toward faster groundspeeds, significantly so only during spring (spring 1.1 $\pm$1.0 ms^{-1}, $p < 0.05$; fall 0.49 $\pm$0.51 ms^{-1}, $p = 0.10$). Groundspeeds changed through the night during spring (LMM; coastal: -0.05 $\pm$0.06 ms^{-1}, $p = 0.121$; inland: 0.32 $\pm$0.04 ms^{-1}, $p < 0.001$) and significantly decreased during fall (LMM; coastal: -0.12 $\pm$0.04 ms^{-1}, $p < 0.001$; inland: -0.12$\pm$0.04 ms^{-1}, $p < 0.001$). We did not find seasonal nor site differences in spectrum width (LMM; $p = 0.471$ and $p = 0.488$ respectively, Figure 3.3b).

Airspeeds of free-flying migrants, groundspeeds minus the influence of winds aloft, also showed strong seasonal differences, with spring migrants averaging 2.3 $\pm$0.4 ms^{-1} faster than fall (LMM; $p < 0.001$, Figure 3.3c). During spring, airspeeds between inland and coastal regions did not differ (LMM; $p < 0.678$), whereas in fall, migrants at inland sites averaged 0.9 $\pm$0.3 ms^{-1} faster (LMM; $p < 0.001$). Airspeeds changed through the night, although generally weakly, during spring (LMM; coastal: 0.06 $\pm$0.06 ms^{-1}, $p < 0.05$; inland: 0.13 $\pm$0.06 ms^{-1}, $p < 0.001$) and fall (LMM; coastal: 0.09 $\pm$0.03 ms^{-1}, $p < 0.001$; inland: -0.01 $\pm$0.03 ms^{-1}, $p = 0.525$).

Although ground- and airspeeds exhibited temporal differences, the marginal variance explained by decile period of the night was less than 3.6%, in comparison to

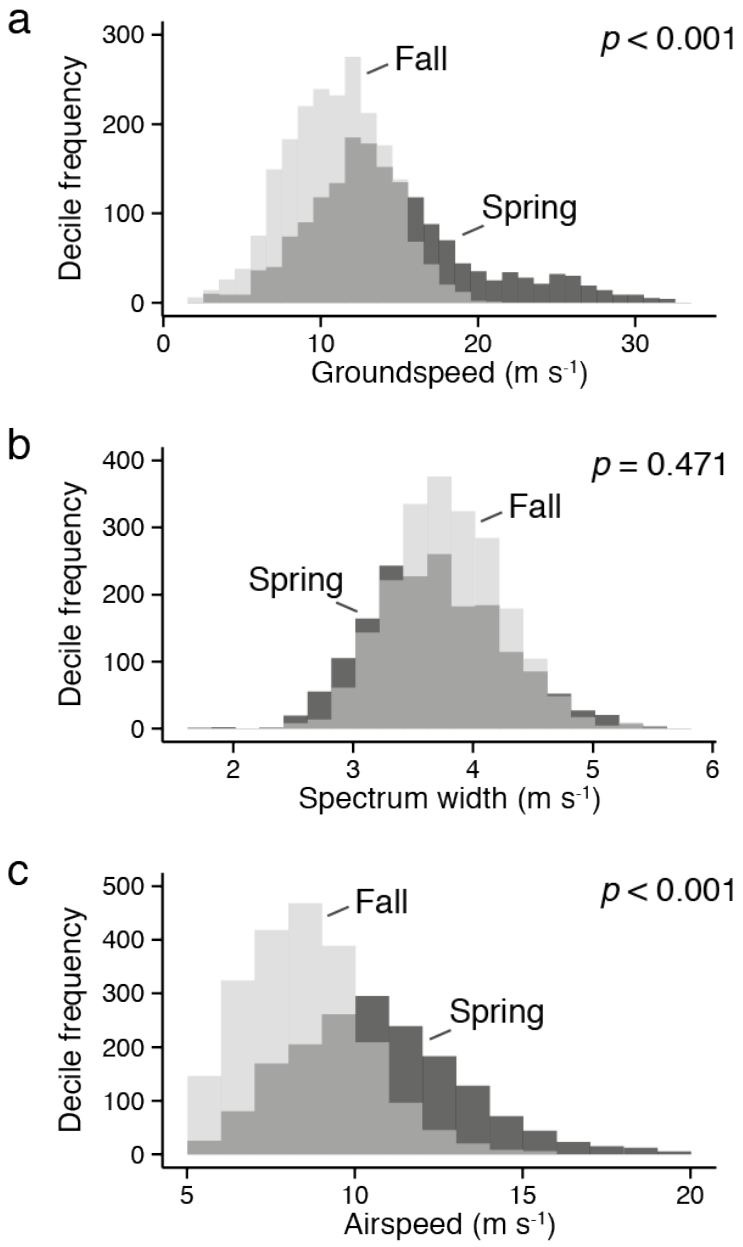

Figure 3.3: (a) Migrant groundspeed, (c) spectrum width, and (c) airspeed distributions during spring (light grey) and fall (dark grey) migratory periods. We excluded airspeeds less than 5.0 ms^{-1} to reduce effects of insect contamination. See Table 3.2 for site-specific summaries of the ground- and airspeeds.

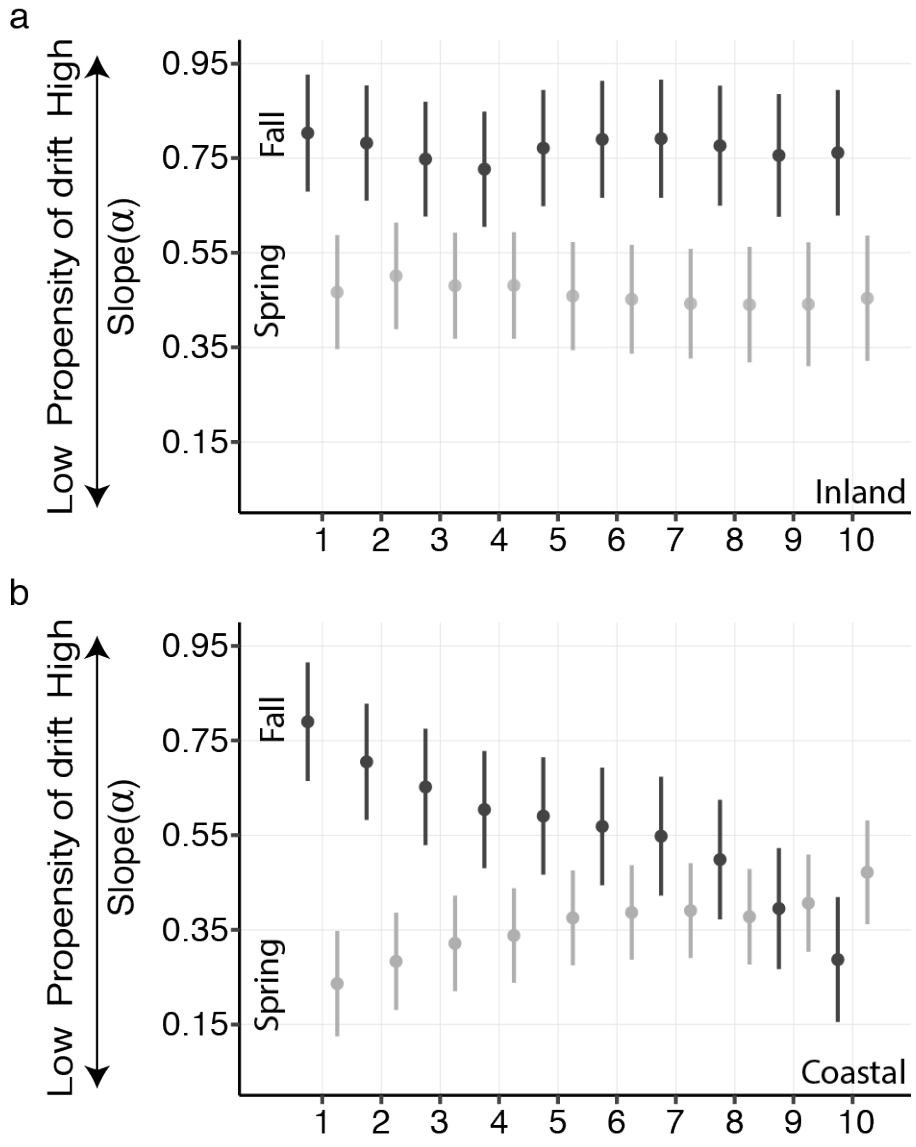

Figure 3.4: (a) Inland and (b) coastal flight strategy during spring (light grey) and fall (dark grey) through the night (decile). Slope of α represents drift propensity; 0–complete wind drift compensation, 1–complete wind drift. Error bars represent 95% confidence intervals. See Table 3.2 for site-specific summaries of the slope of α.

seasonal differences which explained >25% of the marginal variance.

3.3.2 Flight strategy

Migrant track direction was to the northeast during spring for inland and coastal regions, whereas heading was comparatively more northerly for coastal sites (Figure 3.2a, Table 3.1). During fall, track direction was generally due south and heading due southwest (Figure 3.2b, Table 3.1). Overall we found a lower extent of wind drift during spring (slope of $\alpha = 0.39 \pm 0.10$) than in fall (slope of $\alpha = 0.66 \pm 0.12$) (Table 3.2). Inland sites (spring and fall) and coastal sites (spring) showed little temporal variation in flight strategy over the course of the night (Figure 3.4a-b). In contrast, fall migrants at coastal sites showed an increased propensity for compensation through the night (Figure 3.4b). The average PDM during spring for coastal migrants was 38.0 $\pm 3.6^\circ$ and 45.2 $\pm 3.5^\circ$ for inland migrants (Table 3.2). During fall PDM was 207.1 $\pm 4.3^\circ$ for coastal migrants and 195.7 $\pm 4.3^\circ$ for inland migrants (Table 3.2).

3.4 Discussion

3.4.1 Seasonal differences in flight behavior

We observed faster ground- and airspeeds in spring, supporting our hypothesis that migrants fly faster toward rather than away from their breeding grounds. We documented a higher average seasonal airspeed ratio of 1.28 (spring|fall) than those previously reported (1.12-1.19; Karlsson et al. 2012, Nilsson et al. 2013, 2014). By arriving early, migrants are better positioned to have increased access to resources, which can directly influence reproductive fitness (Kokko 1999). Increased airspeeds during spring can also increase flight precision by facilitating greater compensation

(Karlsson et al. 2012). Because airspeeds limit migrants' abilities to fully compensate for diverse wind scenarios, subtle changes may lead to substantial differences in migration speeds. For instance, a bird perfectly compensating for a 7.0 ms^{-1} cross wind would see a 14.4% increase in distance covered for a 6-hour flight with a 2.4 ms^{-1} increase in airspeed (spring 10.6 ms^{-1}, 8.3 fall ms^{-1}).

We found an even greater difference in seasonal groundspeeds (spring|fall; 1.39) relative to airspeeds, which were considerably faster during spring (14.7 ms^{-1}) than during fall (10.6 ms^{-1}). Groundspeeds were consistently faster than airspeeds during both seasons: by 4.1 ms^{-1} in spring and 2.3 ms^{-1} in fall. Seasonal wind regimes are partially responsible for groundspeed differences – on average, migrants experienced more tailwinds in spring and more crosswinds in fall – but deciphering ultimate motivations for changes in airspeeds is difficult and potentially complicated by seasonal age and experience differences, resource competition, compensatory ability, and distance from final destination among other factors. It is also possible that, despite filtering the data, more slow-flying insects were included in the fall samples than the spring samples.

Flight strategies contrasted starkly between seasons, with spring migrants exhibiting greater compensatory tendencies. The difference between mean track and heading directions across the sites was comparatively lower during spring (29.6° ±1.05°) than fall (40.2° ±1.06), similar to what Bäckman and Alerstam (2003) found. The headings of coastal migrants, both in spring and fall, tended to point inland (Figure 3.2a-b). Within night flight strategies were relatively stable, although fall coastal migrants exhibited a more dynamic strategy and compensated more later in the night (Horton et al. 2016c). Geography may partly explain these coastal differences, with northbound spring migrants facing much more land to the north than to the east, and fall migrants encountering a tapering coastline heading south. For migrants over coastal areas, the danger of wind drift over the ocean may also account for differences

in flight strategies. Surprisingly, fall airspeeds were slower at coastal sites (Table 3.2), a strategy that hinders the capacity of migrants to compensate for wind drift (Karlsson et al. 2012). One possible explanation for this observation is that slower airspeeds in coastal areas and later in the night reflect differences in the composition of migrants instead of the changing behavior of individuals. Since migrants with lower airspeeds are more prone to coastward drift, these slower-flying birds should be more numerous in coastal areas; this would explain the counterintuitive airspeed result. This also strongly suggests that birds achieve the observed shift towards a compensatory strategy in coastal areas by increasing their track and heading differences (i.e., α), rather than by increasing their airspeeds.

Seasonal differences in flight behavior may also result from the preponderance of young, inexperienced hatch-year individuals during fall, especially in coastal regions (Ralph 1978, Morris et al. 1996, Woodrey and Moore 1997). Whereas inexperienced migrants don't tend to fly at lower airspeeds (Mitchell et al. 2015), they may be more willing to fly under a greater diversity of wind regimes and may show wider heading distributions (Moore 1984). Age may influence the abilities of migrants to account for wind drift and may explain the occurrence of increased drift during fall (Thorup et al. 2003). Thorup et al. (2003) reported age-dependent wind drift compensation in raptors, with young, first-year individuals showing a greater susceptibility to wind drift. This trend presumably applies to migrant songbirds as well (Ralph 1978), but individual monitoring technology for these assessments in smaller-bodied birds is limited.

Greater dispersion of flight directions could also account for radar-derived airspeed differences across seasons. We predicted this attribute would manifest in seasonally or regionally high measures of spectrum widths (a measure of radial velocity distributions). However, this was not evident in our analysis, suggesting that we can attribute airspeed differences to variation in migrant behavior and not sampling bias

due to volume averaging of radial velocities.

3.4.2 Flight behavior in response to changes in large-scale wind patterns

The observed seasonal, regional, and temporal differences reveal plasticity in birds' flight behaviors. Such plasticity may be important if migrants need to advance their migration phenologies in response to climate change. Decisions made during stopover and in flight influence overall migration speed and may constrain birds' migration strategies without considering additional selection pressures from climate change (Coppack and Both 2002). Trade-offs between decisions about stopover duration and flight speeds define migration speed, and changing seasonal and regional forces shaping migratory life histories will determine how migrants optimize their behaviors to cope with a changing environment (Alerstam 2011).

Dominant wind patterns may have the greatest effect on migration timing by influencing migrant flight speeds (Kemp et al. 2010, La Sorte et al. 2014). In our study, fall migrants faced substantial crosswinds relative to their PDM (46.2° between PDM and mean wind direction), in contrast to spring (31.3°). Summarizing all nocturnal wind directions (not limited to sampling nights), spring nights exhibited more favorable flying conditions, with winds in the general direction of the PDM ±45° on 40.3% of nights; only 22.0% of fall nights showed favorable conditions (Chi-square test: $= 77.0$, $p < 0.001$). Thus, during spring birds encountered more tailwinds, and additionally showed more relative compensatory behaviors. This suggests that spring migrants benefitted from more favorable winds, which required lower offsets to compensate for drift when necessary. Furthermore, birds compensated even though displacement would have been less (relative to fall) if they had drifted.

Climate-change induced shifts in wind intensity may influence migration speed, presumably by altering both stopover duration and in-flight migration speed. Wind speeds over the last ∼30-60 years have declined across much of North America (Pryor

et al. 2009), partly as a result of changes in global climate, and future declines are predicted to be greatest in the eastern United States (∼15% decrease in wind speeds; Pryor and Barthelmie 2011). During fall, weaker opposing winds could yield additional nights that are seasonally favorable for migration, thereby reducing stopover duration by providing more opportunities for flight (Erni et al. 2002, Shamoun-Baranes et al. 2006, Kemp et al. 2010, 2013). In flight, declining speeds of seasonally favorable winds would reduce overall groundspeeds and increase energetic expenditure, both during spring and fall. Under these scenarios we predict overall decreases in levels of wind drift, especially during fall. Lower wind speeds would serve to reduce flight speeds and might reduce seasonal differences in overall phenology. However, because future projections of wind regimes are imperfect, more research is needed to examine the direction and confidence of these changes. Nonetheless, it is clear that these already rapid spring migrations will need to advance further to keep pace with climate change (Coppack and Both 2002). Reduced wind assistance in spring could decrease spatial and temporal flexibility associated with stopover biology.

Additional work is needed to shed light on the motivating factors that drive seasonal flight strategies and the plasticity of these behaviors across greater latitudinal extents. Seasonally appropriate shifts in flight strategy may emerge as migrants approach wintering or breeding grounds (i.e., increased compensation), although no such assessment has been performed to date. Whereas our results demonstrate that migrants are more likely to compensate during spring, we are unable to determine if this pattern varies within the season at more extreme latitudes. Nonetheless, this study demonstrates that weather surveillance radar networks can enable enhanced geographic and temporal coverage to advance our understanding of how migrants moderate migration speeds, cope with wind drift, and alter behaviors across spatial

and temporal gradients.

3.5 Conclusions

Migrants fly more rapidly and precisely in spring than in fall migration. Although causal processes for these differences may be difficult to define explicitly (i.e., for factors like airspeeds that are under migrants' controls), seasonal changes may indicate a more efficient form of flight during spring or migrants' willingness to engage in more costly (i.e., increased efforts toward precision of flights) behaviors to reach breeding grounds in less time. We found greater wind drift compensation during spring, which may be enhanced by faster airspeeds and increased frequency of favorable wind conditions (i.e., less frequent crosswinds). However, these in-flight factors cannot completely account for seasonal differences in migratory phenology, as stopover duration represents a major component of timing. Regardless, these results are important in understanding migratory behavior in Nearctic-Neotropical migrants; variation in flight behaviors suggests that phenotypic plasticity could be an important factor in migrants' phenological responses to climate change.

Table 3.1: Sampling effort, mean track, heading, and wind direction for spring and fall migration seasons at six WSR-88D stations in the eastern United States.

region	radar	season	sampling nights	deciles	track (°) ±95% CI	heading (°) ±95% CI	wind (°) ±95% CI
Inland	KBGM	spring	45	305	36.7 ±4.5	34.2 ±4.6	68.7 ±6.7
		fall	67	526	194.0 ±6.1	233.3 ±3.9	146.3 ±4.5
	KCCX	spring	52	376	35.0 ±4.5	28.8 ±4.5	50.8 ±5.9
		fall	58	445	205.1 ±6.2	231.3 ±4.0	159.3 ±9.6
	KENX	spring	39	241	47.3 ±4.7	33.8 ±4.7	71.3 ±5.7
		fall	46	257	196.7 ±6.6	226.1 ±4.2	150.4 ±5.0
Coastal	KDIX	spring	52	307	40.4 ±4.5	3.3 ±4.6	79.0 ±4.2
		fall	53	321	201.0 ±6.3	245.4 ±4.0	157.1 ±4.6
	KDOX	spring	54	329	37.7 ±4.5	6.9 ±4.5	82.9 ±4.9
		fall	60	359	204.7 ±6.1	238.9 ±4.0	159.1 ±6.2
	KOKX	spring	37	198	49.6 ±4.9	0.7 ±4.9	85.6 ±5.1
		fall	38	221	208.1 ±6.6	251.2 ±4.3	159.5 ±5.7

Table 3.2: Mean groundspeed, airspeed, slope of α, and preferred direction of movement (PDM) for spring and fall migration seasons at six WSR-88D stations in the eastern United States.

region	radar	season	groundspeed (ms^{-1}) ±95% CI	airspeed (ms^{-1}) ±95% CI	slope of α ±95% CI	PDM ±95% CI
Inland	KBGM	spring	14.5±1.3	10.9 ±0.7	0.54 ±0.15	44.6 ±5.0
		fall	11.6 ±0.7	8.9 ±0.5	0.77 ±0.16	195.6 ±6.4
	KCCX	spring	15.1 ±1.2	10.4 ±0.7	0.48 ±0.15	42.2 ±5.0
		fall	10.9 ±0.7	9.0 ±0.5	0.70 ±0.16	199.9 ±6.4
	KENX	spring	15.2 ±1.3	9.7 ±0.7	0.56 ±0.16	49.1 ±5.1
		fall	11.7 ±0.8	8.6 ±0.5	0.88 ±0.17	191.7 ±6.5
Coastal	KDIX	spring	14.4 ±1.2	10.8 ±0.7	0.29 ±0.14	35.5 ±5.0
		fall	10.8 ±0.7	8.1 ±0.5	0.48 ±0.16	206.3 ±6.5
	KDOX	spring	13.7 ±1.2	10.7 ±0.7	0.26 ±0.14	36.8 ±4.9
		fall	10.3 ±0.7	8.2 ±0.5	0.55 ±0.16	204.4 ±6.4
	KOKX	spring	14.0 ±1.3	10.4 ±0.7	0.33 ±0.14	42.4 ±5.4
		fall	10.0 ±0.8	7.6 ±0.5	0.50 ±0.17	211.0 ±6.6

Chapter 4

Where in the air? Aerial habitat use of nocturnally migrating birds

4.1 Introduction

Habitat use is a unifying concept of organismal ecology that connects behavioral plasticity, ecological constraints, and evolutionary adaptations of animals to their environment (MacArthur 1958). The lower atmosphere (i.e., aerosphere) is a heterogeneous, dynamic habitat that is occupied by a host of organisms such as birds, bats, and insects (Diehl 2013). Unlike terrestrial habitats, which often can be characterized at smaller scales and in fewer dimensions, biological occupancy of the aerosphere can extend kilometers in altitude above large areas of Earth's surface. Describing multi-dimensional patterns of use by airborne organisms is essential for characterizing the behavioral processes that drive the distribution and abundance of migrating and foraging animals. Recent technological advances in tracking techniques enable monitoring of long-term airspace use by migratory individuals (Liechti et al. 2013), but the challenges of tracking more than a small number of individuals hampers our inferences about the complete distribution of animals in the aerosphere. Obtaining airspace use distributions, in particular to resolve details of animals' movements across diverse spatial and temporal scales, poses technical challenges that include

processing large amounts of data and exhaustively sampling individuals (Kelly and Horton 2016).

Radar remote sensing is one of the few tools that can accurately quantify multi-dimensional time-series of animal density at high elevations and large spatial extents (Gauthreaux 1971). Radar applications have contributed significant knowledge about biological phenomena, especially bird and insect migration (Chapman et al. 2010, Horton et al. 2016b). Organized networks of weather surveillance radars such as the United States' NEXRAD or Europe's OPERA can provide continental coverage with multiple updates per hour for monitoring migrant passage and distribution (Diehl and Larkin 2005, Dokter et al. 2011). The aim of this chapter is to leverage the NEXRAD network to determine where and when nocturnally migrating birds occupy the airspace and how prevailing wind conditions dictate aerosphere use. We build upon previous examinations of height selection and the influence of winds (e.g., Kemp et al. 2013, Dokter et al. 2013, La Sorte et al. 2015a), examining seasonal and spatial differences in airspace usage. Because wind conditions dramatically influence the efficiency of migratory flight (Pennycuick 1969), particularly in songbirds, we predict birds will select heights with the greatest wind profit (i.e., support a migrant obtains from wind conditions aloft) to maximize tailwind assistance (Kemp et al. 2013). In addition, because nights with profitable winds are less frequent during the fall, we predict correlations with wind profit will be higher during the fall season (Horton et al. 2016b).

4.2 Methods

4.2.1 Weather surveillance radar data

We examined geographic differences in airspace usage following recent evidence from this region of differences in flight strategies between inland and coastal

sites (Horton et al. 2016b, 2016c). We used radar measures from six WSR-88D radars (Figure 4.1), 3 inland (KENX, KBGM, KCCX) and 3 coastal (KOKX, KDIX, and KDOX). Data were downloaded from NOAA's National Centers for Environmental Information (`http://www.ncdc.noaa.gov/has/has.dsselect`) from March 1st to June 15th for 2013-15 and August 1st to November 15th 2013-14. We generated height profiles of reflectivity factor (Z, mm^6m^{-3}) at 10-m intervals from 0.15-2.0 km above ground level (a.g.l., radar antenna heights Table 4.1). We used data from the five lowest elevation sweeps (0.5-4.5°) between a range of 5.0-37.5 km from the radar (La Sorte et al. 2015a). We converted measures of reflectivity factor to reflectivity (η; cm^2km^{-3}) following (Chilson et al. 2012). We manually excluded scans containing non-biological measures (e.g., precipitation, anomalous propagation, etc.) through visual inspection and restricted the sampling duration to the hours between evening and morning civil twilight (sun angle 6° below the horizon). We constructed velocity azimuth displays (VAD), retained samples with VAD fits between 1 and 5 RMSE to limit insect contamination and poor fits, and eliminated samples with airspeeds less than 5.5 ms^{-1} to further reduce insect contamination (Larkin 1991).We categorized the native 5- and 10-minute radar measures between these intervals as tenths of the night (i.e., deciles), averaging measures within these decile periods. We calculated mean flight height by taking the average of the height intervals (10-m) weighted by η.

4.2.2 Winds aloft

To examine wind speed and direction at height intervals occupied by migrants, we used the North American Regional Reanalysis dataset (Mesinger et al. 2006). These data offer a horizontal spatial resolution of ∼32 km, three-hour updates, and 25-hPa pressure-level (i.e., height) intervals of zonal and meridional wind components. We assigned wind measures to decile periods and linked each 10-m height interval of

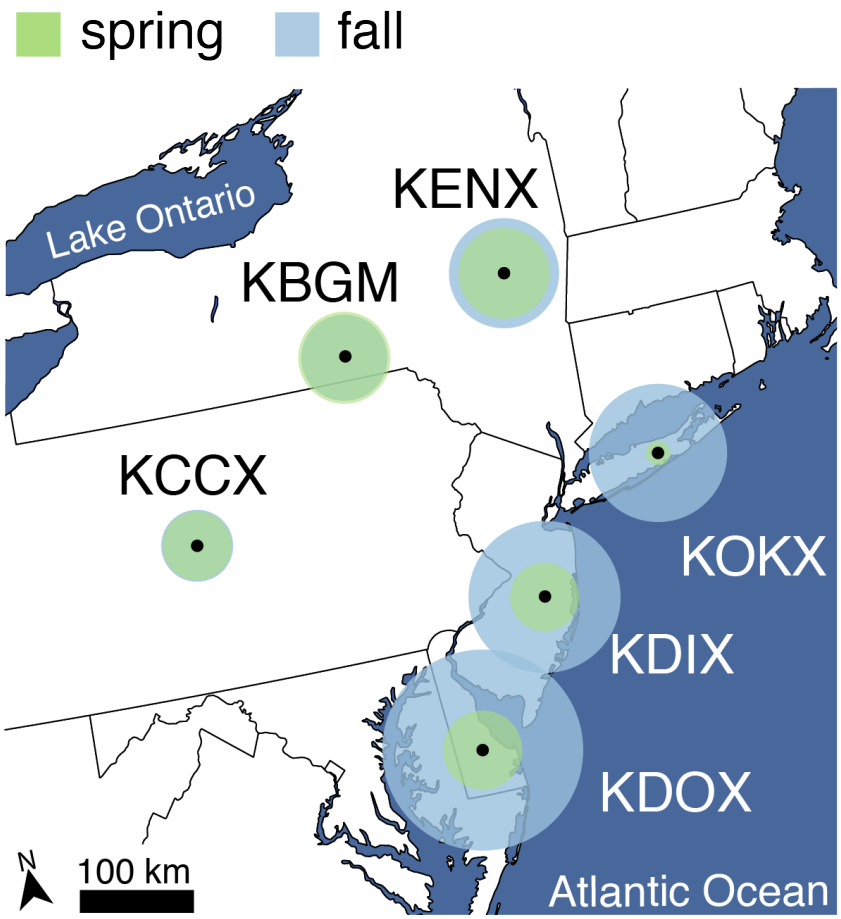

Figure 4.1: WSR-88D locations (black dots). Green (spring) and blue (fall) disk radii represent the seasonal average of migratory activity (η; cm^2km^{-3}) as a summation of time and space.

reflectivity to the closest corresponding spatial and temporal measure. We calculated wind profit following (Kemp et al. 2013) using extracted airspeeds from VAD analysis, and used seasonal and site-specific preferred directions of movement extracted from (Horton et al. 2016b, 2016c), calculated following (Green and Alerstam 2002). We removed from analysis any sets of conditions in which birds could not fully compensate for cross-winds and for which we could not calculate a real solution (Kemp et al. 2013 p. 2013). For each height profile, we determined the minimum and maximum wind profit (ms^{-1}), height of the maximum wind profit, and the height of the 0.50,

0.60, and 0.75 quantile (τ) of wind profit. To determine the respective height of each quantile we calculated the median of height bins with wind profits within 0.25 ms^{-1} of the respective quantile value. We calculated the wind profit used by most migrants by taking the mean of wind profits weighted by the vertical profile of reflectivity.

4.2.3 Statistics

We used two-sample *t*-tests to calculate nightly mean height differences across sites (inland v coastal) and nightly mean seasonal differences in maximum wind profit. We used Pearson's correlation to quantify the correspondence of nightly means of migratory activity (reflectivity) and flight height between and within inland and coastal regions. We used Pearson's correlations to examine the seasonal and regional relationships between nightly mean flight height and the heights of variable with profit gains (τ = 0.50, 0.60, 0.75, and max wind profit).

4.3 Results

We sampled 136 nights during the spring and 134 nights during the fall (Table 4.2). We found higher migratory activity (reflectivity) in fall, particularly over coastal sites (Figure 4.1, Figure 4.2, Figure 4.3). Although trends in average reflectivity varied, activity generally peaked in the first half of the night. Average heights of birds in flight ranged from 119.8 to 1135.6 m (Table 4.2), with birds at inland sites flying higher during the spring than birds at coastal sites (inland, 528.8 ±26.4 m; coastal, 436.0 ±26.3 m; t = 4.9, 407 d.f., p <0.01). During the fall, regional differences in flight height were less apparent (inland, 435.9 ±19.7 m; coastal, 451.4 ±22.8 m; t =

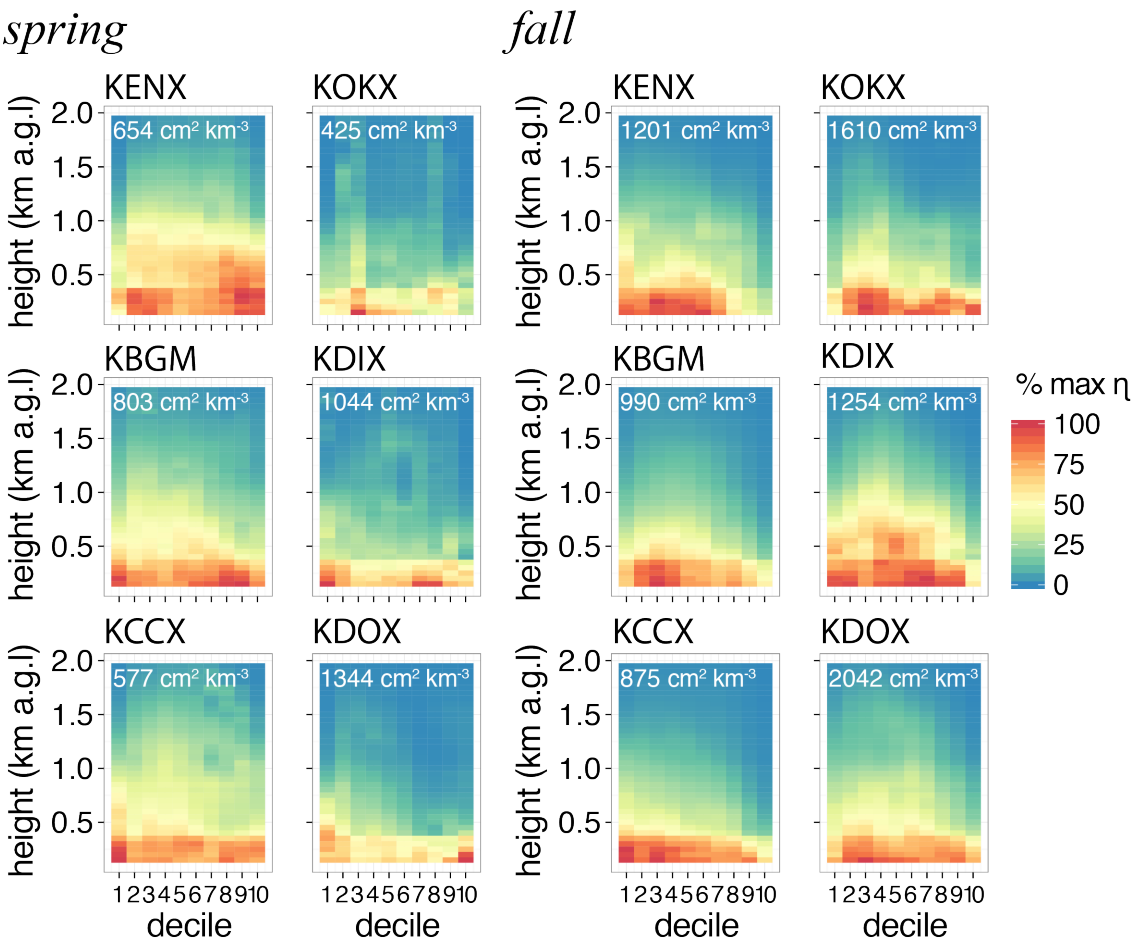

Figure 4.2: Spring and fall spatial and temporal distribution of η. To use a common gradient of intensity, measures are represented as the percent maximum for each seasonal-radar pairing. Height intervals were averaged to 50-m intervals to enable visualization.

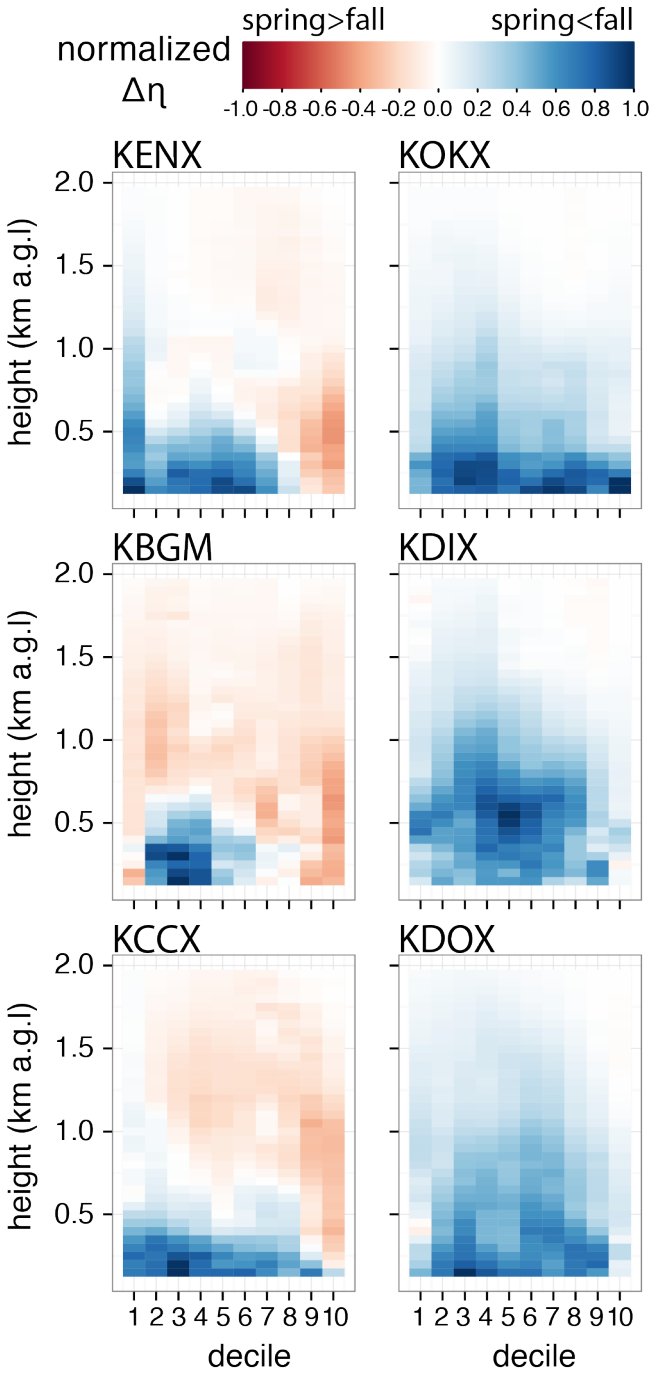

Figure 4.3: Normalized seasonal changes in η. Shades of red represent greater spring migratory activity, whereas blues represent greater fall migratory activity.

-1.0, 402 d.f., $p = 0.313$). Birds flew at peak heights during the first 30% of the night and thereafter tended to decrease in height (Figure 4.2).

Within each region (inland and coastal), migrant activity was positively correlated among radar stations, with six of six possible within region correlations showing statistical significance during spring and fall (hereafter represented as spring 6/6, fall 6/6; Figure 4.4). Correlations between migrant activity at inland and coastal sites were generally weaker or non-significant (spring 1/9, fall 8/9; Figure 4.4). Correlations between mean nightly flight heights showed similar spatial dependence, with significant positive correlations within regions (spring 3/6, fall 5/6, Figure 4.4) but weaker non-significant correlations between regions (spring 1/9, fall 2/9, Figure 4.4).

Maximum wind profits were on average stronger during spring than fall (spring, 6.9 $\pm$0.6 ms^{-1}; fall, 3.3 $\pm$0.4 ms^{-1}; $t = 10.7$, 790 d.f., $p < 0.001$; Figure 4.5). In spring and fall, migrants flew at heights positively correlated with the height of the maximum wind profit, and tended to be weaker for heights with moderate wind assistance (Figure 4.6). Regardless, the absolute value differences between the mean flight heights and wind height quantiles were large ($\tau = 0.50$, 500.6 $\pm$18.3 m; $\tau = 0.60$, 502.6 $\pm$18.2 m; $\tau = 0.75$, 496.4 $\pm$23.1 m; $\tau =$ max, 598.6 $\pm$34.6 m; mean $\pm$95%CI, see Table 4.3 for seasonal and regional differences). Birds flew at heights nearer to maximum wind profit than to the minimum wind profit, suggesting positive selection for wind assistance (spring, $t =$ -5.0, 776 d.f., $p < 0.001$; fall, $t =$ -8.2, 804 d.f., $p < 0.001$; Figure 4.7).

4.4 Discussion

Migrants' flight heights correlated positively with height of the maximum wind profit, although correlations were weaker than expected (Kemp et al. 2013), suggesting more complex relationships between flight height selection. Birds may not select the flight height with optimal wind profit because of time and energy constraints. While higher flight altitudes can extend flight distance because of lower frictional

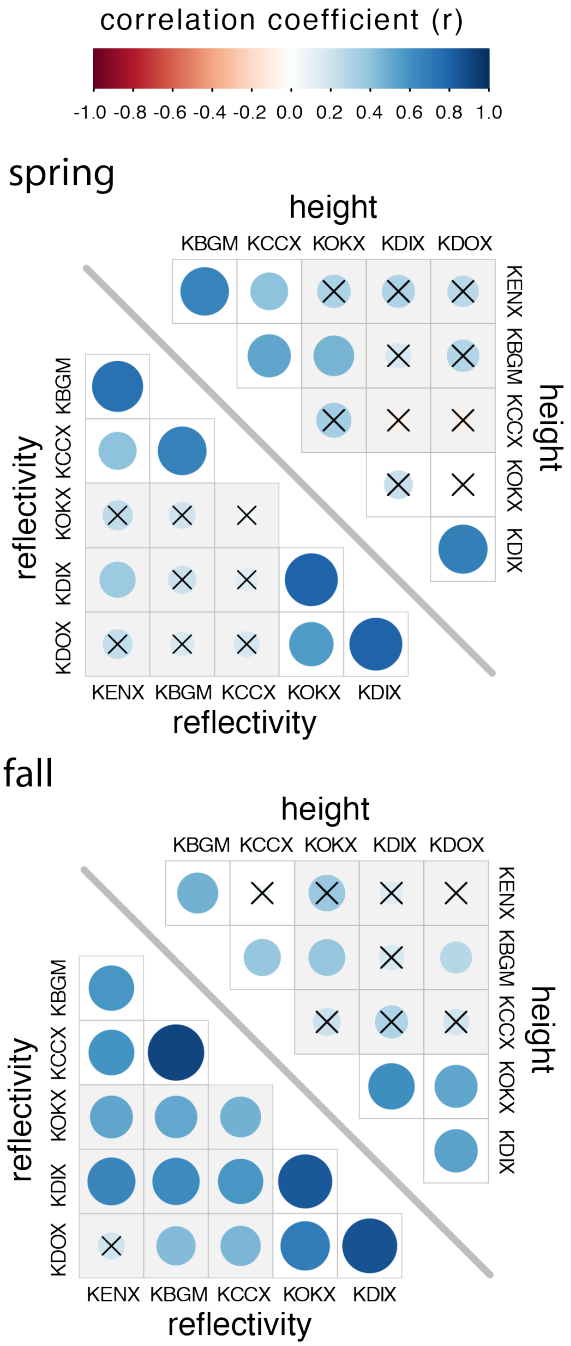

Figure 4.4: Seasonal within (white background) and between (gray background) region correlations of migrant height and activity. X's denote non-significant Pearson's correlation at the $\alpha = 0.05$ level and circle size proportional to correlation strength. We used nightly means for all correlations.

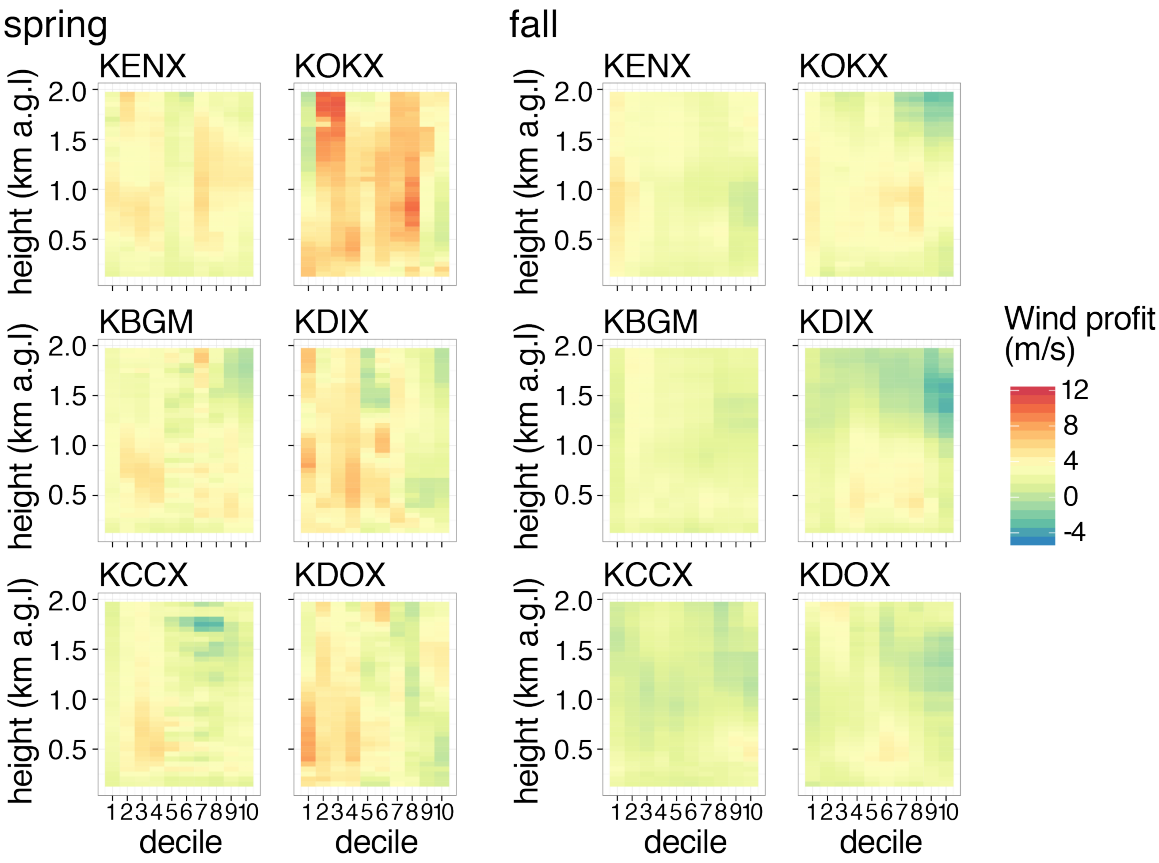

Figure 4.5: Spring and fall spatial and temporal distribution of mean wind profit (ms^{-1}). Height intervals were averaged to 50-m intervals to enable visualization.

resistance (Pennycuick 1969), the cost of water loss due to declining partial pressure (Klaassen 1996) may result in birds selecting flight altitudes with suboptimal wind profit (Kemp et al. 2013). Our results suggest that non-aerodynamic constraints, such as costs associated with the time and energy to sample airspace, navigate, and stop over (Kemp et al. 2013), may cause migrants to seek conditions sufficient, rather than optimal, for flight.

We found strong seasonal shifts in migration activity in the eastern United States. Significantly greater overall migration activity along more coastal routes typified the fall season. Coastal sites showed a nearly 100% increase in summed reflectivity (75.5 to 139.8%) between spring and fall (Figure 4.1). These patterns may indicate

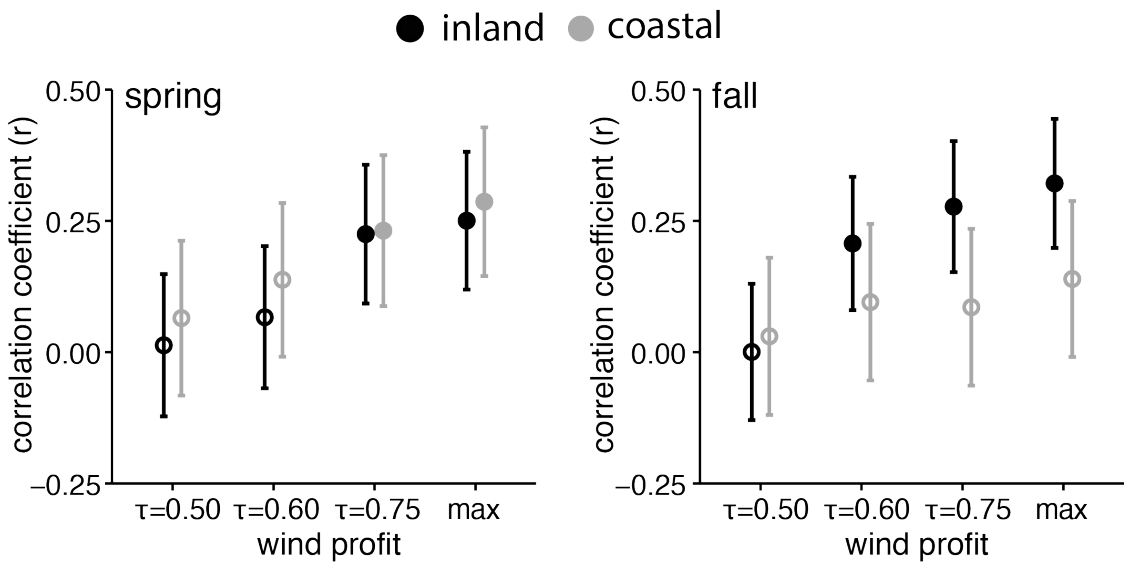

Figure 4.6: Pearson's correlation (±95% confidence intervals) between migrant height and height of variable wind profit gain (τ = 0.50, 0.60, 0.75, and max wind profit). Statistically significant (α = 0.05) Pearson's correlations denoted by filled points. We used nightly means for all correlations.

looped migration patterns (La Sorte et al. 2016), migrants staging for departure from the coast (Stoddard et al. 1983), and possibly population-level drift towards coastal regions (Horton et al. 2016b, Horton et al. 2016c). They demonstrate the importance of coastal airspace habitat for fall migrants, most of which are undertaking their first and most perilous migration. These critical coastal habitats are disproportionately impacted by light pollution and loss of stopover habitat (Newton 2006).

When examining the spatiotemporal differences in migratory activity (Figure 4.3), we surprisingly saw greater migrant activity during the spring than the fall at higher altitudes and later in the night. These changes may reflect spring migrants'

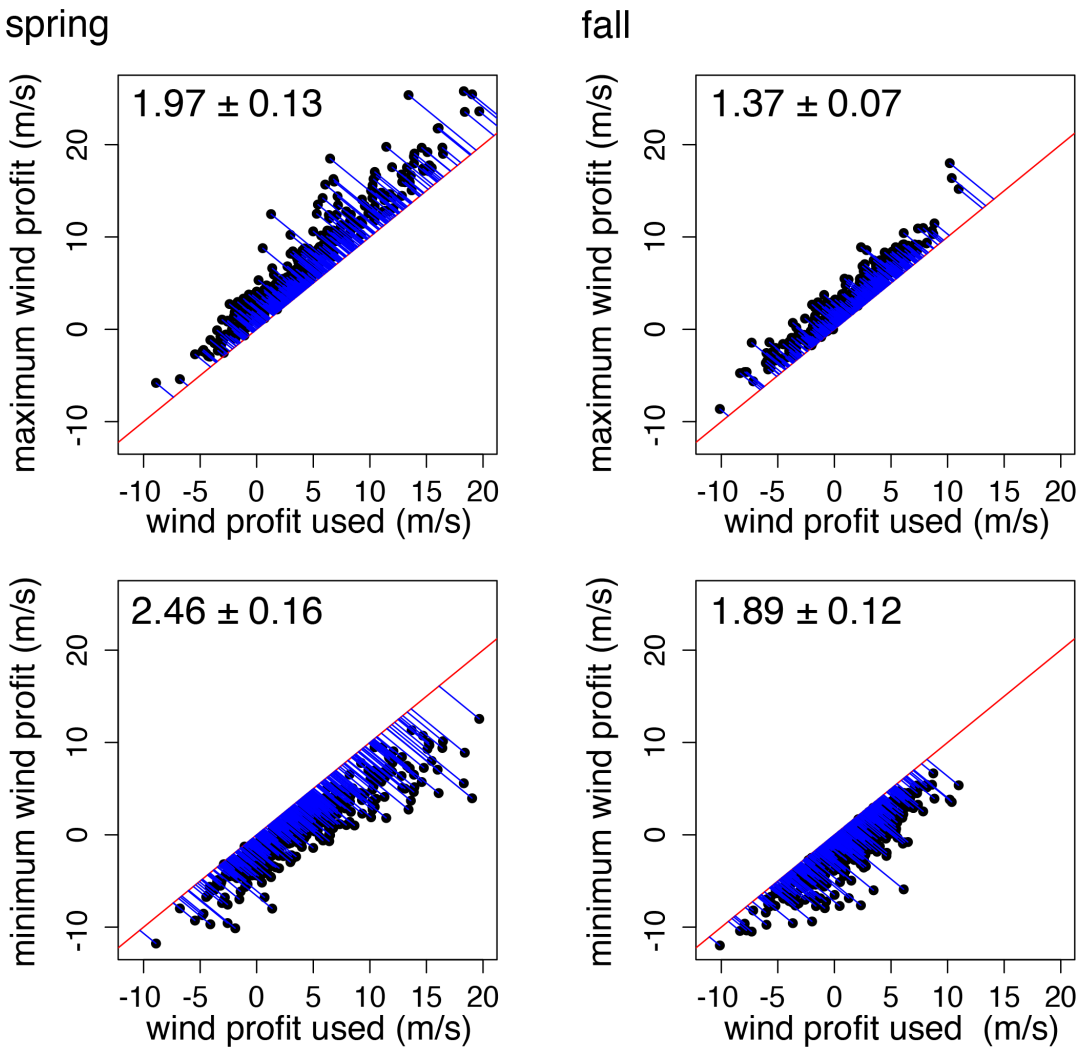

Figure 4.7: Migrants' wind profits versus maximum and minimum wind profits within the 0.15-2km vertical sampling region. Red lines indicate the theoretically perfect positive 1-to-1 correlation between the maximum (top) or minimum (bottom) wind profits available. Values in the upper left are the mean distance (blue segments) from the maximum or minimum (±95% confidence intervals). Points above the red line (top) indicated birds flying in slower than max wind profit winds and points below the line (bottom) are birds flying in faster than minimum wind profits.

willingness to fly for longer durations and at higher altitudes to maximize flight distance, a behavior likely driven by enhanced seasonal tailwind profit.

4.5 Conclusions

This study is one of the first to present a large-scale, multi-season depiction of the distribution of migratory birds in airspace habitats. We predicted flight altitudes would be strongly constrained by wind speed and direction. Migrants tended to fly at altitudes with high wind profits, but these altitudes were not always the stratum with maximum profit. A more complex scenario likely defines relationships between migrants' flight altitudes, winds, and optimality of movements. Because the altitudinal distribution of wind profit can be very complex, with multiple peaks, in addition to the implicit assumptions of wind profit calculations, we recommend additional analyses across larger scales. Larger scale analyses will enhance our understanding of how biogeographic effects shape patterns of aerial habitat selection, especially near presumed ecological barriers. By leveraging the existing radar infrastructure, we can examine these patterns through entire migratory flyways and answer macro-scale questions of avian migration.

Table 4.1: Radar antenna heights (m) above ground level and above sea level.

region	radar	radar antenna height (meters above ground level)	radar antenna height (meters above sea level)
Inland	KBGM	20	509.5
	KCCX	20	753
	KENX	20	576.6
Coastal	KDIX	20	65.4
	KDOX	30	45.2
	KOKX	20	196.5

Table 4.2: Weighted means ±95% CI and range of seasonal flight heights (m a.g.l.) for inland and coastal sites.

region	radar	season	sampling nights	flight height (m a.g.l.) ±95% CI	range of flight heights (m a.g.l.)
Inland	KBGM	spring	70	484.9 ±42.5	155.7 to 1127.9
		fall	96	418.0 ±26.7	188.4 to 762.2
	KCCX	spring	79	543.0 ±46.6	199.6 to 1121.1
		fall	76	424.0 ±36.3	191.8 to 935.5
	KENX	spring	64	559.1 ±46.0	213.3 to 1087.6
		fall	61	479.1 ±41.6	221.5 to 903.3
Coastal	KDIX	spring	72	449.4 ±45.0	144.8 to 1034.9
		fall	63	491.2 ±37.2	253.1 to 870.8
	KDOX	spring	74	438.8 ±42.0	135.5 to 1048.5
		fall	83	438.1 ±38.6	119.8 to 960.7
	KOKX	spring	50	454.6 ±50.8	172.9 to 1135.6
		fall	49	419.8 ±38.1	220.0 to 817.2

Table 4.3: Mean differences (m a.g.l ±95% confidence intervals) between migrant flight height and height of wind profit quantiles. We calculated means from absolute value of the differences.

region	season	wind profit quantile			
		$\tau = 0.50$	$\tau = 0.60$	$\tau = 0.75$	$\tau = \max$
Inland	spring	487.2 ±38.4	502.9 ±37.4	522.7 ±41.9	657.4 ±64.8
	fall	505.6 ±31.1	534.8 ±31.2	535.6 ±39.8	633.9 ±64.5
Coastal	spring	500.7 ±38.2	484.9 ±36.6	451.0 ±53.5	546.4 ±78.8
	fall	510.1 ±40.0	477.7 ±41.4	458.8 ±51.5	533.8 ±69.4

Chapter 5

Seasonal variation in avian flight strategies during spring migration is dictated by wind direction and body size

5.1 Introduction

Movement is ubiquitous among a diverse array of animals and can be a primary means to maximize an individual's fitness. Movement behaviors vary in mode, speed, duration, and scale – and these movements in turn shape the structure and function of aerial, marine, and terrestrial ecosystems (Hansson and Åkesson 2014). Avian migrations represent some of the fastest (Great Snipe, *Gallinago media*; (Klaassen et al. 2011), most distant (Arctic Terns, *Sterna paradisaea*, Egevang et al. 2010), and longest-lasting (Bar-tailed Gotwit, *Limosa lapponica*; Gill et al. 2009) movements recorded on Earth. Variation in these migration behaviors provide valuable insights into understanding animal navigation (Weindler et al. 1996, Alerstam et al. 2001), optimal behavior theory (Alerstam and Hedenström 1998, Alerstam 2011), and biotic responses to recent climate change (Butler 2003, Jonzón et al. 2006).

Even the most basic movements involved in ranging, foraging, and homing may require remarkable feats of orientation and navigation, regardless of the distances traveled. Unique among movements are long-distance seasonal migrations.

Many species of migrant suppress their responses to spatially and temporally proximate resources that would otherwise be sufficient for immediate survival and move seasonally between consistent and well-defined geographic or altitudinal ranges (Dingle 1996, Hansson and Åkesson 2014). In these cases, migration can be seen as a pre-emptive, or programmed (Berthold 1991), movement away from deteriorating local conditions (push) or toward improving conditions (pull) (Rohwer et al. 2005), which ultimately has fitness consequences.

Of all migratory taxa, birds have received the greatest attention (Newton 2008). During migratory journeys that may last weeks or months, birds must decide on when to fly, and once in flight they must make decisions about the direction, speed, and duration of flight. The success of birds' migrations, and thus their survival and fitness, depend strongly on the outcome of these decisions. Varying wind conditions present a major challenge for aerial navigators, and understanding birds' context-dependent responses to winds aloft is fundamental to understanding avian navigation. Barring periods of rain, winds are the most important weather factor determining the departure of migrants (Richardson 1978, 1990). The optimal migration strategy is to select for conditions with tailwinds or weakly opposing headwinds (Alerstam 1979), but extensive geographic variation in dominant wind fields may dictate migration departure during seemingly suboptimal conditions (Liechti 2006, Horton et al. 2016a).

Regional patterns in winds have shaped the migration routes of billions of individuals of hundreds of species as they transition to and from their breeding and wintering grounds (La Sorte et al. 2014, Kranstauber et al. 2015). Biogeography constrains these routes (wintering and breeding location; Moore et al. 1995, Kelly et al. 1999), but seasonal wind regimes may make the use of a particular route optimal during one season and suboptimal in the other (La Sorte et al. 2014, 2016).

Whereas recent system-level investigations of stopover behavior have mapped migration trajectories (La Sorte et al. 2013, 2016), no study has investigated system-level flight strategies across an entire migration flyway. In combination, prevailing winds and birds' flight strategies are important aspects that can define optimal migratory movements (Liechti 2006, Chapman et al. 2011, Horton et al. 2016a), but it remains unresolved whether a migrant's tolerance for selecting opposing winds is context dependent, specifically with respect to proximity to its end destination. This question is grounded in theoretical predictions about migrants' abilities to optimally and systematically adjust their behaviors in free flight.

Optimal migration theory predicts that migrants should tolerate wind drift near the origin of their migratory route and increase the degree to which they compensate for wind drift as they near their ultimate destination (Liechti 2006). But testing this prediction remains a fundamental challenge for understanding the ecology of long distance migration through the aerosphere (the lower atmosphere). Collecting data on *in-flight behaviors* of millions of individuals across a large number of species with high spatial and temporal resolution, across an extensive latitudinal gradient, is a primary constraint. Moreover, even state-of-the-art tracking technology is insufficient to monitor adequate numbers of migrants, especially small passerines that compose a majority of migratory movements (Bridge et al. 2011). And small numbers of tracked individuals may document only a subset of the variation in populations' migratory strategies.

The US network of weather surveillance radar (WSR) stations provides the potential to capture migratory movements at continental scales (Kelly and Horton 2016, Kelly et al. 2016). However, WSR stations do not explicitly detect species or taxonomic identities, a feature that has historically imposed stark limits on the depth of possible inference about bird migration from these sensors. To overcome these constraints, we integrate crowd-sourced data (eBird observations) collected on

the ground by thousands of citizen scientists (Sullivan et al. 2014). The combination of WSR stations and ground-based observations allows us to investigate the degree to which species composition influences the dynamics of migration systems. For example, can we explain broad-scale variation in avian flight behavior across a flyway with information about the morphology and intended destinations of species on the move? There is evidence that body size and morphology may influence the ability of particular species or taxonomic groups to modulate migration behavior (Gauthreaux and Able 1970, Hedenström 2008). Specifically, we hypothesize that large-bodied birds with faster airspeeds would compensate more for wind drift than small-bodied migrants (Alerstam et al. 2007). If these traits are important drivers of migration behavior, understanding their underlying geographic distributions is needed to explain system-level flight patterns.

The central United States offers an ideal locality to test hypotheses rooted in migration theory. The region extends upwards of ∼2500 km from subtropical habitats bordering the Gulf of Mexico, across the grasslands of the Great Plains, and extends into the boreal forest near the Canadian border. Aquatic (Lincoln 1935, Buhnerkempe et al. 2016) and terrestrial (La Sorte et al. 2014) migrants use this region, blurring the classical definitions of the Central, Mississippi, and Eastern Flyways. This region is only minimally influenced by major ecological barriers (e.g., mountains, lakes, deserts, etc.) or leading lines (i.e., coastlines, rivers), that may otherwise alter flight strategies (Horton et al. 2016c). However, as migrants move north through the region in the spring, the direction of the prevailing winds at migration altitudes changes from southerly to westerly (Randall 2015). Thus, migrants are more likely to encounter tailwinds early and crosswinds late in their migration journey. Here, we use data from WSR stations and bird observations from eBird (Sullivan et al. 2014) to test flight strategy predictions originating from optimal migration theory. Additionally, we examine the extent to which body mass, an important morphological trait, determines

how well these predictions are met.

5.2 Material and methods

We used WSR to quantify the intensity and speed of in-flight nocturnal movements and measured changes in track (directions relative to the ground) and heading (body axis direction) to understand the degree to which migrants compensate for wind drift. We integrated these data with ground-based observations (eBird) to characterize the underlying distribution of nocturnal migrants passing through the radar coverage. Ground-based observations were used to understand the temporal and spatial shift in taxonomic identities of migrants, morphological traits (i.e., average body mass), and species trajectories towards breeding range centers. These datasets were used to understand how species-traits drive changing spatial and temporal patterns of wind drift compensation.

5.2.1 Weather surveillance radar data

We used unfiltered (i.e., level-II) **W**eather **S**urveillance **R**adar 19**88** **D**oppler (WSR-88D) data from 20 sites covering a large portion of the central USA from spring 2013 to spring 2015 (21.6° of latitude; Figure 5.1) (Crum and Alberty 1993). To investigate spring behaviors, we acquired radar data from NOAA's National Centers for Environmental Information for the period 1 March to 31 May of each year. The National Weather Service (NWS) within the National Oceanic and Atmospheric Administration (NOAA) operates nineteen of these radars and the Department of Defense (DOD) operates one (KGRK). Every 5 to 10 minutes the radars makes a series of sequential elevation observations (e.g., 0.5, 1.5, ... 19.5°), scanning the airspace from 0 to 359° degrees in azimuth at each elevation. The volume coverage pattern

(i.e., airspace sampling routine) is tailored to the atmospheric conditions, and for this reason sampling update times can vary.

We retained data between evening and morning civil twilight (sun angle 6° below the horizon) and discarded any aerial samples containing weather (i.e., contamination from precipitation that obscured bird movements). Because the number of radar scans (∼900,000) prevented complete manual screening, we used a two-stage approach to remove weather contamination: (1) we removed volume coverage patterns in which 70% of the low elevation sweep volumes (∼0.5°) had correlation coefficient (a polarimetric radar variable) values greater than 0.90 or 70% of the sampling volumes had reflectivity measures greater than 35 dBZ (Stepanian et al. 2016); (2) we visually screened all remaining sweeps (n = 250,552) for weather contamination. Examination of a subset of images following step 1 (KMVX 2013, n = 11,543) revealed that automated filtering by correlation coefficient and reflectivity returned a 2.7% false negative rate (203 of 7,582). However we deemed the false positive rate too high for our biological application (573 of 3,961; 14.5%), mandating the need for manual inspection (step two) (see Figure 5.2 for illustrated workflow). This two-stage process resulted in 231,241 sweeps containing weather-free data.

From weather-free scans, we determined migrant track and heading from radial velocity and correlation coefficient (ρ_{HV}), respectively, from 55 to 1995 m above ground level (a.g.l.) following (Browning and Wexler 1968, Stepanian and Horton 2015). When necessary, radial velocity measures were dealiased following Sheldon et al. (2013) through the WSRLIB package (Sheldon 2015). To limit insect contamination, we excluded velocity azimuth displays (a computation of the mean Doppler velocity to derive migrant track and groundspeed) with RMSE (root mean squared error) less than one, and we removed samples with RMSE greater than five to limit poor fits (Dokter et al. 2011, Horton et al. 2016b). We restricted polarimetric azimuth displays (a computation of the correlation coefficient, ρ_{HV}, to derive heading) to fits

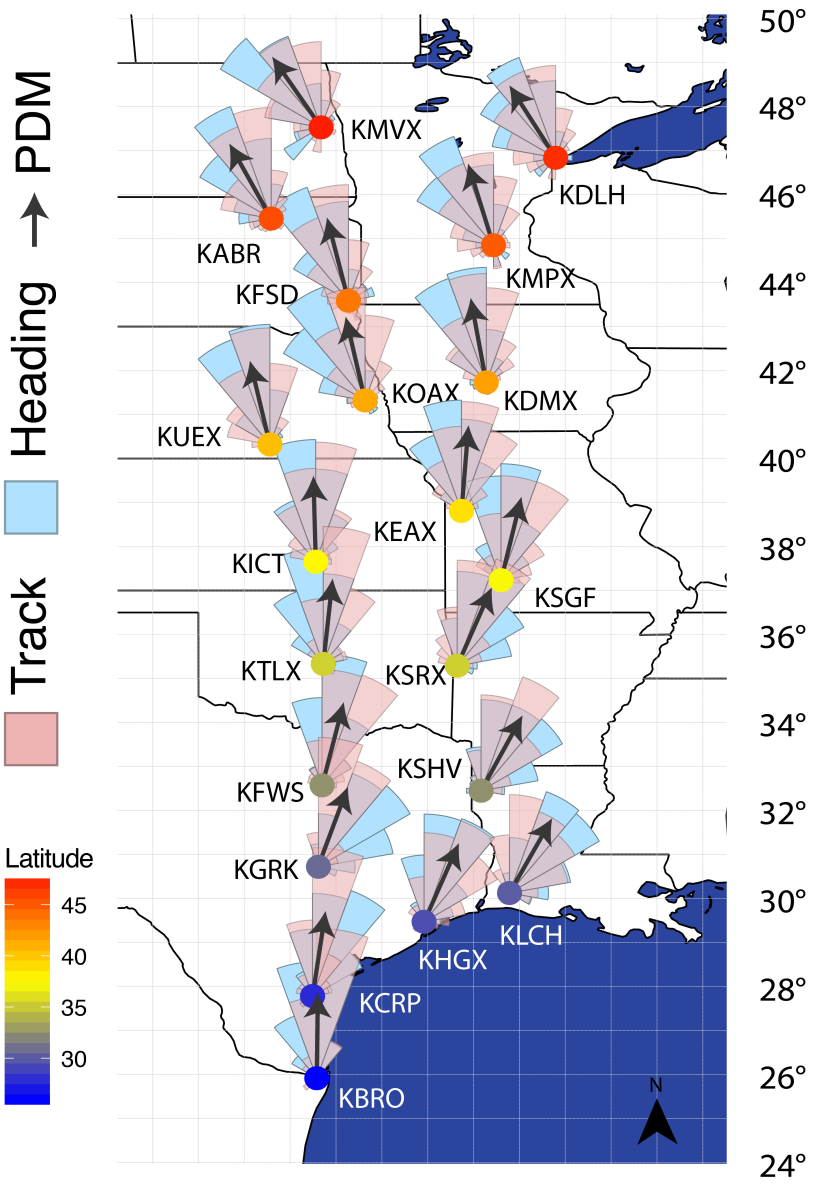

Figure 5.1: Rose diagram showing the distribution of migrant track (pink) and heading (blue) during spring migration (2013-15) from 20 weather surveillance radar (WSR) stations locations in the central USA. Black arrows identify the in-flight preferred direction of movement from complete season model for wind drift. We weighted track and heading distributions by scaled reflectivity factor and used 20° sectors for the plotting of track and heading measures. The color of the WSR stations is based on its latitude.

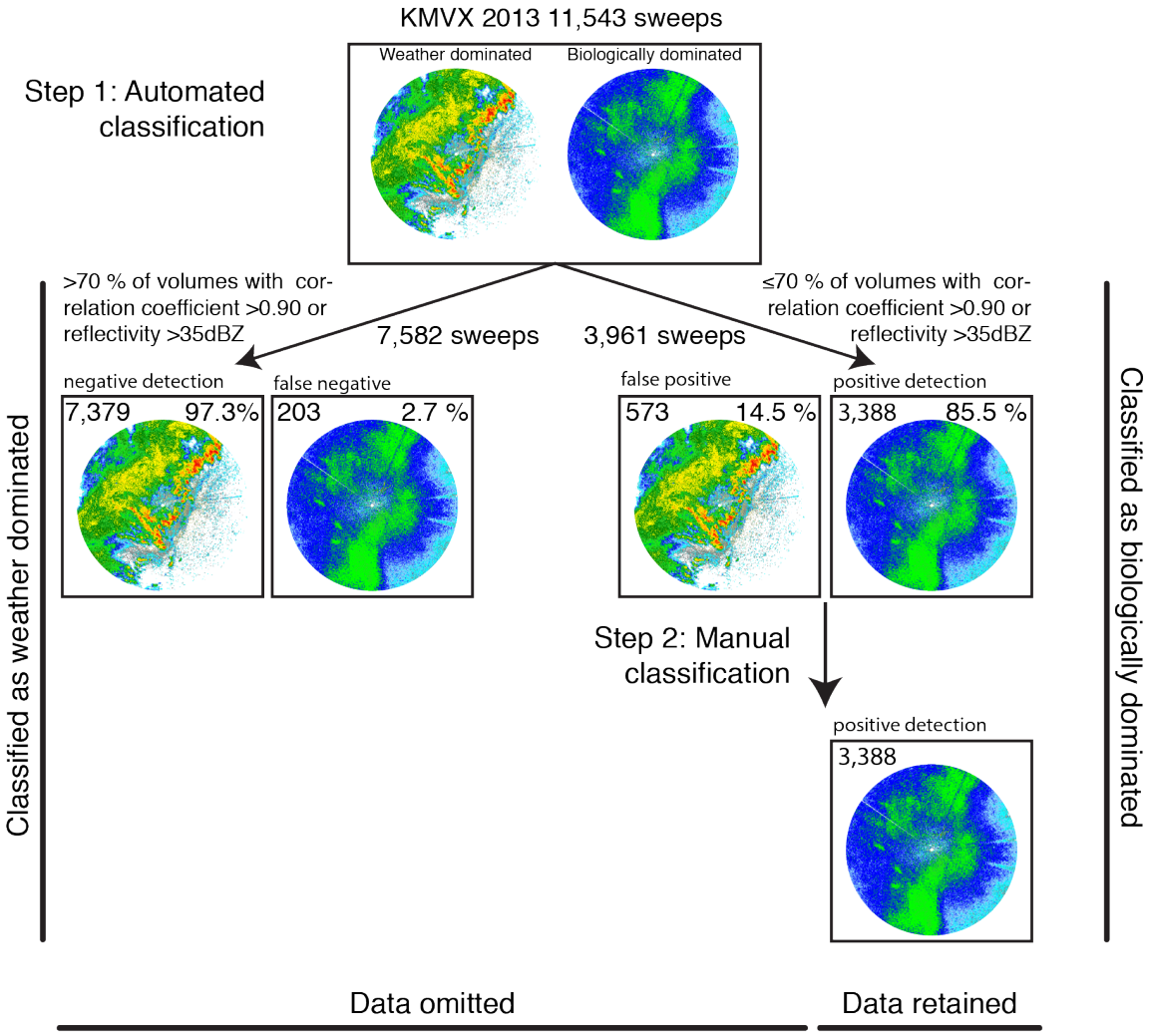

Figure 5.2: Visualization of two-stage (1. automated and 2. manual) radar classification workflow. Data retained following manual classification were further filtered by derived features of flight airspeeds (omitted if <5 ms^{-1}), velocity azimuth display RMSE (omitted if <1 or >5), polarimetric azimuth displays R^2 (omitted if <0.15), and profile heading standard deviation (omitted if $>20°$).

with greater than 15% of the variance explained (when fitting ρ_{HV} to a sinusoid) and an average standard deviation in heading direction that was less than 20° (Stepanian and Horton 2015, Horton et al. 2016c). Profiles of track and heading were weighted by log-scaled reflectivity (a measure that scales with biological density), constructed from the lowest five elevation scans, (0.5-4.5°) from 5 to 37.5 km (Farnsworth et al. 2015).

For statistical weighting and phenological indices of aerial movements, we calculated the large-scale (20 to 125 km) intensity of migratory movements from the lowest elevation sweeps (∼0.5°) of reflectivity. We calculated intensity (i.e., phenology indices) and directional data from the lowest sweep because it provides a large-scale perspective of migratory behaviors, and we constructed vertical profiles of reflectivity at closer ranges and higher elevation scales because they allow a better sampling of the altitudinal distribution of birds (Buler and Diehl 2009). We summarized radar measures to tenths of the night (i.e., deciles) to avoid sampling changes caused by the duration of the night. We only used data from individual radars on nights where two or more radars acquired usable samples (e.g., those that were dominated by biology) through the night and five or more deciles of the night were sampled at the individual radar. Overall, we retained 106,772 sweeps across 238 unique sampling nights (17,080 unique deciles) from three spring migratory seasons.

5.2.2 Winds Aloft

We quantified wind direction and variance aloft using the North American Regional Reanalysis (NARR) data set (Mesinger et al. 2006). NARR models zonal and meridional wind components every three hours at 25 hPa increments at a gridded 32-km spatial resolution. To characterize general nocturnal wind patterns, regardless of migratory activity and precipitation conditions, we extracted 03:00 UTC wind speeds and directions from measures between typical avian flight height ranges of 350

and 650 meters above ground level (875 -975 hPa)(La Sorte et al. 2015a, Horton et al. 2016a), weighting directions by wind speed. All dates between 1 March and 31 May from 2013 to 2015 were used to characterize average wind patterns.

For linking biological measures with wind speeds and directions, we aligned the nearest radar measures by time and height above ground level (55 to 1995 m). We weighted the vertical structure of wind speed and direction by vertical profiles of reflectivity. We weighted decile measures of wind direction by the product of migration intensity and wind speed. In addition to determining the dominant wind regimes within the radar coverage areas, we used winds aloft to calculate migrant airspeed (powered flight speed). Knowing groundspeed, wind direction, and wind speed, we calculated migrant airspeeds through vector subtraction. We eliminated radar samples with migrant airspeeds greater than 30 ms^{-1} ($n = 67$ deciles, $\sim$0.99 quantile). As an additional step to limit insect contamination, we eliminated decile samples with airspeeds less than 5 ms^{-1} (Larkin 1991; Gauthreaux and Belser 1998).

5.2.3 eBird

We used spatio-temporal exploratory models (STEM) (Fink et al. 2010) to estimate weekly probability of occurrence of nocturnally migrating bird species using bird observations from eBird (Sullivan et al. 2014) compiled during the period 2004 to 2011. From 446 species, we classified 234 as nocturnal migrants, 175 of which had probabilities of occurrence >than 0 in our sampling area (see Table 5.1). STEM models use underlying landscape (landcover, elevation), temporal (year, day of year, time of day), location (latitude and longitude), and effort (duration, distance, number of observers) information to learn associations of species occurrence. For the STEM analysis, eBird data were limited to stationary and traveling counts ($\leq$ 8.1 km) with start times between 05:00 and 20:00 and counts that were less than 3 hours in duration. The weekly estimates of probability of occurrence for each species were rendered at

130,751 points at a density of *ca.* 15 per 30 × 30 km within the contiguous USA using a geographically stratified random design (SRD) (see Figure 5.3). We used previously described methods to remove SRD points that contained very low probabilities of occurrence (La Sorte et al. 2014). Specifically, we converted weekly estimates of probability of occurrence to zero that were less than or equal to the 80th percentile of the non-zero occurrence probabilities for that week, and if the 80th percentile was <0.0175, which defined our minimum probability threshold, the probability threshold was set to 0.0175.

We calculated the mean probability of occurrence for species at each WSR station during each week using the SRD points that occurred within a 125 km radius of each WSR station (see Figure 5.3). We defined presence/absence for the species richness calculations if the mean probability of occurrence of a species at a WSR station was greater than 0.0175 (La Sorte et al. 2014). We derived body mass estimates for each of the 175 species from Dunning (2008) – sex- and subspecies-specific masses were averaged following La Sorte et al. (2015b). To summarize behavioral differences among major taxonomic groupings, we investigated the region's three most species-rich orders: songbirds (Passeriformes; $n = 127$, mean mass = 22.4 g), shorebirds (Charadriiformes; $n = 18$, mean mass = 159.4 g), and waterfowl (Anseriformes; $n = 14$, mean mass = 851.6 g).

We used Nature Serve breeding range map polygons (Ridgely et al. 2007) to estimate the direction of movement and distance between centers of species' distributions and radar locations for the 175 species. We used the angles and distances to predict the population-level direction of movement of species reflected in the radar measures. For each radar station, we calculated the angle from the station to the center of the breeding range following formulae by (Snyder 1987). We calculated the shortest geographic distance (i.e., the great-circle distance) between the breeding range center and radar location using the Haversine formula (Sinnott 1984). We only

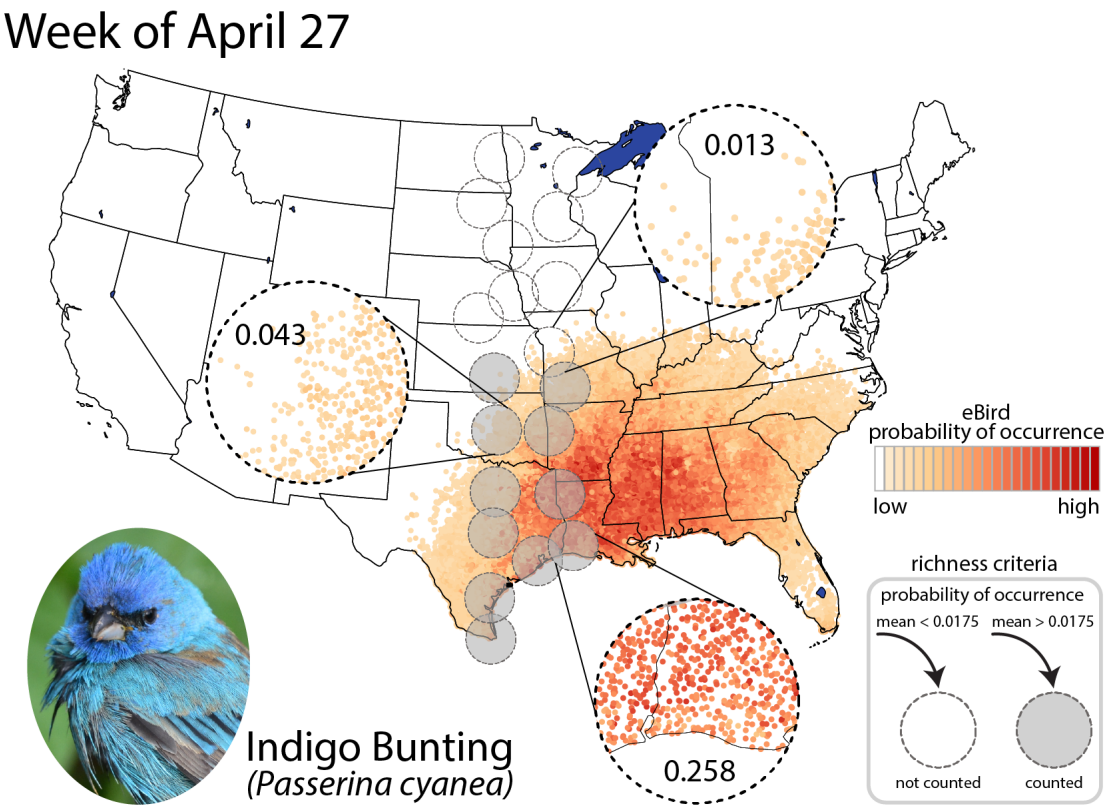

Figure 5.3: Schematic representation of the probability of occurrence of the Indigo Bunting (*Passerina cyanea*) during the week of 27 April across points of a stratified random design (SRD) rendered at a density of *ca.* 15 points per 30 × 30 km (130,751 points in total). SRD points counted towards species richness (gray) if the mean probability of occurrence within the radar domain (125 km radius) was greater than 0.0175. Mean probabilities of occurrence are displayed in the three magnified radar domains (e.g., 0.258). SRD points with a probability of occurrence less than 0.020 are not displayed.

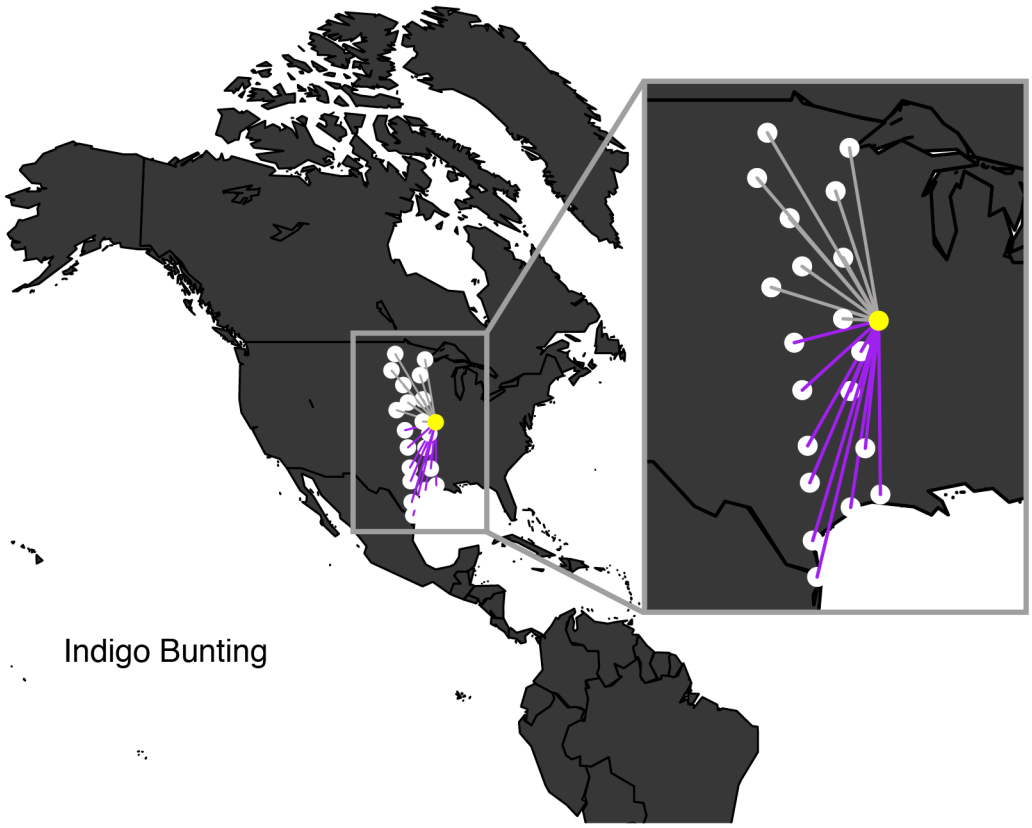

Figure 5.4: Visual representation for Indigo Bunting (*Passerina cyanea*) of the angle toward the geographic center of the breeding range. Note, angles were not considered for radar locations north of the geographic center of the breeding range (gray lines).

retained distances having angles $< 90°$ and $> 270°$ because these species should be making progress northward towards their breeding range. For each radar station and week, we calculated the mean angle of all species (Figure 5.4, Figure 5.5), weighted by the proportional occurrence from STEM models. The proportional occurrence was calculated weekly, dividing species-specific STEM model occurrences within the radar domain by the weekly summed total occurrence (for all species) within the radar domain.

A primary approach we used to assess species-level differences in flight strategies was through analysis of early vs. peak season migration. We took this approach because large-bodied waterfowl characterize early season spring migration, whereas

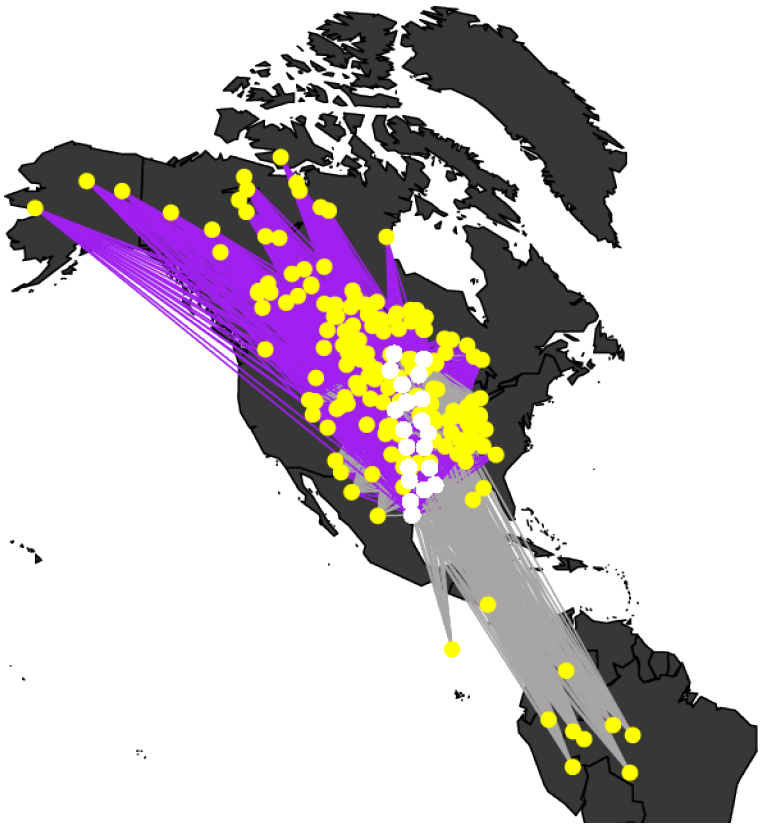

Figure 5.5: Visual representation for all of the species considered in the analysis ($n = 175$) of the angle toward the geographic center of each species' breeding range. Note, angles were not considered for radar locations north of the center each species breeding range (gray lines).

songbirds dominate peak season migration (Saunders 1959). To delineate early and peak migratory periods, we estimated the maximum daily increase in species richness at each radar site. This was achieved by fitting a generalized additive model (GAM; Wood 2011) to radar-specific measures of species richness based on STEM estimates. Across sites, the average maximum increase occurred on 23 April. To create balanced temporal periods, we defined the early phase as 17 March to 23 April and the peak phase between 24 April and 31 May. Each period contains 38 days. The early phase constituted an average (±SD) species richness of 87.05 ±29.39 and average body mass

of 309.31 ±202.73 g. Comparatively, the peak period had an average species richness of 116.22 ±15.98 and body mass of 162.08 ±94.44 g. The paired differences across periods by radar were significantly different in both accounts (richness: t_{19} = -4.80, p <0.001; body mass: t_{19} = 5.00, p <0.001).

5.2.4 Statistical analysis

We used the methods of Green and Alerstam (2002) to determine degree of compensation for wind drift. In brief, a mixed model approach is used to regress radar measures of track on the difference between track and heading (α) (Green and Alerstam 2002). The α parameter is used to derive two important metrics describing migrant flight strategy: (1) slope of α versus track, a measure of the propensity of drift (0– complete wind drift compensation, 1– complete wind drift), and (2) y-intercept, a measure of preferred direction of movement (Chapman et al. 2011, Kemp et al. 2012). Propensity of drift is equivalent elsewhere to the degree of compensation. We limited our analyses to samples with α between -120 and 120. We further regressed site-specific measures of the slope of α on radar latitude to examine latitudinal variation in the propensity of drift.

To limit pseudoreplication from repeated measures of decile samples, we included a number of random effects: station, year, and ordinal date as random intercepts and α as a random slope. These were grouped as follows: α|ordinal date, α|station:year, and α|station:year:ordinal date. These analyses were weighted by scaled radar reflectivity. All statistical analyses were conducted in R version 3.0.2 (R Core Team 2017), and linear mixed models implemented using the lme4 and lmerTest packages (Kuznetsova et al. 2014, Bates et al. 2014).

We used paired *t*-tests to contrast early and peak season factors (e.g., airspeed, slope of α, preferred direction of movement, species richness, body mass, etc.). All

summary statistics are reported with 95% confidence intervals.

5.3 Results

5.3.1 Weather surveillance radar data

Migratory activity increased during the second week of April and peaked between 30 April and 20 May. Date of peak reflectivity correlated with latitude (r = 0.89, t_{18} = 8.02, p <0.001), showing a 10-day difference between latitudinal extremes (KBRO and KMVX) (Figure 5.6). Overall, track direction averaged slightly more eastward-facing (3.20° ±5.66) than heading (359.13° ±6.78) (Figure 5.1). Flight directions changed systematically with latitude, with track shifting 2.30° ±0.48 (p <0.001) and heading 3.23° ±0.61 (p <0.001) westward with each increase in degree latitude. Airspeeds declined throughout the season for 18 of 20 sites, most sharply for high latitude sites (Figure 5.7a). Airspeeds averaged 1.53 ±0.85 ms^{-1} faster during the early period as compared to the peak period (t_{19} = -3.84, p <0.01).

Across the entire season, the propensity of drift did not change significantly with latitude (slope = 0.006 ±0.007, p = 0.083). However, early and peak season movements showed divergent flight strategy relationships with latitude (Figure 5.8). Early season movements showed a non-significant change in propensity of drift with latitude (slope = -0.006 ±0.01, p = 0.28), while peak movements showed an increasing propensity of drift with latitude (slope = 0.013 ±0.008, p <0.05). Propensity of drift was significantly lower earlier (mean = 0.23 ±0.07) in the season compared to later (mean = 0.42 ±0.06) in the season (mean of differences = 0.18, t_{19} = 3.51, p <0.01).

Radar-derived preferred direction of movement shifted westward with increasing latitude for both early (slope = 2.27° ±0.82, p <0.001) and peak periods (slope = 2.75° ±0.88, p <0.001) (Figure 5.1, Figure 5.11). The mean paired differences at radar stations in preferred direction of movement between early and peak season

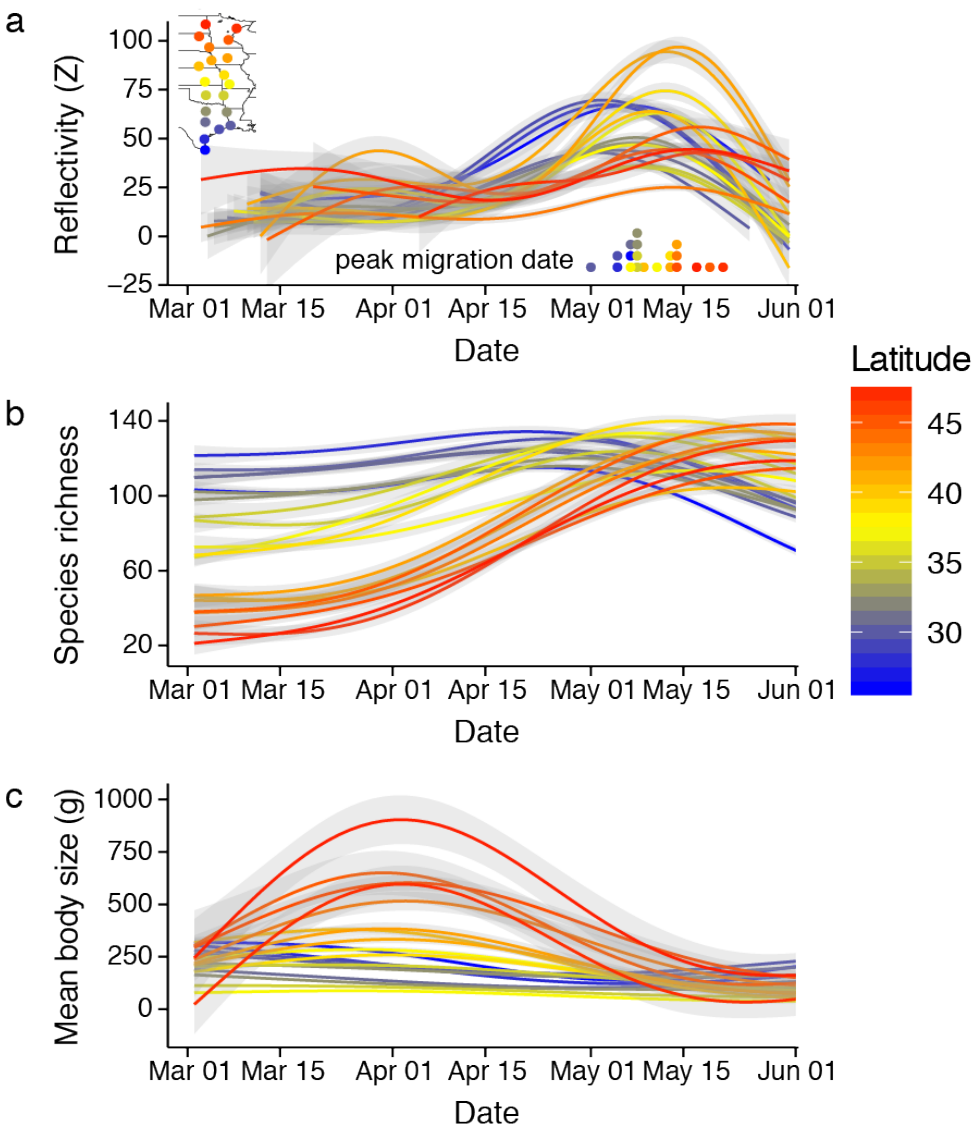

Figure 5.6: Bird migration characterizations by time and latitude in the central USA. (a) Reflectivity as measured by 20 weather surveillance radar (WSR) stations during spring migration (2013-15). The fitted lines and 95% confidence bands are from generalized additive models. The colored points are the estimated peak migration date (highest modeled reflectivity) for each WSR station. Points depicted in multiple rows because of overlapping date. (b) Weekly species richness and (c) mean body size of migrating birds based on STEM estimates of probability of occurrence using bird observations from eBird.

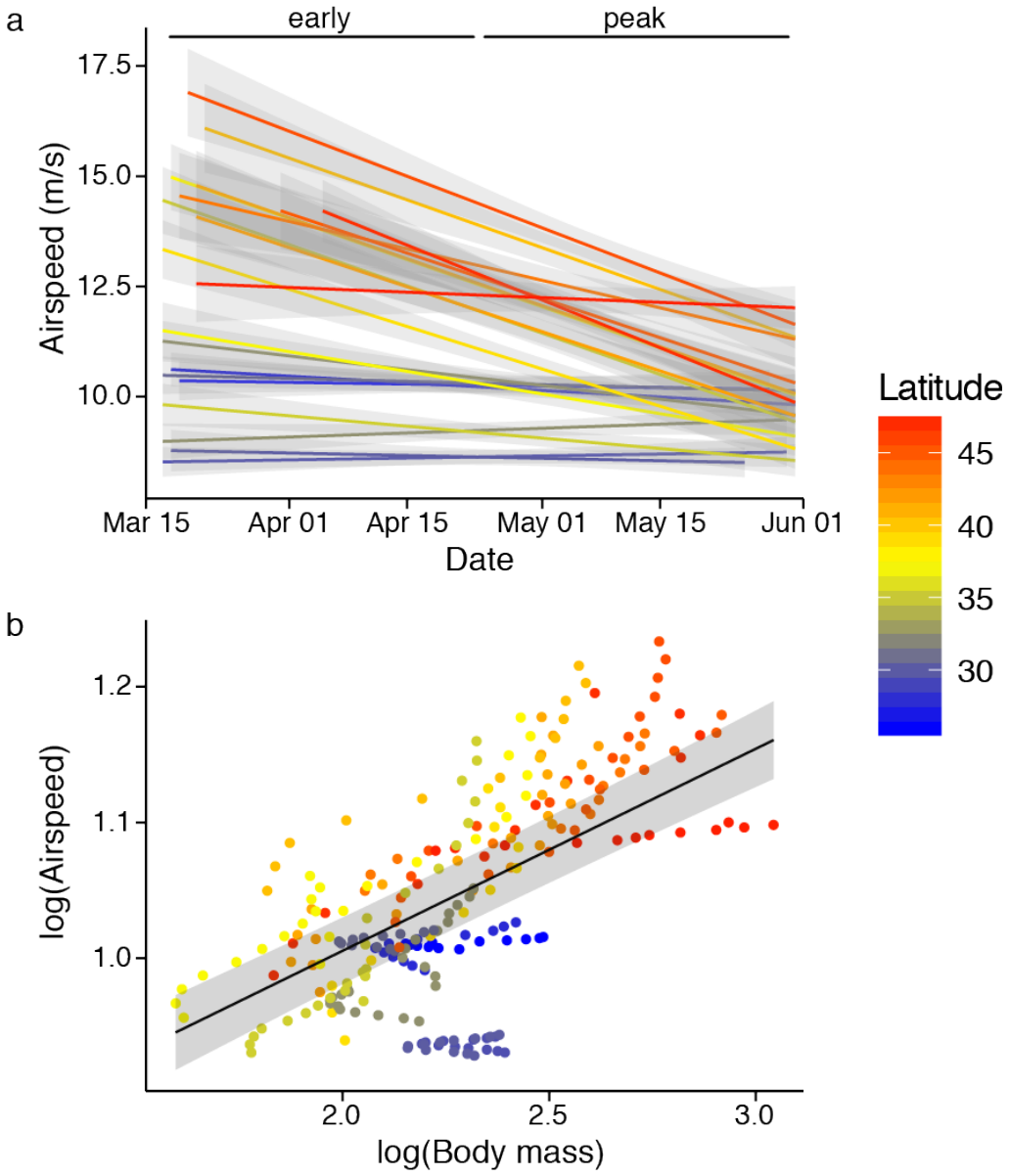

Figure 5.7: (a) Airspeeds of migrants from 17 March to 31 May measured at 20 weather surveillance radar stations during spring migration (2013-15). The fitted lines and 95% confidence bands are from least squares linear models. (b) Log-transformed predicted migrant airspeed (ms^{-1}) and averaged body mass (g). The fitted line and 95% confidence band is from a linear mixed model with radar ID and ordinal date as random effects.

movements was 3.89°, with no statistical difference between early and peak season directions ($t_{19} = 1.55$, $p < 0.14$).

5.3.2 eBird

Species richness generally increased throughout the season, rising more rapidly with increasing latitude (Figure 5.6b). The average body mass of species detected at each WSR station increased sharply early in the season and then decreased after the peak body size, particularly for northern sites (i.e., KMVX, KDLH, KABR, KMPX; Figure 5.6c). This marked peak in migrant body size centered on early April was driven by shifts in species composition (Figure 5.9); large-bodied Anseriformes dominated early season occurrence patterns but gave way to small-bodied Passeriformes during peak movement periods. Like radar-derived preferred directions of movement, our eBird predicted directions of movement shifted westward with increasing latitude for both early (slope = 2.83° ±0.84, p <0.001) and peak periods (slope = 2.46° ±1.22, p <0.001) (Figure 5.11).

Average distance to range center decreased with increasing ordinal date (20 of 20 sites, latitude as random effect: slope = -11.31±0.37, p <0.001, df = 239, Marginal $R^2 = 0.63$) and increasing latitude (ordinal date as random effect: slope = -19.30 ±3.56, df = 246, Marginal $R^2 = 0.10$) (Figure 5.10).

5.3.3 Combining radar and eBird

At a weekly time interval, body mass estimated from eBird STEM models explained variation in average airspeed (slope = 0.15 ±0.020, p <0.001, df = 94.79, marginal $R^2 = 0.35$; Figure 5.7b). Predicted direction of movement from eBird explained 64-66% of the variation in radar-derived preferred direction of movement estimates (early season: $r = 0.80$, df = 18, p <0.001; peak season: $r = 0.81$, df = 18,

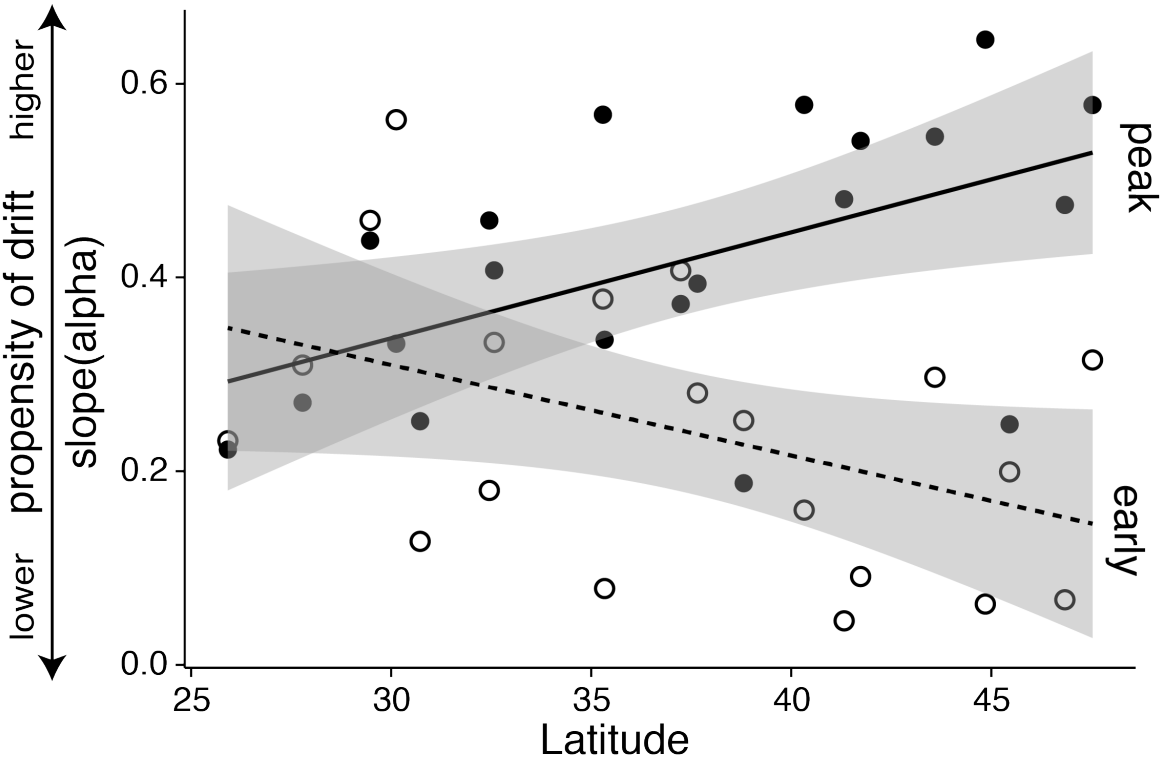

Figure 5.8: Wind drift propensity across latitudes during early (17 March to 23 April; hollow points, dotted line) and peak (24 April to 31 May; solid points, solid line) spring migratory periods at 20 weather surveillance radar stations during spring migration (2013-15). Slope of α represents drift propensity; 0 is complete compensation for wind, 1 is complete drift with wind. The fitted line and 95% confidence bands are from least squares linear regression.

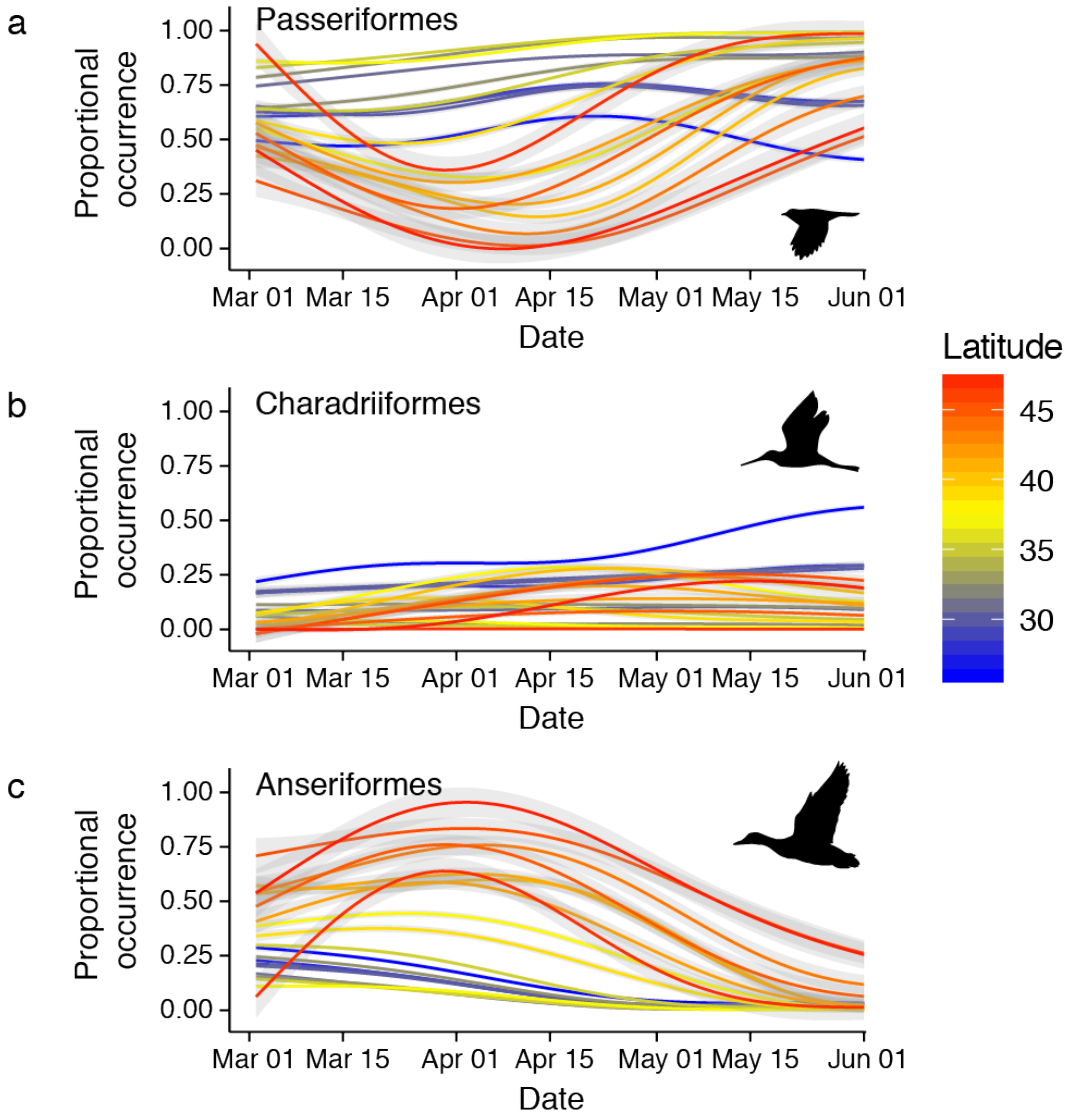

Figure 5.9: Proportional occurrence of (a) songbirds (Passeriformes, 127 species), (b) shorebirds (Charadriiformes, 18 species), and (c) waterfowl (Anseriformes, 14 species) at 20 weather surveillance radar stations at a weekly temporal resolution during spring migration summarized during the period 2004-2011. Proportional occurrence is the sum of taxonomic occurrence divided by the sum of taxonomic occurrence across the three orders derived from STEM models. Fitted lines and 95% confidence bands are from generalized additive models applied to each WSR station. The color of the fitted lines corresponds to the latitude of the WSR station.

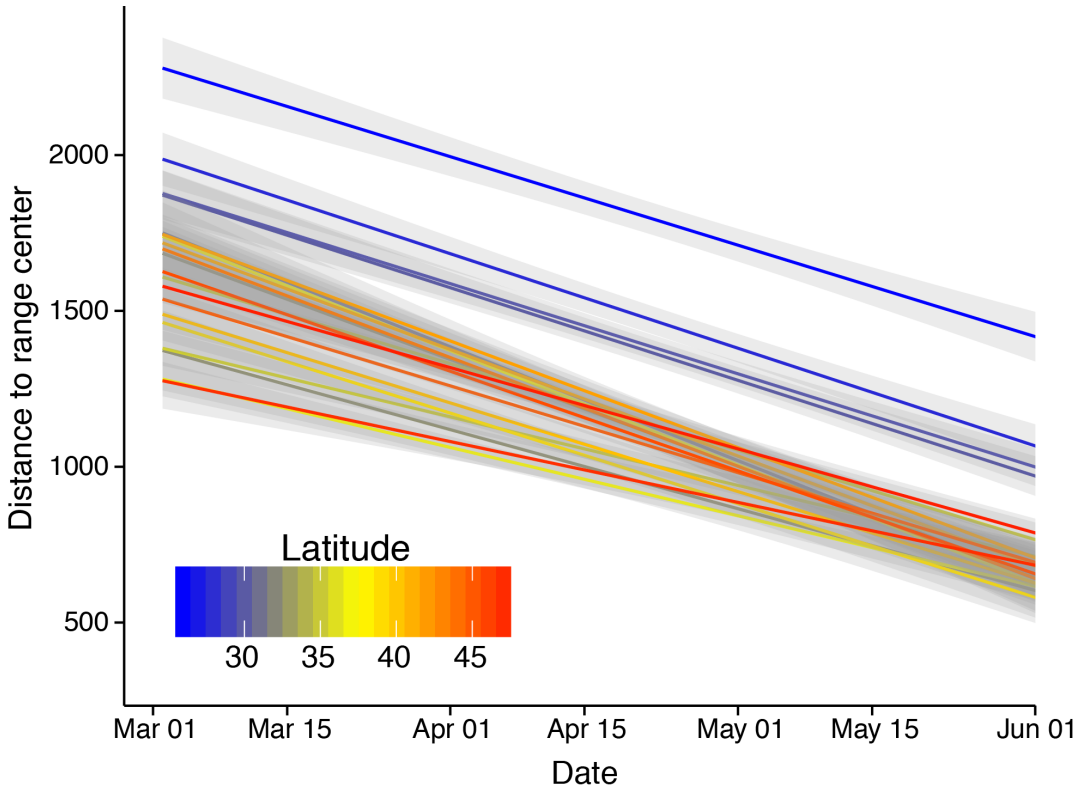

Figure 5.10: Average distance between the geographic center of each species' breeding range ($n = 175$) and 20 weather surveillance radar (WSR) stations. Only distances with angles between range center and radar locations $< 90°$ and $> 270°$ were included. Radar location color scaled in accordance to latitude. The fitted lines and 95% confidence bands are from least squares linear models fit for each WSR station.

p <0.001; Figure 5.11).

5.3.4 Wind

Seasonal wind direction originated increasingly from the west at higher latitudes (slope = 5.82° ±1.54, p <0.001, r = 0.87) and became more variable in direction at higher latitudes (slope of variance = 1.83° ±0.26, p <0.001, r = 0.96) (Figure 5.12a-b). Similarly, although less dramatically, wind directions weighted by migratory activity showed a westerly shift at higher latitudes across early (slope = 1.26° ±0.64, p <0.01) and peak migration periods (slope = 1.53° ±1.08, p <0.05) (Figure 5.12c). Additionally, winds used by migrants were more variable in direction with increasing latitude, more weakly so for early movements (slope = 0.43° ±0.47, $p = 0.09$) than peak migration periods (slope = 1.23° ±0.39, p <0.001) (Figure 5.12d).

5.4 Discussion

We show for the first time how in-flight strategies of migratory birds change across a broad latitudinal gradient. The extent to which migrants adjusted for wind drift varied through central USA. Faster-flying migrants, who are better able to compensate for wind drift, dominated the early migration period. Early season migrants did not change their propensity of drift with increasing latitude, although across latitudes the propensity of drift was significantly lower in the early phase as compared to peak phase. Peak season migrants showed similar levels of wind drift at low latitudes compared to early season migrants, however they increased their propensity to drift with increasing latitude. Thus, peak season migrants at high latitudes drifted more than did early season migrants passing through the same regions. Ground-based records of species composition corroborate the seasonal shift from early large-bodied,

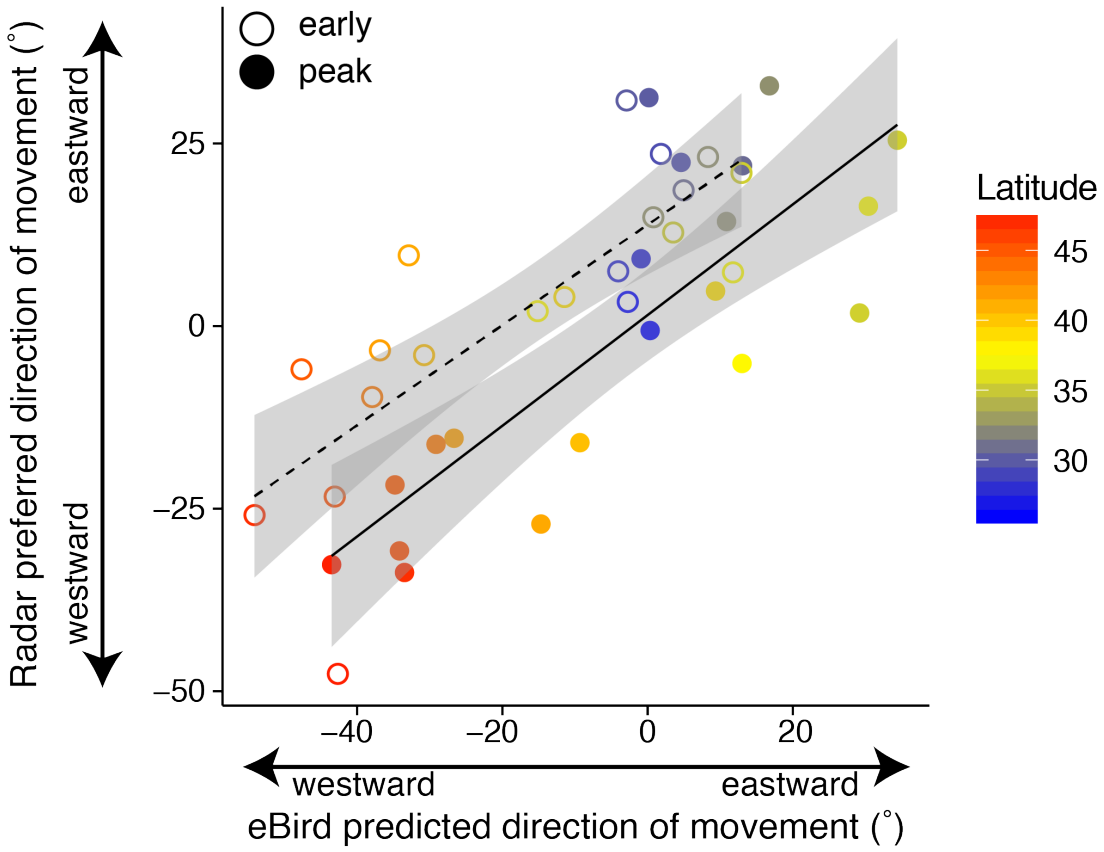

Figure 5.11: Radar preferred direction of movement and eBird predicted direction of movement during early (17 March to 23 April; hollow points, dotted line) and peak (24 April 24 to 31 May; solid points, solid line) spring migratory periods at 20 weather surveillance radar (WSR) stations during spring migration (2013-15). Fitted lines and 95% confidence bands estimate associations during early (dashed, R^2 = 0.64) and peak season migration (solid, R^2 = 0.66). WSR station color corresponds to its latitude.

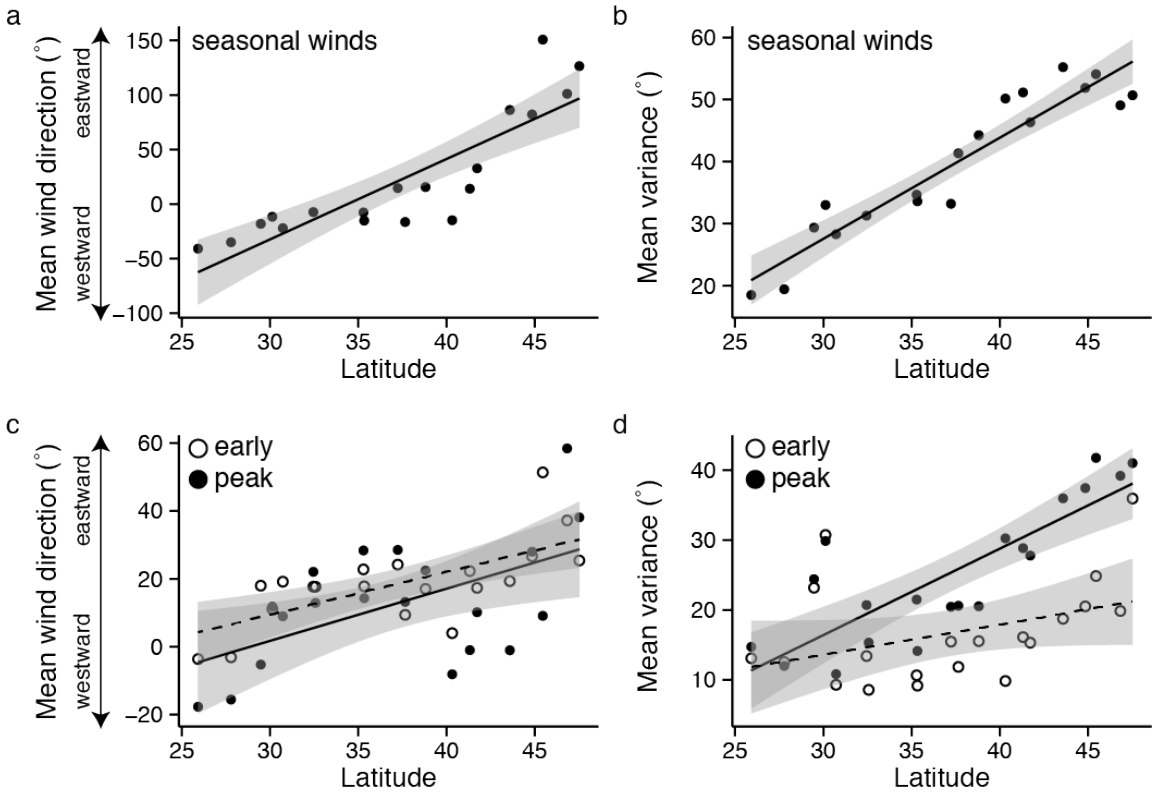

Figure 5.12: (a) Wind direction and (b) variance in wind direction weighted by wind speed between 1 March and 31 May regardless of migratory activity across radar latitudes. Winds modeled from 3 UTC between 350 and 650 m above ground level. (c) Wind direction and (d) variance in wind direction during early (17 March to 23 April; hollow points, dotted line) and peak (24 April to 31 May; solid points, solid line) spring migratory periods weighted by the product of migratory activity and wind speed. The fitted lines and 95% confidence bands are from least squares linear models.

faster flying migrants to peak-period small-bodied, slower flying migrants, lending insight to the temporal differences in flight strategies.

A migrant's maximum airspeed limits its ability to compensate for wind drift (Alerstam 1979, Green and Alerstam 2002). We found seasonal declines in airspeeds through our study region. Large-bodied birds, which can fly faster as a function of their morphology, have greater capacity to counter wind drift (Pennycuick 1969, Alerstam and Hedenström 1998, Alerstam et al. 2007, Hedenström 2008). We showed that average body mass from ground-based observations scaled positively with in-flight nocturnal airspeeds, strengthening the linkage of these disparate data sets. Our results suggest that differences in morphology of migrants (e.g., between waterfowl and songbirds) underlie some of the temporal and geographic differences we observed in flight behavior of nocturnally migrating birds moving through the center on North America. This is evidence that changes in species composition as reflected in morphology, such as body size, is an important consideration in understanding the broad-scale dynamics of migration systems.

Migration systems are complex and embody the integration of numerous biotic and abiotic components. We suggest that primary drivers of patterns in compensation for wind drift are driven by species' morphology, and geographic and seasonal variation in wind direction. Winds aloft, in particular, may be an important factor determining the seasonal composition of migrants within a flyway. Geographic tendencies in wind direction and speed may shape observed flight behaviors, as well as their phenologies. The low-level nocturnal jet stream of the Great Plains brings strong, southerly winds from the Gulf of Mexico, generally peaking in intensity through the mid-latitudes of the United States (Walters et al. 2008). The low-level jet influences spring migratory pathways (La Sorte et al. 2014) and nightly flight behaviors (e.g., flight height selection; Wainwright et al. 2016). Additionally, this low-level jet, in concert with polar and subtropical jets (i.e., those that drive synoptic weather

patterns west to east; Archer and Caldeira 2008, Pena-Ortiz et al. 2013), helps to explain our findings of winds originating increasingly from the west at higher latitudes, in addition to greater seasonal variation in wind directions at more northerly sites. Our findings carry particular significance when considering the implications of projected changes in the region's prevailing winds under global warming. The low level jet in the south is projected to increase in strength (Cook et al. 2008), and the prevailing westerlies in the north are projected to decrease in strength (Francis and Vavrus 2012, Li et al. 2012); the former may increase migration speeds, while the latter may diminish the need for compensation (La Sorte and Fink 2016). In total, these changes may enhance flight efficiency during spring migration.

In the context of bird flight strategies, optimal migration theory predicts that migrants should increase compensation to minimize time and energy expenditure as they approach their end destination (Liechti 2006). However, this is predicated on the expectation that the wind environment is constant across the latitudinal gradient. We found that with increasing latitude wind directions were increasingly in opposition to directions of movement (radar and eBird). Our initial prediction was very general and did not account for this possibility. Divergent flight strategies are not surprising given the prevailing biogeography of winds aloft (e.g., McLaren et al. 2012, 2014) and the divergent capacity of migrants to compensate for drift based on body size as a determinant of flight speed. Birds moving towards the northwest contend increasingly with westerly crosswinds at higher latitudes, compounding the effort needed to compensate for wind drift during a westward shift in directions of movement with increasing latitude. These factors suggest that peak season migrants do not compensate for increasingly unfavorable winds. It must be noted, however, that it remains difficult to assess the influence of pseudodrift in our findings, specifically for peak season movements. The non-uniformity in preferred flight directions among different species or populations and their choice to fly under different wind conditions can manifest

in the appearance of enhanced levels of drift (i.e., pseudodrift) (Evans 1966, Nisbet and Drury 1967, Alerstam 1978). Our statistical approach aimed to limit pseudodrift, accounting for inter-night variation in flight direction using random effects and leaving the fixed effects to describe average patterns within the migratory periods. However, without detailed knowledge of the relationship between the probability of departure and wind direction and speed, quantifying pseudodrift remains a principle challenge. The question of the general behavioral mechanisms that enable individual migrants to cope with these unfavorable conditions and ultimately arrive precisely at their destinations remains open. These findings clearly contrast with predictions from migration theory and highlight the need for more empirical studies to understand how stochastic natural environments shape migratory behaviors across spatial and temporal scales.

Understanding the flight strategies of hundreds of species of nocturnally migrating birds at large spatial scales is intrinsically challenging. Natural history, in addition to morphology and atmospheric characteristics, are factors that may govern in-flight wind drift strategies. For instance, wintering and breeding site specificity, geographic range, and incidence and potential for stopover may yield context-dependent flight strategies. Only recently has work begun to broaden our knowledge of the geographic positioning of flyways (La Sorte et al. 2014), and species-specific seasonal flyway usage (La Sorte et al. 2016). We documented a shift in the preferred direction of movement across latitudes, with increasingly westerly directions at higher latitudes. We were able to reproduce this pattern with information about species composition from ground-based eBird observations and direction to destination, which suggests that this phenomenon occurs because species with northerly distributions tend to have range centers in western North America (Figure 5.5). Our study area covers portions of two major flyways utilized by aquatic and terrestrial species, which are critical to understanding migratory systems that feed a significant portion of the breeding range

of North America's migratory bird species. These taxonomically diverse flyways have received little attention, especially at a system-level. Our work adds to a growing literature detailing the plasticity of system-level flight characteristics (e.g., daily, seasonal, and geographic, (Horton et al. 2016a, 2016b, 2016c, Van Doren et al. 2016). Landscape and climate changes make quantifying behavioral plasticity paramount to understand how migrants cope with broad-scale environmental change.

5.5 Conclusions

This is the first study to examine migratory flight strategies across an entire flyway. We used radar and ground-based observations to quantify and qualify large-scale movements, revealing phenological differences in flight activity, characterized by a shifting mosaic of underlying species composition. The linkage between these data and the ability to substantiate one another points to the future of large-scale analyses for whole migratory systems, revealing dominant flight strategies and their determinants for millions of migrating birds.

Table 5.1: Composition of nocturnally migrating bird species used in analyses. Distance between breeding and wintering grounds derived from Nature Serve range map polygons (Ridgely et al. 2007). Body mass estimates for each of the 175 species from Dunning (2008) – sex and subspecies-specific masses were averaged following La Sorte et al. (2015).

Common Name	*Scientific Name*	Distance (km) (breeding - wintering)	Body Mass (g)	Order	Family
Acadian Flycatcher	*Empidonax virescens*	3457.7	12.6	Passeriformes	Tyrannidae
Alder Flycatcher	*Empidonax alnorum*	7184.7	12.7	Passeriformes	Tyrannidae
American Avocet	*Recurvirostra americana*	1703.2	304.48	Charadriiformes	Recurvirostridae
American Golden-Plover	*Pluvialis dominica*	11962.8	151.47	Charadriiformes	Charadriidae
American Redstart	*Setophaga ruticilla*	3997.3	8.24	Passeriformes	Parulidae
American Robin	*Turdus migratorius*	1031.8	78.5	Passeriformes	Turdidae
American Tree Sparrow	*Spizella arborea*	2359.6	17.83	Passeriformes	Emberizidae
American Wigeon	*Mareca americana*	3222.6	754.61	Anseriformes	Anatidae
Ash-throated Flycatcher	*Myiarchus cinerascens*	1365.9	28.2	Passeriformes	Tyrannidae
Baird's Sandpiper	*Calidris bairdii*	11410.1	40.97	Charadriiformes	Scolopacidae
Baltimore Oriole	*Icterus galbula*	2894.8	32.83	Passeriformes	Icteridae
Bay-breasted Warbler	*Dendroica castanea*	4287.6	11.8	Passeriformes	Parulidae
Bell's Vireo	*Vireo bellii*	1537.3	8.5	Passeriformes	Vireonidae
Belted Kingfisher	*Megaceryle alcyon*	1884.9	148	Coraciiformes	Alcedinidae
Black-billed Cuckoo	*Coccyzus erythropthalmus*	5669.2	50.9	Cuculiformes	Cuculidae

Common Name	*Scientific Name*	Distance (km) (breeding - wintering)	Body Mass (g)	Order	Family
Black-capped Vireo	*Vireo atricapilla*	1186.1	8.99	Passeriformes	Vireonidae
Black-chinned Sparrow	*Spizella atrogularis*	488	11.3	Passeriformes	Emberizidae
Black-throated Gray Warbler	*Dendroica nigrescens*	2195.7	8.7	Passeriformes	Parulidae
Black Phoebe	*Sayornis nigricans*	78.3	18.63	Passeriformes	Tyrannidae
Black Turnstone	*Arenaria melanocephala*	3132.7	126.21	Charadriiformes	Scolopacidae
Blackburnian Warbler	*Dendroica fusca*	4942.1	9.74	Passeriformes	Parulidae
Blackpoll Warbler	*Dendroica striata*	6911.5	11.84	Passeriformes	Parulidae
Blue-gray Gnatcatcher	*Polioptila caerulea*	786.8	5.8	Passeriformes	Polioptilidae
Blue-headed Vireo	*Vireo solitarius*	2735	15.3	Passeriformes	Vireonidae
Blue-winged Teal	*Spatula discors*	3604.3	359.44	Anseriformes	Anatidae
Blue-winged Warbler	*Vermivora cyanoptera*	2354.1	8.9	Passeriformes	Parulidae
Blue Grosbeak	*Passerina caerulea*	1497.6	27.39	Passeriformes	Cardinalidae
Bobolink	*Dolichonyx oryzivorus*	8109.5	31.46	Passeriformes	Icteridae
Bohemian Waxwing	*Bombycilla garrulus*	2010.1	54.41	Passeriformes	Bombycillidae
Brown-crested Flycatcher	*Myiarchus tyrannulus*	715.6	35.45	Passeriformes	Tyrannidae
Brown Creeper	*Certhia americana*	270.4	8.1	Passeriformes	Certhiidae
Brown Thrasher	*Toxostoma rufum*	942.4	68.8	Passeriformes	Mimidae
Bufflehead	*Bucephala albeola*	2110.2	397.46	Anseriformes	Anatidae
Bullock's Oriole	*Icterus bullockii*	2069.9	37.9	Passeriformes	Icteridae

Common Name	*Scientific Name*	Distance (km) (breeding - wintering)	Body Mass (g)	Order	Family
Canada Warbler	*Wilsonia canadensis*	5217.1	10.04	Passeriformes	Parulidae
Canvasback	*Aythya valisineria*	2656.3	1202	Anseriformes	Anatidae
Cape May Warbler	*Dendroica tigrina*	4126.9	10.04	Passeriformes	Parulidae
Cassin's Sparrow	*Peucaea cassinii*	342.2	18.9	Passeriformes	Emberizidae
Cedar Waxwing	*Bombycilla cedrorum*	1607.7	31.58	Passeriformes	Bombycillidae
Chestnut-collared Longspur	*Calcarius ornatus*	1780.5	20.3	Passeriformes	Calcariidae
Chestnut-sided Warbler	*Dendroica pensylvanica*	3458.6	9.29	Passeriformes	Parulidae
Chimney Swift	*Chaetura pelagica*	5072.9	23.6	Apodiformes	Apodidae
Chipping Sparrow	*Spizella passerina*	1839.1	12.2	Passeriformes	Emberizidae
Cinnamon Teal	*Spatula cyanoptera*	1090	377.45	Anseriformes	Anatidae
Clay-colored Sparrow	*Spizella pallida*	2910.2	11.2	Passeriformes	Emberizidae
Common Nighthawk	*Chordeiles minor*	6980.5	79.3	Caprimulgiformes	Caprimulgidae
Common Yellowthroat	*Geothlypis trichas*	2156.4	9.54	Passeriformes	Parulidae
Connecticut Warbler	*Oporornis agilis*	6587.6	13.3	Passeriformes	Parulidae
Dark-eyed Junco	*Junco hyemalis*	1183.4	19.5	Passeriformes	Emberizidae
Dickcissel	*Spiza americana*	3533.9	26.18	Passeriformes	Cardinalidae
Dunlin	*Calidris alpina*	3489.2	51.89	Charadriiformes	Scolopacidae
Eastern Bluebird	*Sialia sialis*	836	27.5	Passeriformes	Turdidae
Eastern Kingbird	*Tyrannus tyrannus*	7071.6	39.85	Passeriformes	Tyrannidae

Common Name	*Scientific Name*	Distance (km) (breeding - wintering)	Body Mass (g)	Order	Family
Eastern Meadowlark	*Sturnella magna*	359.4	91.76	Passeriformes	Icteridae
Eastern Phoebe	*Sayornis phoebe*	1795.5	19.7	Passeriformes	Tyrannidae
Eastern Towhee	*Pipilo erythrophthalmus*	569.8	40.03	Passeriformes	Emberizidae
Eastern Wood-Pewee	*Contopus virens*	4888.3	13.9	Passeriformes	Tyrannidae
Field Sparrow	*Spizella pusilla*	512.2	12.5	Passeriformes	Emberizidae
Fox Sparrow	*Passerella iliaca*	2453.5	33.25	Passeriformes	Emberizidae
Golden-cheeked Warbler	*Dendroica chrysoparia*	1992.7	9.9	Passeriformes	Parulidae
Golden-crowned Kinglet	*Regulus satrapa*	812.1	6.19	Passeriformes	Regulidae
Golden-winged Warbler	*Vermivora chrysoptera*	3682.3	8.74	Passeriformes	Parulidae
Grasshopper Sparrow	*Ammodramus savannarum*	1343.9	17.61	Passeriformes	Emberizidae
Gray-cheeked Thrush	*Catharus minimus*	7256.8	31.58	Passeriformes	Turdidae
Great Blue Heron	*Ardea herodias*	1196.4	2523.41	Pelecaniformes	Ardeidae
Great Crested Flycatcher	*Myiarchus crinitus*	2848.5	32.1	Passeriformes	Tyrannidae
Great Egret	*Ardea alba*	914	871.33	Pelecaniformes	Ardeidae
Greater White-fronted Goose	*Anser albifrons*	4204.8	2506.39	Anseriformes	Anatidae
Greater Yellowlegs	*Tringa melanoleuca*	7123.1	161.74	Charadriiformes	Scolopacidae
Green-tailed Towhee	*Pipilo chlorurus*	1342.3	29.4	Passeriformes	Emberizidae
Green-winged Teal	*Anas crecca*	2281.9	341.89	Anseriformes	Anatidae
Groove-billed Ani	*Crotophaga sulcirostris*	89.9	82.04	Cuculiformes	Cuculidae

Common Name	*Scientific Name*	Distance (km) (breeding - wintering)	Body Mass (g)	Order	Family
Harris's Sparrow	*Zonotrichia querula*	3195	35.5	Passeriformes	Emberizidae
Henslow's Sparrow	*Ammodramus henslowii*	1088.2	12.8	Passeriformes	Emberizidae
Hermit Thrush	*Catharus guttatus*	2052.6	30.1	Passeriformes	Turdidae
Hooded Oriole	*Icterus cucullatus*	1060.1	24.3	Passeriformes	Icteridae
Hooded Warbler	*Wilsonia citrina*	1943.4	10.54	Passeriformes	Parulidae
House Wren	*Troglodytes aedon*	1142	10.85	Passeriformes	Troglodytidae
Hudsonian Godwit	*Limosa haemastica*	12785.2	253.29	Charadriiformes	Scolopacidae
Indigo Bunting	*Passerina cyanea*	2317.6	14.69	Passeriformes	Cardinalidae
Kentucky Warbler	*Oporornis formosus*	2315.7	14	Passeriformes	Parulidae
Killdeer	*Charadrius vociferus*	1610.1	96.44	Charadriiformes	Charadriidae
Lapland Longspur	*Calcarius lapponicus*	2782.3	27.84	Passeriformes	Calcariidae
Lark Bunting	*Calamospiza melanocorys*	1585.4	37.6	Passeriformes	Emberizidae
Lark Sparrow	*Chondestes grammacus*	1143.2	29	Passeriformes	Emberizidae
Le Conte's Sparrow	*Ammodramus leconteii*	2227.1	13	Passeriformes	Emberizidae
Least Flycatcher	*Empidonax minimus*	3545.6	10	Passeriformes	Tyrannidae
Least Sandpiper	*Calidris minutilla*	5981.3	22.88	Charadriiformes	Scolopacidae
Lesser Nighthawk	*Chordeiles acutipennis*	841.7	48.42	Caprimulgiformes	Caprimulgidae
Lesser Scaup	*Aythya affinis*	3673.7	819.45	Anseriformes	Anatidae
Lincoln's Sparrow	*Melospiza lincolnii*	2518.8	16.6	Passeriformes	Emberizidae

Common Name	*Scientific Name*	Distance (km) (breeding - wintering)	Body Mass (g)	Order	Family
Loggerhead Shrike	*Lanius ludovicianus*	567.5	51.59	Passeriformes	Laniidae
Long-billed Curlew	*Numenius americanus*	2005	583.86	Charadriiformes	Scolopacidae
Long-billed Dowitcher	*Limnodromus scolopaceus*	5770.1	104.4	Charadriiformes	Scolopacidae
Louisiana Waterthrush	*Parkesia motacilla*	2381.1	19.9	Passeriformes	Parulidae
Magnolia Warbler	*Dendroica magnolia*	3686.1	8.14	Passeriformes	Parulidae
Marbled Godwit	*Limosa fedoa*	2700.9	357.02	Charadriiformes	Scolopacidae
Marsh Wren	*Cistothorus palustris*	1117.9	10.8	Passeriformes	Troglodytidae
Mountain Plover	*Charadrius montanus*	1165.3	95.74	Charadriiformes	Charadriidae
Mourning Warbler	*Oporornis philadelphia*	4721.6	11.74	Passeriformes	Parulidae
Nashville Warbler	*Vermivora ruficapilla*	2695.1	8.09	Passeriformes	Parulidae
Nelson's Sparrow	*Ammodramus nelsoni*	2169.3	15.11	Passeriformes	Emberizidae
Northern Flicker	*Colaptes auratus*	1448.7	131.46	Piciformes	Picidae
Northern Mockingbird	*Mimus polyglottos*	115.9	48.5	Passeriformes	Mimidae
Northern Parula	*Parula americana*	2259.3	7.84	Passeriformes	Parulidae
Northern Pintail	*Anas acuta*	3217.1	944.62	Anseriformes	Anatidae
Northern Rough-winged Swallow	*Stelgidopteryx serripennis*	1745.4	15.69	Passeriformes	Hirundinidae
Northern Shoveler	*Spatula clypeata*	3495.2	612.56	Anseriformes	Anatidae
Northern Shrike	*Lanius excubitor*	2221.4	63.41	Passeriformes	Laniidae
Northern Waterthrush	*Parkesia noveboracensis*	4774.4	16.3	Passeriformes	Parulidae

Common Name	*Scientific Name*	Distance (km) (breeding - wintering)	Body Mass (g)	Order	Family
Olive-sided Flycatcher	*Contopus cooperi*	6760.5	32.1	Passeriformes	Tyrannidae
Orange-crowned Warbler	*Vermivora celata*	2906	9.19	Passeriformes	Parulidae
Orchard Oriole	*Icterus spurius*	2485.6	19.44	Passeriformes	Icteridae
Ovenbird	*Seiurus aurocapilla*	3206.4	18.8	Passeriformes	Parulidae
Painted Bunting	*Passerina ciris*	1569.9	15.54	Passeriformes	Cardinalidae
Palm Warbler	*Dendroica palmarum*	3084.5	10.3	Passeriformes	Parulidae
Philadelphia Vireo	*Vireo philadelphicus*	4078.9	11.5	Passeriformes	Vireonidae
Pine Warbler	*Dendroica pinus*	752.2	11.79	Passeriformes	Parulidae
Prairie Warbler	*Dendroica discolor*	1785.1	7.64	Passeriformes	Parulidae
Prothonotary Warbler	*Protonotaria citrea*	2527	14.3	Passeriformes	Parulidae
Red-eyed Vireo	*Vireo olivaceus*	4086.7	16.06	Passeriformes	Vireonidae
Red-headed Woodpecker	*Melanerpes erythrocephalus*	505	71.6	Piciformes	Picidae
Red-naped Sapsucker	*Sphyrapicus nuchalis*	1553.9	48.49	Piciformes	Picidae
Ring-necked Duck	*Aythya collaris*	2337.2	704.55	Anseriformes	Anatidae
Ringed Kingfisher	*Megaceryle torquata*	34.5	317	Coraciiformes	Alcedinidae
Rose-breasted Grosbeak	*Pheucticus ludovicianus*	3701.9	42	Passeriformes	Cardinalidae
Ross's Goose	*Anser rossii*	3322.4	1635.99	Anseriformes	Anatidae
Ruby-crowned Kinglet	*Regulus calendula*	2076.3	6.19	Passeriformes	Regulidae
Ruddy Duck	*Oxyura jamaicensis*	1176.9	608.15	Anseriformes	Anatidae

Common Name	*Scientific Name*	Distance (km) (breeding - wintering)	Body Mass (g)	Order	Family
Sage Thrasher	*Oreoscoptes montanus*	1523.6	44.2	Passeriformes	Mimidae
Sandhill Crane	*Antigone canadensis*	3024.1	4296.22	Gruiformes	Gruidae
Savannah Sparrow	*Passerculus sandwichensis*	2561.6	19.97	Passeriformes	Emberizidae
Say's Phoebe	*Sayornis saya*	2404	20.9	Passeriformes	Tyrannidae
Scarlet Tanager	*Piranga olivacea*	4900.6	28.2	Passeriformes	Cardinalidae
Scissor-tailed Flycatcher	*Tyrannus forficatus*	2187.3	39.3	Passeriformes	Tyrannidae
Seaside Sparrow	*Ammodramus maritimus*	138.5	22.16	Passeriformes	Emberizidae
Sedge Wren	*Cistothorus platensis*	593.4	9.04	Passeriformes	Troglodytidae
Semipalmated Sandpiper	*Calidris pusilla*	7141.5	27.5	Charadriiformes	Scolopacidae
Smith's Longspur	*Calcarius pictus*	3542	26.66	Passeriformes	Calcariidae
Snow Bunting	*Plectrophenax nivalis*	1913.4	42.2	Passeriformes	Calcariidae
Song Sparrow	*Melospiza melodia*	753.4	21.91	Passeriformes	Emberizidae
Spotted Towhee	*Pipilo maculatus*	503.1	39.28	Passeriformes	Emberizidae
Summer Tanager	*Piranga rubra*	3310.3	29.13	Passeriformes	Cardinalidae
Swainson's Thrush	*Catharus ustulatus*	5715.2	30.3	Passeriformes	Turdidae
Swainson's Warbler	*Limnothlypis swainsonii*	1603.9	18.9	Passeriformes	Parulidae
Swamp Sparrow	*Melospiza georgiana*	1898.2	16.1	Passeriformes	Emberizidae
Tennessee Warbler	*Vermivora peregrina*	4825.6	8.9	Passeriformes	Parulidae
Upland Sandpiper	*Bartramia longicauda*	9372.1	158.92	Charadriiformes	Scolopacidae

Common Name	*Scientific Name*	Distance (km) (breeding - wintering)	Body Mass (g)	Order	Family
Veery	*Catharus fuscescens*	7925	31.9	Passeriformes	Turdidae
Vermilion Flycatcher	*Pyrocephalus rubinus*	954.2	14.4	Passeriformes	Tyrannidae
Vesper Sparrow	*Pooecetes gramineus*	1715.1	25.68	Passeriformes	Emberizidae
Warbling Vireo	*Vireo gilvus*	2563.1	12.67	Passeriformes	Vireonidae
Western Kingbird	*Tyrannus verticalis*	3107.9	39.6	Passeriformes	Tyrannidae
Western Meadowlark	*Sturnella neglecta*	877.5	100.06	Passeriformes	Icteridae
Western Sandpiper	*Calidris mauri*	7193.1	27.82	Charadriiformes	Scolopacidae
White-crowned Sparrow	*Zonotrichia leucophrys*	2396.1	28	Passeriformes	Emberizidae
White-eyed Vireo	*Vireo griseus*	1122.6	11.4	Passeriformes	Vireonidae
White-faced Ibis	*Plegadis chihi*	343.9	616.89	Pelecaniformes	Threskiornithidae
White-throated Sparrow	*Zonotrichia albicollis*	1839.9	24.4	Passeriformes	Emberizidae
Willet	*Tringa semipalmata*	3023.2	245.7	Charadriiformes	Scolopacidae
Willow Flycatcher	*Empidonax traillii*	4046.6	13.39	Passeriformes	Tyrannidae
Wilson's Phalarope	*Steganopus tricolor*	9218.6	59.39	Charadriiformes	Scolopacidae
Wilson's Warbler	*Wilsonia pusilla*	3952.2	6.96	Passeriformes	Parulidae
Winter Wren	*Troglodytes troglodytes*	1127.8	9.74	Passeriformes	Troglodytidae
Wood Duck	*Aix sponsa*	469.4	657.59	Anseriformes	Anatidae
Wood Thrush	*Hylocichla mustelina*	2822.3	50.09	Passeriformes	Turdidae
Worm-eating Warbler	*Helmitheros vermivorum*	2057.7	14.16	Passeriformes	Parulidae

Common Name	*Scientific Name*	Distance (km) (breeding - wintering)	Body Mass (g)	Order	Family
Yellow-bellied Flycatcher	*Empidonax flaviventris*	4053.9	11.8	Passeriformes	Tyrannidae
Yellow-bellied Sapsucker	*Sphyrapicus varius*	2897.5	50.3	Piciformes	Picidae
Yellow-billed Cuckoo	*Coccyzus americanus*	5981.6	64	Cuculiformes	Cuculidae
Yellow-breasted Chat	*Icteria virens*	2466.4	24.89	Passeriformes	Parulidae
Yellow-green Vireo	*Vireo flavoviridis*	3412.7	17.59	Passeriformes	Vireonidae
Yellow-throated Vireo	*Vireo flavifrons*	2699	18	Passeriformes	Vireonidae
Yellow-throated Warbler	*Dendroica dominica*	1424.3	9.69	Passeriformes	Parulidae
Yellow Warbler	*Dendroica petechia*	3740	10.22	Passeriformes	Parulidae

References

Able, K. P. 1975. The orientation of passerine nocturnal migrants following offshore drift. Auk 94:320–330.

Able, K. P. 1977. The flight behaviour of individual passerine nocturnal migrants: a tracking radar study. Animal Behaviour 25:924–935.

Able, K. P., and M. A. Able. 1997. Development of sunset orientation in a migratory bird: No calibration by the magnetic field. Animal Bahviour 53:363–368.

Alerstam, T. 1978. A graphical illustration of pseudodrift. Oikos 30:409–412.

Alerstam, T. 1979. Wind as selective agent in bird migration. Ornis Scandinavica 10:76–93.

Alerstam, T. 2011. Optimal bird migration revisited. Journal of Ornithology 152:5–23.

Alerstam, T., G. A. Gudmundsson, M. Green, and A. Hedenström. 2001. Migration along orthodromic sun compass routes by Arctic birds. Science 291:300–303.

Alerstam, T., and A. Hedenström. 1998. The development of bird migration theory. Journal of Avian Biology 29:343–369.

Alerstam, T., A. Hedenström, and S. Åkesson. 2003. Long-distance migration: Evolution and determinants. Oikos 103:247–260.

Alerstam, T., and S. Petterson. 1976. Do birds use waves for orientation when migrating across the sea? Nature 259:205–207.

Alerstam, T., M. Rosén, J. Bäckman, P. G. P. Ericson, and O. Hellgren. 2007. Flight speeds among bird species: allometric and phylogenetic effects. PLOS Biology 5:e197.

Archer, C. L., and K. Caldeira. 2008. Historical trends in the jet streams. Geophysical Research Letters 35:L08803.

Aristotle, and D. M. Balme. 1991. History of animals. Books VII-X Books VII-X. Harvard University Press, Cambridge, Mass.

Arlt, D., P. Olsson, J. W. Fox, M. Low, and T. P*ä*rt. 2015. Prolonged stopover duration characterises migration strategy and constraints of a long-distance migrant songbird. Animal Migration 2:47–62.

B*ä*ckman, J., and T. Alerstam. 2003. Orientation scatter of free-flying nocturnal passerine migrants: Components and causes. Animal Behaviour 65:987–996.

B*ä*ckman, J., J. Pettersson, and R. Sandberg. 1997. The influence of fat stores on magnetic orientation in day-migrating Chaffinch, *Fringilla coelebs*. Ethology 103:247–256.

Bates, D., M. M*ä*chler, B. Bolker, and S. Walker. 2014. Fitting linear mixed-effects models using lme4. arXiv:1406.5823 [stat].

Berthold, P. 1991. Genetic control of migratory behaviour in birds. Trends in Ecology and Evolution 6:254–258.

Bingman, V. P., K. P. Able, and P. Kerlinger. 1982. Wind drift, compensation, and the use of landmarks by nocturnal bird migrants. Animal Behaviour 30:49–53.

Bonadonna, F., C. Bajzak, S. Benhamou, K. Igloi, P. Jouventin, H. P. Lipp, and G. Dell'Omo. 2005. Orientation in the Wandering Albatross: interfering with magnetic perception does not affect orientation performance. Proceedings of the Royal Society B: Biological Sciences 272:489–495.

Bowlin, M. S., W. W. Cochran, and M. Wikelski. 2005. Biotelemetry of New World thrushes during migration: Physiology, energetics and orientation in the wild. Integrative and Comparative Biology 45:295–304.

Bowlin, M. S., D. A. Enstrom, B. J. Murphy, E. Plaza, P. Jurich, and J. Cochran. 2015. Unexplained altitude changes in a migrating thrush: Long-flight altitude data from radio-telemetry. The Auk 132:808–816.

Bridge, E. S., J. F. Kelly, A. Contina, R. M. Gabrielson, R. B. MacCurdy, and D. W. Winkler. 2013. Advances in tracking small migratory birds: A technical review of light-level geolocation. Journal of Field Ornithology 84:121–137.

Bridge, E. S., K. Thorup, M. S. Bowlin, P. B. Chilson, R. H. Diehl, R. W. Fl*é*ron, P. Hartl, R. Kays, J. F. Kelly, W. D. Robinson, and M. Wikelski. 2011. Technology on the move: Recent and forthcoming innovations for tracking migratory birds. BioScience 61:689–698.

Browning, K. A., and R. Wexler. 1968. The determination of kinematic properties of a wind field using Doppler radar. Journal of Applied Meteorology 7:105–113.

Bruderer, B., and F. Liechti. 1998. Flight behavior of nocturnally migrating birds in coastal areas – crossing or coasting. Journal of Avian Biology:499–507.

Buhnerkempe, M. G., C. T. Webb, A. A. Merton, J. E. Buhnerkempe, G. H. Givens, R. S. Miller, and J. A. Hoeting. 2016. Identification of migratory bird flyways in North America using community detection on biological networks. Ecological Applications 26:740–751.

Buler, J. J., and D. K. Dawson. 2014. Radar analysis of fall bird migration stopover sites in the northeastern U.S. The Condor 116:357–370.

Buler, J. J., and R. H. Diehl. 2009. Quantifying bird density during migratory stopover using weather surveillance radar. IEEE Transactions on Geoscience and Remote Sensing 47:2741–2751.

Butler, C. J. 2003. The disproportionate effect of global warming on the arrival dates of short-distance migratory birds in North America. Ibis 145:484–495.

Chapman, J. W., R. H. G. Klaassen, V. A. Drake, S. Fossette, G. C. Hays, J. D. Metcalfe, A. M. Reynolds, D. R. Reynolds, and T. Alerstam. 2011. Animal orientation strategies for movement in flows. Current Biology 21:R861–R870.

Chapman, J. W., R. L. Nesbit, L. E. Burgin, D. R. Reynolds, A. D. Smith, D. R. Middleton, and J. K. Hill. 2010. Flight orientation behaviors promote optimal migration trajectories in high-flying insects. Science 327:682–685.

Chapman, J. W., C. Nilsson, K. S. Lim, J. Bäckman, D. R. Reynolds, and T. Alerstam. 2015a. Adaptive strategies in nocturnally migrating insects and songbirds: Contrasting responses to wind. Journal of Animal Ecology: 85:115–124.

Chapman, J. W., C. Nilsson, K. S. Lim, J. Bäckman, D. R. Reynolds, T. Alerstam, and A. M. Reynolds. 2015b. Detection of flow direction in high-flying insect and songbird migrants. Current Biology 25:R751–R752.

Chilson, P. B., W. F. Frick, P. M. Stepanian, J. R. Shipley, T. H. Kunz, and J. F. Kelly. 2012. Estimating animal densities in the aerosphere using weather radar: To Z or not to Z? Ecosphere 3:art72.

Cochran, W. W., and C. G. Kjos. 1985. Wind drift and migration of thrushes: A telemetry study. Illinois Natural History Survey Bulletin 33:297–330.

Cook, K. H., E. K. Vizy, Z. S. Launer, and C. M. Patricola. 2008. Springtime intensification of the Great Plains low-level jet and ,midwest precipitation in GCM simulations of the twenty-first century. Journal of Climate 21:6321–6340.

Coppack, T., and C. Both. 2002. Predicting life-cycle adaptation of migratory birds to global climate change. Ardea 38-90:369–378.

Crum, T. D., and R. L. Alberty. 1993. The WSR-88D and the WSR-88D operational support facility. Bulletin of the American Meteorological Society 74:1669–1687.

Crum, T. D., R. L. Alberty, and D. W. Burgess. 1993. Recording, archiving, and using WSR-88D data. Bulletin of the American Meteorological Society 74:645–653.

Deppe, J. L., M. P. Ward, R. T. Bolus, R. H. Diehl, A. Celis-Murillo, T. J. Zenzal, F. R. Moore, T. J. Benson, J. A. Smolinsky, L. N. Schofield, D. A. Enstrom, E. H. Paxton, G. Bohrer, T. A. Beveroth, A. Raim, R. L. Obringer, D. Delaney, and W. W. Cochran. 2015. Fat, weather, and date affect migratory songbirds' departure decisions, routes, and time it takes to cross the Gulf of Mexico. Proceedings of the National Academy of Sciences 112:E6331-E6338.

Deutschlander, M. E., and R. Muheim. 2009. Fuel reserves affect migratory orientation of thrushes and sparrows both before and after crossing an ecological barrier near their breeding grounds. Journal of Avian Biology 40:85–89.

Deutschlander, M. E., and R. Muheim. 2010. Magnetic orientation in migratory songbirds. Pages 314–323 in M. D. B. Moore, editor. Encyclopedia of Animal Behavior. Academic Press, Oxford.

Diehl, R. H. 2013. The airspace is habitat. Trends in Ecology Evolution 28:377–379.

Diehl, R. H., J. M. Bates, D. E. Willard, and T. P. Gnoske. 2014. Bird mortality during nocturnal migration over Lake Michigan: A case study. The Wilson Journal of Ornithology 126:19–29.

Diehl, R. H., and R. P. Larkin. 2005. Introduction to the WSR-88D (NEXRAD) for ornithological research. Pages 876–888 in C. J. Ralph and T. D. Rich, editors. Bird Conservation Implementation and Integration in the Americas: Proceedings of the Third International Partners in Flight Conference. USDA Forest Service, Gen. Tech. Rep. PSW-GTR-191.

Diehl, R. H., R. P. Larkin, and J. E. Black. 2003. Radar observations of bird migration over the Great Lakes. The Auk 120:278–290.

Dingle, H. 1996. Migration: The biology of life on the move. Oxford University Press, Oxford, New York.

Dingle, H., and V. A. Drake. 2007. What is migration? BioScience 57:113–121.

Dokter, A. M., F. Liechti, H. Stark, L. Delobbe, P. Tabary, and I. Holleman. 2011. Bird migration flight altitudes studied by a network of operational weather radars. Journal of The Royal Society Interface 8:30–43.

Dokter, A. M., J. Shamoun-Baranes, M. U. Kemp, S. Tijm, and I. Holleman. 2013. High altitude bird migration at temperate latitudes: A synoptic perspective on wind assistance. PLOS ONE 8:e52300.

Dunning, J. B. J. 2008. CRC handbook of avian body masses, Second Edition. Boca Raton, FL.

Egevang, C., I. J. Stenhouse, R. A. Phillips, A. Petersen, J. W. Fox, and J. R. D. Silk. 2010. Tracking of Arctic terns *Sterna paradisaea* reveals longest animal migration. Proceedings of the National Academy of Sciences 107:2078–2081.

Erni, B., F. Liechti, L. G. Underhill, and B. Bruderer. 2002. Wind and rain govern the intensity of nocturnal bird migration in central Europe – a log-linear regression analysis. Ardea 90:155–166.

Evans, and O'Brien. 2002. Flight calls of migratory birds: Eastern North American landbirds. [CD-ROM.].

Evans, P. R. 1966. Migration and orientation of passerine night migrants in northeast England. Journal of Zoology 150:319–348.

Farnsworth, A. 2005. Flight calls and their value for future ornithological studies and conservation research. Auk 122:733–746.

Farnsworth, A., S. A. Gauthreaux, and D. van Blaricom. 2004. A comparison of nocturnal call counts of migrating birds and reflectivity measurements on Doppler radar. Journal of Avian Biology 35:365–369.

Farnsworth, A., B. M. Van Doren, W. M. Hochachka, D. Sheldon, K. Winner, J. Irvine, J. Geevarghese, and S. Kelling. 2016. A characterization of autumn nocturnal migration detected by weather surveillance radars in the northeastern US. Ecological Applications 26:752–770.

Fink, D., W. M. Hochachka, B. Zuckerberg, D. W. Winkler, B. Shaby, M. A. Munson, G. Hooker, M. Riedewald, D. Sheldon, and S. Kelling. 2010. Spatiotemporal

exploratory models for broad-scale survey data. Ecological Applications 20:2131–2147.

Fortin, D., F. Liechti, and B. Bruderer. 1999. Variation in the nocturnal flight behaviour of migratory birds along the northwest coast of the Mediterranean Sea. Ibis 141:480–488.

Francis, J. A., and S. J. Vavrus. 2012. Evidence linking Arctic amplification to extreme weather in mid-latitudes. Geophysical Research Letters 39:L06801.

Gauthreaux, S. A. 1971. A radar and direct visual study of passerine spring migration in southern Louisiana. Auk 88:343–365.

Gauthreaux, S. A., and K. P. Able. 1970. Wind and the direction of nocturnal songbird migration. Nature 228:476–477.

Gauthreaux, S. A., and C. G. Belser. 1998. Displays of bird movements on the WSR-88D: patterns and quantification. Weather and Forecasting 13:453–464.

Gauthreaux, S. A., C. G. Belser, and D. V. Blaricom. 2003. Using a network of WSR-88D weather surveillance radars to define patterns of bird migration at large spatial scales. Pages 335–346 in P. Berthold, E. Gwinner, and E. Sonnenschein, editors. Avian migration. Springer-Verlag, Berlin Heidelberg, Germany.

Gill, R. E., T. L. Tibbitts, D. C. Douglas, C. M. Handel, D. M. Mulcahy, J. C. Gottschalck, N. Warnock, B. J. McCaffery, P. F. Battley, and T. Piersma. 2009. Extreme endurance flights by landbirds crossing the Pacific Ocean: Ecological corridor rather than barrier? Proceedings of the Royal Society of London B: Biological Sciences 276:447–457.

Green, M., and T. Alerstam. 2002. The problem of estimating wind drift in migrating birds. Journal of Theoretical Biology 218:485–496.

Hahn, S., T. Emmenegger, S. Lisovski, V. Amrhein, P. Zehtindjiev, and F. Liechti. 2014. Variable detours in long-distance migration across ecological barriers and their relation to habitat availability at ground. Ecology and Evolution 4:4150–4160.

Hansson, L.-A., and S. Åkesson. 2014. Animal movement across scales. Oxford University Press.

Hawkes, L. A., S. Balachandran, N. Batbayar, P. J. Butler, P. B. Frappell, W. K. Milsom, N. Tseveenmyadag, S. H. Newman, G. R. Scott, P. Sathiyaselvam, J. Y. Takekawa, M. Wikelski, and C. M. Bishop. 2011. The trans-Himalayan flights

of bar-headed geese *(Anser indicus)*. Proceedings of the National Academy of Sciences 108:9516–9519.

Hedenström, A. 2008. Adaptations to migration in birds: Behavioural strategies, morphology and scaling effects. Philosophical Transactions of the Royal Society B: Biological Sciences 363:287–299.

Hochachka, W. M., D. Fink, R. A. Hutchinson, D. Sheldon, W.-K. Wong, and S. Kelling. 2012. Data-intensive science applied to broad-scale citizen science. Trends in Ecology Evolution 27:130–137.

Holling, C. S. 1973. Resilience and stability of ecological systems. Annual Review of Ecology and Systematics 4:1–23.

Horton, K. G., B. M. V. Doren, P. M. Stepanian, A. Farnsworth, and J. F. Kelly. 2016a. Where in the air? Aerial habitat use of nocturnally migrating birds. Biology Letters 12:20160591.

Horton, K. G., W. G. Shriver, and J. J. Buler. 2015a. A comparison of traffic estimates of nocturnal flying animals using radar, thermal imaging, and acoustic recording. Ecological Applications 25:390–401.

Horton, K. G., P. M. Stepanian, C. E. Wainwright, and A. K. Tegeler. 2015b. Influence of atmospheric properties on detection of wood-warbler nocturnal flight calls. International Journal of Biometeorology 59:1385–1394.

Horton, K. G., B. M. Van Doren, P. M. Stepanian, A. Farnsworth, and J. F. Kelly. 2016b. Seasonal differences in landbird migration strategies. The Auk 133:761–769.

Horton, K. G., B. M. Van Doren, P. M. Stepanian, W. M. Hochachka, A. Farnsworth, and J. F. Kelly. 2016c. Nocturnally migrating songbirds drift when they can and compensate when they must. Scientific Reports 6:21249.

Jonzén, N., A. Lindén, T. Ergon, E. Knudsen, J. O. Vik, D. Rubolini, D. Piacentini, C. Brinch, F. Spina, L. Karlsson, M. Stervander, A. Andersson, J. Waldenström, A. Lehikoinen, E. Edvardsen, R. Solvang, and N. C. Stenseth. 2006. Rapid advance of spring arrival dates in long-distance migratory birds. Science 312:1959–1961.

Karlsson, H., C. Nilsson, J. Bäckman, and T. Alerstam. 2012. Nocturnal passerine migrants fly faster in spring than in autumn: a test of the time minimization hypothesis. Animal Behaviour 83:87–93.

Kelly, J. F., and K. G. Horton. 2016. Toward a predictive macrosystems framework for migration ecology. Global Ecology and Biogeography 25:1159–1165.

Kelly, J. F., K. G. Horton, P. M. Stepanian, K. M. de Beurs, T. Fagin, E. S. Bridge, and P. B. Chilson. 2016. Novel measures of continental-scale avian migration phenology related to proximate environmental cues. Ecosphere 7:1–13.

Kelly, J. F., R. Smith, D. M. Finch, F. R. Moore, and W. Yong. 1999. Influence of summer biogeography on wood warbler stopover abundance. Condor 101:76–85.

Kemp, M. U., J. Shamoun-Baranes, A. M. Dokter, E. Van Loon, and W. Bouten. 2013. The influence of weather on the flight altitude of nocturnal migrants in mid-latitudes. Ibis 155:734–749.

Kemp, M. U., J. Shamoun-Baranes, H. Van Gasteren, W. Bouten, and E. E. Van Loon. 2010. Can wind help explain seasonal differences in avian migration speed? Journal of Avian Biology 41:672–677.

Kemp, M. U., J. Shamoun-Baranes, E. E. Van Loon, J. D. McLaren, A. M. Dokter, and W. Bouten. 2012. Quantifying flow-assistance and implications for movement research. Journal of Theoretical Biology 308:56–67.

Klaassen, M. 1996. Metabolic constraints on long-distance migration in birds. The Journal of Experimental Biology 199:57–64.

Klaassen, R. H. G., T. Alerstam, P. Carlsson, J. W. Fox, and Å. Lindström. 2011. Great flights by great snipes: long and fast non-stop migration over benign habitats. Biology Letters 7:833–835.

Kokko, H. 1999. Competition for early arrival in migratory birds. Journal of Animal Ecology 68:940–950.

Kranstauber, B., R. Weinzierl, M. Wikelski, and K. Safi. 2015. Global aerial flyways allow efficient travelling. Ecology Letters 18:1338–1345.

Kunz, T. H., E. B. Arnett, B. M. Cooper, W. P. Erickson, R. P. Larkin, T. Mabee, M. L. Morrison, M. D. Strickland, and J. M. Szewczak. 2007. Assessing impacts of wind-energy development on nocturnally active birds and bats: A guidance document. Journal of Wildlife Management 71:2449–2486.

Kuznetsova, A., P. B. Brockhoff, and R. H. B. Christensen. 2014. lmerTest: Tests in linear mixed effects models. R package version 2.0-20.

Larkin, R. P. 1991. Flight speeds observed with radar, a correction: slow "birds" are insects. Behavioral Ecology and Sociobiology 29:221–224.

Larkin, R. P., W. R. Evans, and R. H. Diehl. 2002. Nocturnal flight calls of Dickcissels and Doppler radar echoes over south Texas in spring. Journal of Field Ornithology 73:2–8.

Larkin, R. P., and D. Thompson. 1980. Flight speeds of birds observed with radar: Evidence for two phases of migratory flight. Behavioral Ecology and Sociobiology 7:301–317.

La Sorte, F. A., and D. Fink. 2016. Projected changes in prevailing winds for transatlantic migratory birds under global warming. Journal of Animal Ecology.

La Sorte, F. A., D. Fink, W. M. Hochachka, J. P. DeLong, and S. Kelling. 2013. Population-level scaling of avian migration speed with body size and migration distance for powered fliers. Ecology 94:1839–1847.

La Sorte, F. A., D. Fink, W. M. Hochachka, A. Farnsworth, A. D. Rodewald, K. V. Rosenberg, B. L. Sullivan, D. W. Winkler, C. Wood, and S. Kelling. 2014. The role of atmospheric conditions in the seasonal dynamics of North American migration flyways. Journal of Biogeography 41:1685–1696.

La Sorte, F. A., D. Fink, W. M. Hochachka, and S. Kelling. 2016. Convergence of broad-scale migration strategies in terrestrial birds. Proceedings of the Royal Society B: Biological Sciences 283:20152588.

La Sorte, F. A., W. M. Hochachka, A. Farnsworth, D. Sheldon, B. M. V. Doren, D. Fink, and S. Kelling. 2015a. Seasonal changes in the altitudinal distribution of nocturnally migrating birds during autumn migration. Royal Society Open Science 2:150347.

La Sorte, F. A., W. M. Hochachka, A. Farnsworth, D. Sheldon, D. Fink, J. Geevarghese, K. Winner, B. M. Van Doren, and S. Kelling. 2015b. Migration timing and its determinants for nocturnal migratory birds during autumn migration. Journal of Animal Ecology 84:1202–1212.

Lefcheck, J. S. 2015. piecewiseSEM: Piecewise structural equation modeling in R for ecology, evolution, and systematics. arXiv:1509.01845 [q-bio].

Lehrer, M., editor. 1997. Wehner, R. Pages 145–185 Orientation and communication in arthropods. Birkhäuser Basel, Basel.

Liechti, F. 2006. Birds: Blowin' by the wind? Journal of Ornithology 147:202–211.

Liechti, F., W. Witvliet, R. Weber, and E. Bächler. 2013. First evidence of a 200-day non-stop flight in a bird. Nature Communications 4.

Lincoln, F. C. 1935. The waterfowl flyways of North America. U.S. Dept. of Agriculture, Circular No. 342. Washington, D.C.

Li, W., L. Li, M. Ting, and Y. Liu. 2012. Intensification of Northern Hemisphere subtropical highs in a warming climate. Nature Geoscience 5:830–834.

Lok, T., O. Overdijk, and T. Piersma. 2015. The cost of migration: Spoonbills suffer higher mortality during trans-Saharan spring migrations only. Biology Letters 11:20140944.

MacArthur, R. H. 1958. Population ecology of some warblers of northeastern coniferous forests. Ecology 39:599–619.

McLaren, J. D., J. Shamoun-Baranes, and W. Bouten. 2012. Wind selectivity and partial compensation for wind drift among nocturnally migrating passerines. Behavioral Ecology 23:1089–1101.

McLaren, J. D., J. Shamoun-Baranes, A. M. Dokter, R. H. G. Klaassen, and W. Bouten. 2014. Optimal orientation in flows: Providing a benchmark for animal movement strategies. Journal of The Royal Society Interface 11:20140588.

Mesinger, F., G. DiMego, E. Kalnay, K. Mitchell, P. C. Shafran, W. Ebisuzaki, D. Jovi?, J. Woollen, E. Rogers, E. H. Berbery, M. B. Ek, Y. Fan, R. Grumbine, W. Higgins, H. Li, Y. Lin, G. Manikin, D. Parrish, and W. Shi. 2006. North American Regional Reanalysis. Bulletin of the American Meteorological Society 87:343–360.

Mitchell, G. W., B. K. Woodworth, P. D. Taylor, and D. R. Norris. 2015. Automated telemetry reveals age specific differences in flight duration and speed are driven by wind conditions in a migratory songbird. Movement Ecology 3:19.

Moore, F. R. 1984. Age-dependent variability in the migratory orientation of the Savannah Sparrow *Passerculus sandwichensis*. The Auk 101:875–880.

Moore, F. R., S. A. J. Gauthreaux, P. Kerlinger, and T. R. Simons. 1995. Habitat requirements during migration: important link in conservation. Pages 121–144 in T. E. Martin and D. M. Finch, editors. Ecology and management of neotropical migratory birds. Oxford University Press, New York, Oxford.

Morris, S. R., D. W. Holmes, and M. E. Richmond. 1996. A ten-year study of the stopover patterns of migratory passerines during fall migration on Appledore Island, Maine. The Condor 98:395–409.

Morris, S. R., M. E. Richmond, and D. W. Holmes. 1994. Patterns of stopover by warblers during spring and fall migration on Appledore Island, Maine. Wilson Bulletin 106:703–718.

Möller, M., and R. Wehner. 1988. Path integration in desert ants, *Cataglyphis fortis*. Proceedings of the National Academy of Sciences 85:5287–5290.

Nevitt, G. A., M. Losekoot, and H. Weimerskirch. 2008. Evidence for olfactory search in Wandering Albatross, *Diomedea exulans*. Proceedings of the National Academy of Sciences 105:4576–4581.

Newton, I. 2006. Can conditions experienced during migration limit the population levels of birds? Journal of Ornithology 147:146–166.

Newton, I. 2008. The migration ecology of birds. Academic Press, London, England.

Nilsson, C., J. Bäckman, and T. Alerstam. 2014. Seasonal modulation of flight speed among nocturnal passerine migrants: Differences between short- and long-distance migrants. Behavioral Ecology and Sociobiology 68:1799–1807.

Nilsson, C., R. H. G. Klaassen, and T. Alerstam. 2013. Differences in speed and duration of bird migration between spring and autumn. The American Naturalist 181:837–845.

Nisbet, I. C. T., and W. H. J. Drury. 1967. Orientation of spring migrants studied by radar. Bird-Banding 38:173–186.

Odum, E. P. 1971. Fundamentals of ecology. Philadelphia: W. B. Saunders Company.

Pena-Ortiz, C., D. Gallego, P. Ribera, P. Ordonez, and M. D. C. Alvarez-Castro. 2013. Observed trends in the global jet stream characteristics during the second half of the 20th century. Journal of Geophysical Research: Atmospheres 118:2702–2713.

Pennycuick, C. J. 1969. The mechanics of bird migration. Ibis 111:525–556.

Peterson, A. C., G. J. Niemi, and D. H. Johnson. 2014. Patterns in diurnal airspace use by migratory landbirds along an ecological barrier. Ecological Applications 25:673–684.

Pryor, S. C., and R. J. Barthelmie. 2011. Assessing climate change impacts on the near-term stability of the wind energy resource over the United States. Proceedings of the National Academy of Sciences 108:8167–8171.

Pryor, S. C., R. J. Barthelmie, D. T. Young, E. S. Takle, R. W. Arritt, D. Flory, W. J. Gutowski, A. Nunes, and J. Roads. 2009. Wind speed trends over the contiguous United States. Journal of Geophysical Research: Atmospheres 114:D14105.

QGIS Development Team. 2015. QGIS Geographic Information System. Open Source Geospatial Foundation.

Ralph, C. J. 1978. Disorientation and possible fate of young passerine coastal migrants. Bird Banding 49:237–247.

Randall, D. 2015. An introduction to the global circulation of the atmosphere. Princeton University Press, Princeton.

R Core Team. 2017. R: A language and environment for statistical computing. R Foundation for Statistical Computing. Vienna, Austria.

Richardson, W. J. 1978. Timing and amount of bird migration in relation to weather: A review. Oikos 30:224–272.

Richardson, W. J. 1982. Northeastward reverse migration of birds over Nova Scotia, Canada, in autumn: A radar study. Behavioral Ecology and Sociobiology 10:193–206.

Richardson, W. J. 1990. Timing of bird migration in relation to weather: Updated review. Pages 78–101 Bird migration. Spring-Verlag, Berlin.

Richardson, W. J. 1991. Wind and orientation of migrating birds: A review. Experientia 60:226–249.

Ridgely, R. S., T. F. Allnutt, T. Brooks, D. K. McNicol, D. W. Mehlman, B. E. Young, and J. R. Zook. 2007. Digital distribution maps of the birds of the Western Hemisphere. NatureServe, Arlington, Virginia, USA.

Rohwer, S., L. K. Butler, and D. R. Froehlich. 2005. Ecology and demography of east-west differences in molt scheduling of neotropical migrant passerines. Pages 87–105 Birds of Two Worlds: The Ecology and Evolution of Migration. Johns Hopkins University Press, Baltimore, Maryland.

Ross, J. C., and P. E. Allen. 2014. Random Forest for improved analysis efficiency in passive acoustic monitoring. Ecological Informatics 21:34–39.

Sandberg, R. 1994. Interaction of body condition and magnetic orientation in autumn migrating Robins, *Erithacus rubecula*. Animal Behaviour 47:679–686.

Sandberg, R., F. R. Moore, J. Bäckman, and M. Lhmus. 2002. Orientation of nocturnally migrating Swainson's Thrush at dawn and dusk: Importance of energetic condition and geomagnetic cues. The Auk 119:201–209.

Saunders, A. A. 1959. Forty years of spring migration in southern Connecticut. The Wilson Bulletin 71:208–219.

Schaub, M., F. Liechti, and L. Jenni. 2004. Departure of migrating European Robins, *Erithacus rubecula*, from a stopover site in relation to wind and rain. Animal Behaviour 67:229–237.

Schmaljohann, H., F. Liechti, and B. Bruderer. 2007. Songbird migration across the Sahara: the non-stop hypothesis rejected! Proceedings of the Royal Society of London B: Biological Sciences 274:735–739.

Sergio, F., A. Tanferna, R. De Stephanis, L. L. Jiménez, J. Blas, G. Tavecchia, D. Preatoni, and F. Hiraldo. 2014. Individual improvements and selective mortality shape lifelong migratory performance. Nature 515:410–413.

Shaffer, S. A., Y. Tremblay, H. Weimerskirch, D. Scott, D. R. Thompson, P. M. Sagar, H. Moller, G. A. Taylor, D. G. Foley, B. A. Block, and D. P. Costa. 2006. Migratory shearwaters integrate oceanic resources across the Pacific Ocean in an endless summer. Proceedings of the National Academy of Sciences 103:12799–12802.

Shamoun-Baranes, J., E. Van Loon, H. Van Gasteren, J. Van Belle, W. Bouten, and L. Buurma. 2006. A comparative analysis of the influence of weather on the flight altitudes of birds. Bulletin of the American Meteorological Society 87:47–61.

Sheldon, D. 2015. WSRLIB: MATLAB toolbox for weather surveillance radar.

Sheldon, D., A. Farnsworth, J. Irvine, B. Van Doren, K. Webb, T. G. Dietterich, and S. Kelling. 2013. Approximate Bayesian inference for reconstructing velocities of migrating birds from weather radar. Association for the Advancement of Artificial Intelligence:1334–1340.

Silvertown, J. 2009. A new dawn for citizen science. Trends in Ecology Evolution 24:467–471.

Sinnott, R. W. 1984. Virtues of the haversine. Sky and Telescope 68:158–159.

Snyder, J. P. 1987. Map projections: A working manual. USGS Numbered Series, U.S. Government Printing Office, Washington, D.C.

Stepanian, P. M., and K. G. Horton. 2015. Extracting migrant flight orientation profiles using polarimetric radar. IEEE Transactions on Geoscience and Remote Sensing 53:6518–6528.

Stepanian, P. M., K. G. Horton, V. M. Melnikov, D. S. Zrnić, and S. A. Gauthreaux. 2016. Dual-polarization radar products for biological applications. Ecosphere 7:1-27.

Stoddard, P. K., J. E. Marsden, and T. C. Williams. 1983. Computer simulation of autumnal bird migration over the western North Atlantic. Animal Behaviour 31:173–180.

Strigul, N., D. Pristinski, D. Purves, J. Dushoff, and S. Pacala. 2008. Scaling from trees to forests: Tractable macroscopic equations for forest dynamics. Ecological Monographs 78:523–545.

Sullivan, B. L., J. L. Aycrigg, J. H. Barry, R. E. Bonney, N. Bruns, C. B. Cooper, T. Damoulas, A. A. Dhondt, T. Dietterich, A. Farnsworth, D. Fink, J. W. Fitzpatrick, T. Fredericks, J. Gerbracht, C. Gomes, W. M. Hochachka, M. J. Iliff, C. Lagoze, F. A. La Sorte, M. Merrifield, W. Morris, T. B. Phillips, M. Reynolds, A. D. Rodewald, K. V. Rosenberg, N. M. Trautmann, A. Wiggins, D. W. Winkler, W.-K. Wong, C. L. Wood, J. Yu, and S. Kelling. 2014. The eBird enterprise: An integrated approach to development and application of citizen science. Biological Conservation 169:31–40.

Thorup, K., T. Alerstam, M. Hake, and N. Kjellen. 2003. Bird orientation: Compensation for wind drift in migrating raptors is age dependent. Proceedings of the Royal Society B: Biological Sciences 270:S8–11.

Thorup, K., T. Alerstam, M. Hake, and N. Kjellén. 2006. Traveling or stopping of migrating birds in relation to wind: an illustration for the Osprey. Behavioral Ecology 17:497–502.

Van Doren, B. M., K. G. Horton, P. M. Stepanian, D. S. Mizrahi, and A. Farnsworth. 2016. Wind drift explains the reoriented morning flights of songbirds. Behavioral Ecology 27:1122–1131.

Van Doren, B. M., D. Sheldon, J. Geevarghese, W. M. Hochachka, and A. Farnsworth. 2014. Autumn morning flights of migrant songbirds in the northeastern United States are linked to nocturnal migration and winds aloft. The Auk 132:105–118.

Wainwright, C. E., P. M. Stepanian, and K. G. Horton. 2016. The role of the US Great Plains low-level jet in nocturnal migrant behavior. International Journal of Biometeorology 60:1531–1542.

Walters, C. K., J. A. Winkler, R. P. Shadbolt, J. van Ravensway, and G. D. Bierly. 2008. A long-term climatology of southerly and northerly low-level jets for the central United States. Annals of the Association of American Geographers 98:521–552.

Weimerskirch, H., Y. Cherel, K. Delord, A. Jaeger, S. C. Patrick, and L. Riotte-Lambert. 2014. Lifetime foraging patterns of the Wandering Albatross: Life on the move! Journal of Experimental Marine Biology and Ecology 450:68–78.

Weindler, P., R. Wiltschko, and W. Wiltschko. 1996. Magnetic information affects the stellar orientation of young bird migrants. Nature 383:158–160.

Wikelski, M., E. M. Tarlow, A. Raim, R. H. Diehl, R. P. Larkin, and G. H. Visser. 2003. Avian metabolism: Costs of migration in free-flying songbirds. Nature 423:704–704.

Wohlgemuth, S., B. Ronacher, and R. Wehner. 2001. Ant odometry in the third dimension. Nature 411:795–798.

Woodrey, M. S., and F. R. Moore. 1997. Age-related differences in the stopover of fall landbird migrants on the coast of Alabama. The Auk 114:695–707.

Wood, S. 2015. mgcv: Mixed GAM computation vehicle with GCV/AIC/REML smoothness estimation.

Wood, S. N. 2011. Fast stable restricted maximum likelihood and marginal likelihood estimation of semiparametric generalized linear models. Journal of the Royal Statistical Society: Series B (Statistical Methodology) 73:3–36.

Zehnder, S., S. Åkesson, F. Liechti, and B. Bruderer. 2001. Nocturnal autumn bird migration at Falsterbo, south Sweden. Journal of Avian Biology 32:239–248.

Zrnić, D. S., and A. Ryzhkov. 1998. Observations of insects and birds with a polarimetric radar. IEEE Transactions on Geoscience and Remote Sensing 36:661–668.